ENGINEERING MANAGEMENT OF AGROTRONICS OF GRAIN PRODUCTION BY AGRICULTURAL ENTERPRISESS

THE ACADEMY OF MANAGEMENT AND ADMINISTRATION IN OPOLE

Ivan Rogovskii, Iwona Mastowska, Józef Kaczmarek, Liudmyla Titova, Mikola Ohiienko, Oleksandr Nadtochiy

ENGINEERING MANAGEMENT OF AGROTRONICS OF GRAIN PRODUCTION BY AGRICULTURAL ENTERPRISES

Monograph

Opole 2020

Authors are responsible for content of the materials.

TABLE OF CONTENTS

PREFACE

The basis of the monograph on the problem of ensuring sustainable human development, in particular environmental management that involves increasing the efficient use of existing resources and modern technologies of grain production. From the solution of this problem depends the food security of the country. Gross harvest of the grain portion of the crop must be sufficient to provide food grains at the level of international standards (up to 1 ton per population of Ukraine), as well as seed, feed grain and raw materials for other sectors of the economy.

The monograph aims to increase the gross grain harvest part of the crop of modern production technologies.

The main scientific results obtained by the authors in preliminary studies include the scientific and technical basis for structuring the existing 157 models combine the park, identifying multiple diferenciales structures technology agricultural companies of the grain production on the area of 58 hectares in the 21120 ha depending on krupnotovarnogo production with the possibility of finding internal mechanisms of development and pursuing their own interests for their development. In previous studies it was found that modern agrominera provision does not contain a clear recommendation of of its technical characteristics. The authors propose a method of determining the optimal cultivated area under crops for associativity, additively, grouped by homogeneous indicators in the totality of their deterministic characteristics. In scientific asset research team, also is the allocation of the group of ten dominating factors: agrolandscapes characteristics of the agricultural companies of the grain production, soil and climatic conditions, resource potential, technological support, technical support, system nasonville, adaptability of crop rotation, organization of work, staffing, social conditions. The coefficient of concordance we establish the existence of some rational and interrelated parameter values of each of the ten factors that can influence directly the

farming enterprise. Previous scientific studies indicate the relevance of the solution of scientific problems of optimization of Park of combine harvesters for the permissible grain losses for agricultural enterprises with different levels of marketability based on the modeling of rates of harvest operations and engineering management of grain production in Ukraine.

Full matrix studies on the importance of various factors for increasing grain production in agricultural enterprises, the intensification of engineering management of domestic and foreign scientists was carried out.However, it was indirectly established that technological (1.52 rank), technical (2.04 rank) and organizational (3.14) factors are the main factors with a total concordance coefficient of 0.841. The authors confirmed the existence of a number of agronomic, technological, technical and social problems: ensuring maximum agro-landscape adaptability of land use, technologicalization of production and adaptability of the fleet structure to specific conditions of grain harvesting, ensuring minimum grain losses in all harvesting operations, application of crop rotations varieties adapted to mechanized harvesting, optimization of the system "field - combine - transport - grain flow" in a single production process with a given rate of harvesting within 2-4 thousand tons of grain per day, strict adherence to technological discipline in all operations for grain production crops, harmony of technical support of agricultural trials with observance of the set pace of their carrying out, introduction of system control of quality of works and their performance in the set volumes

CHAPTER 1. EXPERIMENTAL STUDIES OF DRYING CONDITIONS OF GRAIN CROPS WITH HIGH MOISTURE CONTENT IN LOW-PRESSURE ENVIRONMENT

During the experimental studies of drying grain crops with high moisture content in a low-pressure environment, the influence of residual pressure in a peri-seed environment and seed heating temperature on drying exposure and laboratory germination have been investigated. These experimental studies have been carried out by means of the experimental facility and its attachments that make it possible to provide residual pressure within the range of 10 – 80 kPa and seed heating temperature of +20 – +40 ºC.

Having processed the experimental data, regression equations of drying exposure and laboratory germination of grain crops with high moisture content by the example of corn seeds have been derived. The characteristic curves plotted based on the regression equations show that the minimum drying exposure and, simultaneously, the maximum laboratory germination can be achieved by applying residual pressure of 45 kPa and seed heating temperature of not more than +30 ºC.

In order to dry seeds with high moisture content, convection drying in a fixed, slow-moving and pseudo-fluidized bed is currently used in seed farming and breeding. It is implemented in chamber, conveyer, hopper and column dryers.

In order to stimulate moisture transfer in a seed, heating, which is provided by an air flow at the temperature of not more than 65 ºC, is used. The upper temperature value is determined by the fact that at this temperature level there is intensive exudation of moisture, but seed proteins are not denaturized. There are mild temperature conditions developed for various crops, which are

necessary to follow during seed drying in different convection dryers, in order to reduce the risk of thermal damage.

In spite of the developed measures for reducing thermal damage of seeds during drying, dried seeds have lower germinating ability and germinating power and less even germination compared to the undried ones. It can be explained by the difference in the properties of individual seeds and non-linear behavior of the temperature conductivity of a seed bed, which results in overheating and under-drying of individual seeds. In order to improve sowing qualities of seeds, it is necessary to decrease their thermal damage after drying by means of reducing the influence or the avoidance of a temperature field as well as the increase in the uniformity of seed drying.

Investigations *(Kotov B.I. et al., 2018; Kuznetsov Y.A. et al., 2018)* show that drying without seed damage is possible, if seed heating temperature of most grain crops does not exceed 40 – 45 ºC. At the same time, the change in moisture content does not exceed 5 – 6% in one technological cycle, since, if drying rate is higher, cracks can appear in a seed *(Zahoranová A. et al., 2016)*. In addition, it has been determined that if there is an increase in the initial moisture content of a seed, there is a decrease in the maximum acceptable temperature of seed heating *(Gorobets V.G. et al. 2018; Gorobets V.G. et al. 2018)*. In order to prevent seed damage during drying, the author *(Kuznetsov Y.A. et al. 2017)* suggests using mild drying temperature conditions. However, mild temperature conditions may result in under-drying of seeds. In addition, the existing heat generators do not always provide the required stable temperature conditions *(Dobrin D. et al. 2015)*.

One of the advanced methods of drying seeds is drying in a low-pressure environment *(Kotov B. et al. 2015)*. In this case, seed drying is more even and heating temperature is lower, compared to the one used in a convection method *(Kroulík M. et al. 2016; Karaj S. et al. 2011)*.

Research *(Paziuk, V.M. et al. 2018; Bogaert L. et al. 2018)* shows that intensive moist removal can be provided during continued seed heating to the temperature, which is close to the permissible one. Other researchers suggest using a vacuum-pulse method, in order to improve drying rate *(Lukaszuk J. et al. 2008)*. However, the use of these methods may result in thermal seed damage *(Rekas A. et al. 2017)*.

Scientific papers *(Paleliulko M.I. et al. 2015; Gorji A. et al. 2010)* present the idea that intensive moist removal in a low-pressure medium is possible during cyclic heating, vacuum treatment and blowing under air-pressure through a heat-exchange apparatus *(Gorobets V.G. et al. 2018)*. However, these papers do not consider the influence of operating conditions on the sowing qualities of seeds.

Most of the above mentioned papers do not consider the influence of the operating conditions of drying in a low-pressure environment both on the sowing qualities of seeds and on their drying exposure simultaneously. That is why, it is necessary to substantiate the parameters, which provide drying in a low-pressure environment with minimum exposure and maximum germinating ability after drying.

In order to investigate the mutual influence of operating conditions and optimize the number of experiments, a multi-factor experiment procedure (Paziuk, V.M. et al. 2018; Bogaert L. et al. 2018) was used. The planning matrix of the experiments was conducted according to D-optimal second-order plans (Lukaszuk J. et al. 2008), based on the theory of joint efficient estimates, which was developed by an American statistician J. Kiefer. At the same time, Box-Behnken design (B–B3) was used for a three-factor experiment.

Drying exposure was determined by measuring the time, during which moisture content of the pre-moistened seed was changed by 6%. Such a change in moisture content was registered by periodic weighing of the seed mass that was used in the experiments. The level of thermal damage was evaluated based

on laboratory germination, which was determined according to State Standards of Ukraine 4138-2002.

Regression coefficients, their relevance, adequacy, reproducibility and the homogeneity of the regression equations were determined by means of Wolfram Mathematica 13 software. Graphical interpretation of the regression equations was realized in MathCad 13 software environment.

In order to substantiate drying conditions of seeds in a low-pressure environment with minimum exposure and maximum generating ability after drying, a simple laboratory-scale plant, which is a cylindrical vessel, where residual pressure up to 2 kPa (Fig. 1.1) can be created inside, was developed. Seed heating was conducted by means of an external heater, which is not a part of a drying chamber.

Since the seeds of every grain crop have their own individual drying characteristics, the determination of the common patterns of their drying in a low-pressure environment requires a great number of experimental studies. In order to reduce the amount of experimental work, a sample weight of corn seeds weighting 715 g was taken as an example. Its drying properties can be considered as those, which are typical of most grain crops, to a certain extend.
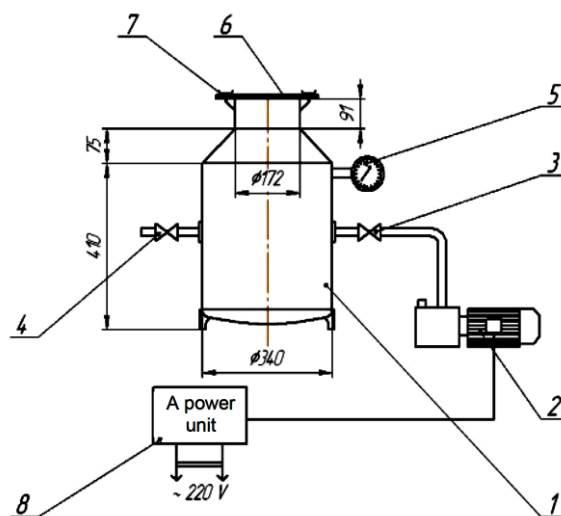
a)

b)

Fig. 1.1 Laboratory-scale plant design (a) and its general view (b):

1 – a drying chamber; 2 – a rotary vane-type vacuum low-pressure pump; 3 – a vacuum pressure tap; 4 – a tap for releasing vacuum; 5 – a vacuum meter; 6 – a lid with a seal; 7 – a locking mechanism; 8 – a power unit

The following independent factors, which are the main operating parameters of seed drying in a low-pressure environment, were chosen: p – residual pressure in a drying chamber, kPa; t – seed heating temperature, ºC.

Their values and variability interval are represented in Table 1.1.

In the course of experimental investigations, sample weight of corn seeds was periodically heated to the required temperature during 5 min and was exposed to a low-pressure air environment during 10 min. At the end of every period sample weight mass was measured and the amount of the evaporated moisture was determined. The measurement of sample weight mass and the amount the evaporated moisture was conducted until the change in moisture content of corn seeds reached 6 %.

Table 1.1

Values and coding of the levels of independent factors during experimental investigation of the operating conditions of drying moist seeds in low-pressure environment

Variability level	Independent factors	
	Residual pressure, p, kPa	**Seed heating temperature, t, °C**
Low (-1)	10	20
Medium (0)	45	30
High (+1)	80	40
Variability interval	35	10

Implementation of a D-optimal plan, according to the data presented in Table 1, resulted in the derivation of the regression equations of drying exposure and seed germinating ability. Having conducted the analysis for regression coefficients, their adequacy, reproducibility and correspondence to a certain dependence, the regression equations acquire the following form.

Regression equation of drying exposure:

$$\tau_{ex} = 608.151 + 1.06 \cdot p - 13.73 \cdot t. \tag{1.1}$$

Regression equation of laboratory germination of seeds:

$$K_{ger} = 81.37 + 0.12 \cdot p + 0.972 \cdot t - 0.028 \cdot t^2. \tag{1.2}$$

The analysis of the regression equations (1.1) and (1.2) shows that drying exposure is greatly affected by heating temperature t and laboratory germination is influenced both by seed heating temperature t and residual pressure in a drying chamber p. Based on the equation (1.1), drying exposure τex was plotted versus residual pressure p without airflow. (Fig. 1.2).
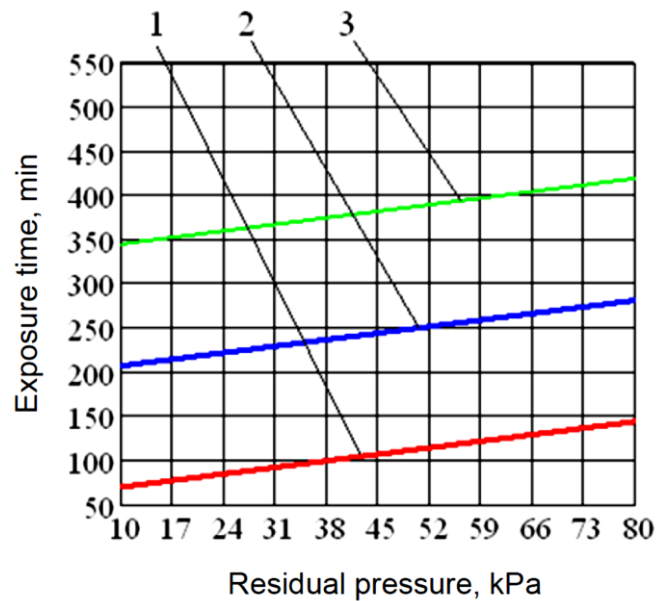
Fig. 1.2 - Drying exposure-vs-residual pressure characteristic curves at various temperature without airflow:

1 – 40 °C, 2 – 30 °C, 3 – 20 °C

According to the characteristic curves presented in Fig. 3, drying exposure τex linearly depends on residual pressure p. The decrease in residual pressure p results in the linear decrease of drying exposure τex. If seed heating temperature t is reduced, drying exposure τex increases. These characteristic curves show that the minimum drying exposure (69.6 min) can be achieved at the lowest level of redisual pressure p = 10 kPa and the seed heating temperature of t = 40 °C. The significant influence of seed heating temperature t on drying exposure τex can be explained by the fact that during seed drying in a low-pressure environment, it is cooled down due to the evaporation of seed surface moisture with simultaneous decrease of moisture diffusion rate. That is why, seed heating reduces exposure.

In addition, seed heating temperature t is a significant factor that influences laboratory germination and therefore, it affects the level of thermal damage of seeds (equation (1.2)). It is shown in Fig. 1.3.
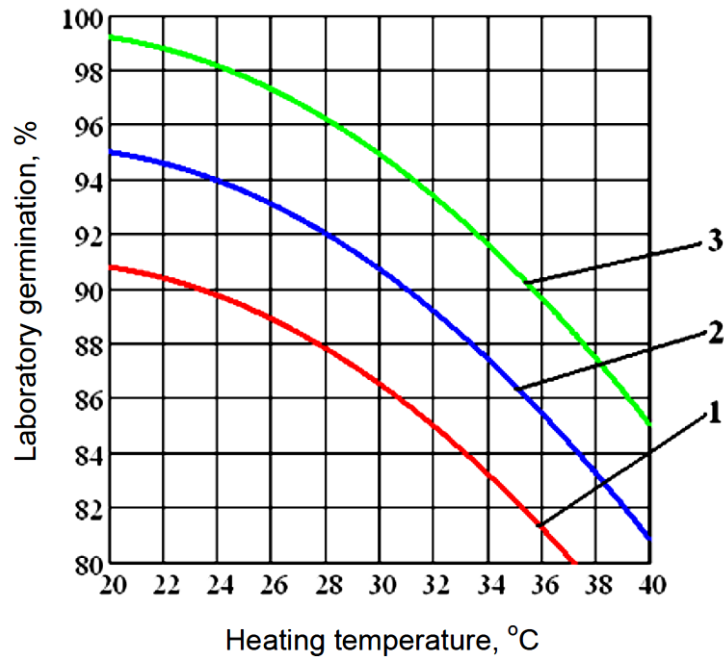
Fig. 1.3 Laboratory germination-vs-seed heating temperature curves at various residual pressure:

1 – 10 kPa, 2 – 45 kPa, 3 – 80 kPa

The increase of seed heating temperature t and the decrease of residual pressure p result in the reduction of seed laboratory germination Kgerm. This is due to the fact that there is an increase of possible degradation of seed protein structures, if seed heating temperature t increases.

The increase of seed heating temperature t and the decrease of residual pressure p result in the reduction of laboratory germination of seeds Kgerm and simultaneous decrease in drying exposure τex. In order to find rational values of the operating conditions of drying in a low-pressure environment, drying exposure and laboratory germination-vs-seed heating temperature curves at various residual pressure were plotted in one of the graphs (Fig. 1.4). Their cross point defines the minimum value of drying exposure and the maximum value of the laboratory germination of seeds.
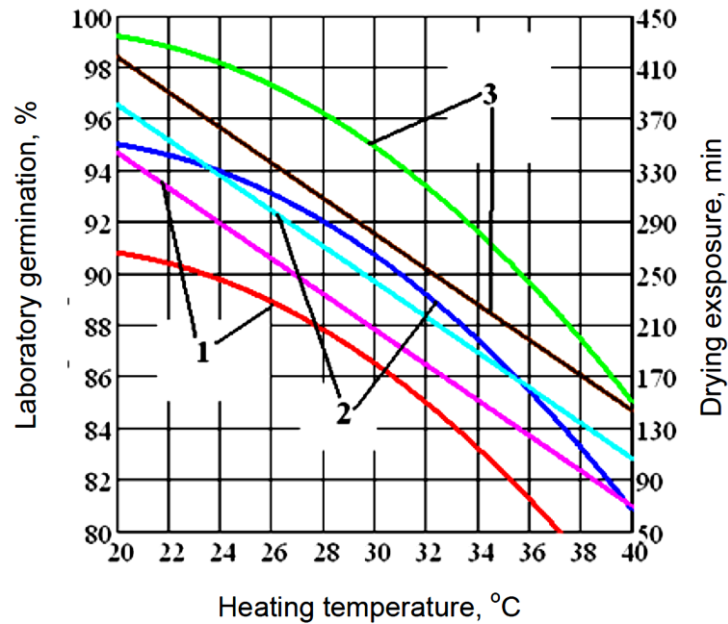
Fig. 1.4 - Laboratory germination and drying exposure-vs-seed heating temperature curves at various residual pressure:

1 – 10 kPa, 2 – 45 kPa, 3 – 80 kPa

According to the curves presented in Fig. 4, the minimum drying exposure with the lowest level of thermal damage, which is expressed as laboratory germination, can be achieved at seed heating temperature of not more than 30 ºC and at residual pressure being equal to 45 kPa. In case of corn seeds with initial moisture content being 20%, the minimum drying exposure is equal to 240 min and laboratory germination is 91.8 %. It means that intensive drying in a low-pressure environment can be conducted at the temperature levels, which are 10 – 15 ºC lower than those used during convection drying, ensuring germinating conditions.

Conclusions to chapter 1

Experimental investigations show that it is possible to reduce the level of thermal damage and drying exposure of the seeds of grain crops with high moisture content by drying at the pressure in a peri-seed environment being equal to 30 – 45 kPa and at seed heating temperature of +25 – +30 °C.

CHAPTER 2. ENGINEERING MANAGEMENT OF TWO-PHASE COULTER SYSTEMS OF SEEDING MACHINES FOR IMPLEMENTING PRECISION FARMING TECHNOLOGIES

The paper covers process flow-sheets and design implementation of two-phase coulter systems of seeding machines for precision farming technologies. A mathematical model of the movement of a two-phase coulter system has been developed and simulation modelling has been conducted. As a result, the ability of a two-phase coulter system to operate a specified working mode, if such operating parameters as, for example, the amplitude and the frequency of irregularities entering a coulter system, the mass of a slot cutter and an indenting disk, a damping coefficient, an amplification coefficient etc. are changed, given that there are systematic and random errors of measuring and control elements, has been determined. A technology evaluation of a two-phase coulter system operation was conducted in the field environment by determining the variation coefficients of a seeding depth, the distance between plants in a row, field germination capacity and the average soil consistency in the area of a plant location. Technical and economic assessment of the application of a two-phase coulter system on row-crop seeding machines has been conducted.

Together with soil preparation and crop tending, one of the main conditions for obtaining high yields of tilled crops is the distribution of crop seeds according to agronomical requirements *(Vlăduţ D.I. et al., 2018)*. It contributes to the provision of plants with the necessary amount of light, moist, heat and nutrients *(Aliev E.B. et. al., 2018)*.

A change in soil resistance and irregularities in the soil surface while a seeding machine is in operation cause coulter oscillations in a longitudinal-vertical plane, which results in its unstable motion at the selected depth *(Rogovskii I.L. et. al., 2019)*. If there is an increase in the movement speed of a

seeding machine, the amplitude of coulter oscillations in a longitudinal-vertical plane increases as well, which results in greater non-uniformity of seeding depth *(Kotov B.I. et. al., 2019).* The existing designs of coulter systems of seeding machines do not provide the sufficient accuracy of distributing tilled crop seeds in the soil *(Bulgakov V. et. al., 2018).*

In the course of solving the problem of the improvement of sowing quality level, a high quality tilled crop sowing achievement hypothesis was made, according to which, in order to improve the quality level of tilled crop sowing, it is necessary to apply a two-phase way of seed covering *(Dinesh J., 2009).*

a)   *b)*

c)   *d)*
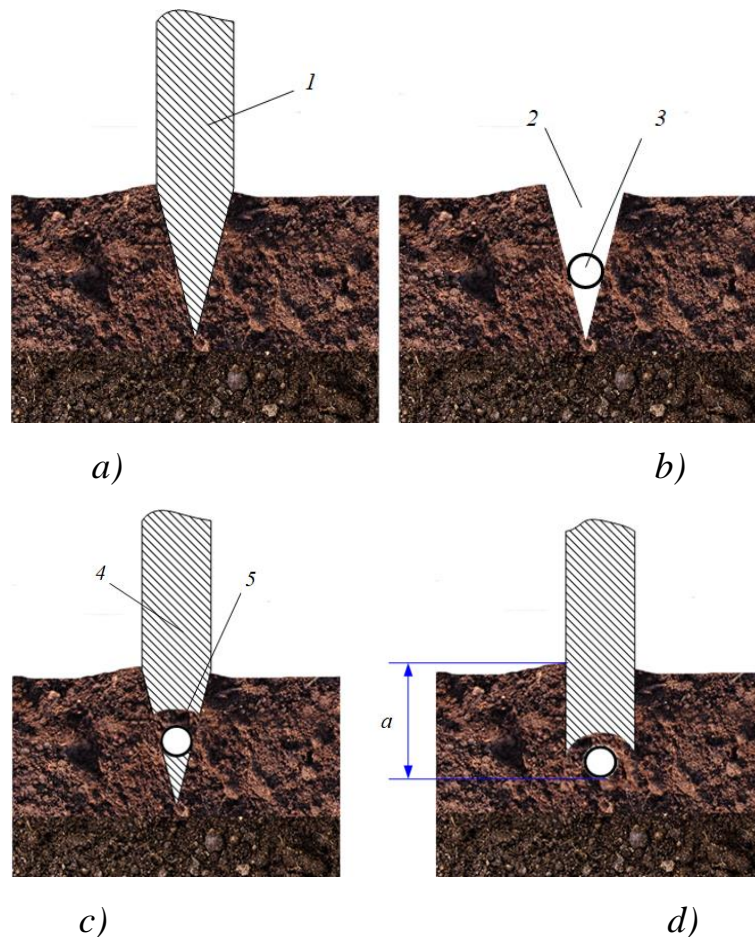
Fig. 2.1 - The main stages of two-phase seed covering

a, b – the first phase; c, d – the second phase of seed covering

1 – a slot cutting disk; 2 – a slot; 3 – a seed; 4 – an indenting disk; 5 – working edges of an indenting disk; α – seeding depth

If such a way of sowing is used, the process of seed covering is performed in two phases *(Kanehl P., 2010)* and each phase includes two stages (Fig. 2.1).

The cycle of the four stages *(Komiwes V. et. al., 2006)* of implementing the suggested method is the following:

▪ the first stage: a slot cutting disk cutter 1 penetrates the soil and makes a slot 2 with favorable geometrical parameters for seed self-blocking between the side walls of a slot without its rolling along a row *(Bulgakov V et. al., 2017)*;

▪ the second stage: a seed 3 is loaded in a slot 2 and, depending on a seed size, it is blocked at various depth (however, it is shallower than the target one) and is arranged along the slot axis *(Asejeva A. et. al., 2013)*;

▪ the third stage: an indenting disk 4 of certain geometrical parameters moves along a slot and cuts wet side walls of the soil by means of its working edges 5; due to the form of a disk groove, during cutting the soil moves down and covers the seed that is located in a slot and, simultaneously, it compacts around it *(Croitoru Şt. et. al., 2017)*;

▪ the fourth stage: an indenting disk 4 moves a seed together with the compacted soil to the target seeding depth a; slot covering is performed in a traditional way *(Aksenov A.G., 2018)*.

Such a two-phase way of tilled crop sowing makes it possible to provide seed covering 1 (Fig. 2.2) in a wet soil layer 4. The nucleus 2 of moistened soil that is compacted to 1,3 g/cm^3 *(Nilesh N.J. et. al., 2015)* is formed around a seed and a fine structure 3 can be formed above. A seed is covered at the target depth (with permissible variation) a irrespective of the state of irregularities and soil density *(Rohokale A.B. et. al., 2014)*. In addition, the uniformity of seed distribution along a row, which is provided by a seeding machine, is not violated and the deviation of seed placement relative to a row center line is reduced to a minimum   *(Shen Qiang et. al., 2015)*.
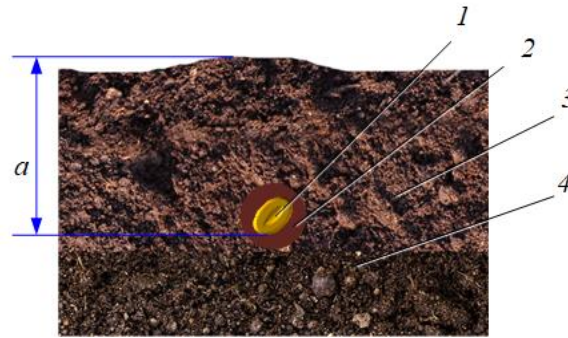
Fig. 2.2 - Image of a seed covered in the soil

1 – seed; 2 – nucleus of compacted and moistened soil; 3 – fine structure;

4 – wet soil layer; a – seeding depth

The purpose of research is to improve the quality of planting row crops in modern farming technologies by study parameters of two-phase coulter systems of seeding machines.

In order to implement the suggested two-phase method of covering tilled crop seeds, a corresponding design of a coulter system has been developed. It has been determined that, when a disk deepens into the soil, the resistance force of the soil is the influencing factor for the running depth of an indenting disk and it depends on the type of soil and its physical and mechanical characteristics etc. Here, the values of the above stated characteristics are changed to a considerable extend over the field area depending on the coordinates of a seeding unit in the field. It means that it is necessary to take into account position-determined soil characteristics, namely, its position-determined consistency.

In the further analysis of a coulter system, position-determined information about soil consistency with the possibility of automated correction of an indenting disk position (Fig. 2.3) is taken into account, which should be able to provide the effective operation of a correction device and a coulter system as a whole within a wide range of operating conditions.

The position of a slot cutter is controlled by a position sensor *D* and its signal is applied to an adder unit *S*. A manual adjustment signal U_3 is applied to an adder unit as well. A signal *λ(t)* is obtained at the output and it is sent to the control module of a servo-drive unit. A feedback control signal *Ž(t)* from the position sensor of an indenting disk and the signal *R(x,y)* from the unit of calculation of position-determined soil consistency are sent to this module as well. The later one operates based on the information about the current coordinated of a seeding unit in the field and a position-determined soil consistency map.
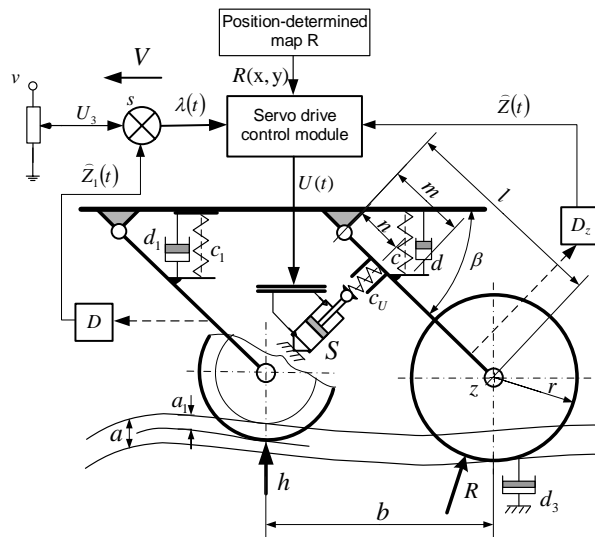
Fig. 2.3 - Scheme of a two-phase coulter system with an automated indenting disk correction system

Fig. 2.4 presents the scheme of an automated indenting disk correction system.

A signal *R(x,y)* is sent from the reading unit (PC card) of a soil map to the calculation unit of position-determined soil consistency. A signal *γ(x,y)* from a global positioning system sensor is applied to the same block. The output signal of this block is the signal *R(x,y,t)*, which is normalized relative to the amplitude and synchronized with the world coordinates. An output signal *λ(t)* serves as a tracking (purpose) signal. This signal is formed as a result of applying the signal

$\check{Z}_1(t)$ from the sensor D of a slot cutter position and the signal $\check{Z}_1(t)$ from a feedback sensor D_Z that controls an indenting disk position to an adder unit. A setter *3* with an output signal U_3 is used for manual controlling of an indenting disk position relative to a slot cutter. On one hand, the purpose is achieved by means of managing slot cutter running at the depth α_1, on the other hand, it is reached by the influence of a pneumatic drive on the drawbar of the radial hanger of an indenting disk (controlled by a sensor D_Z with an output feedback signal $\check{Z}(t)$). As a result, the target seeding depth $Z(t)$ is achieved at the output of the system.
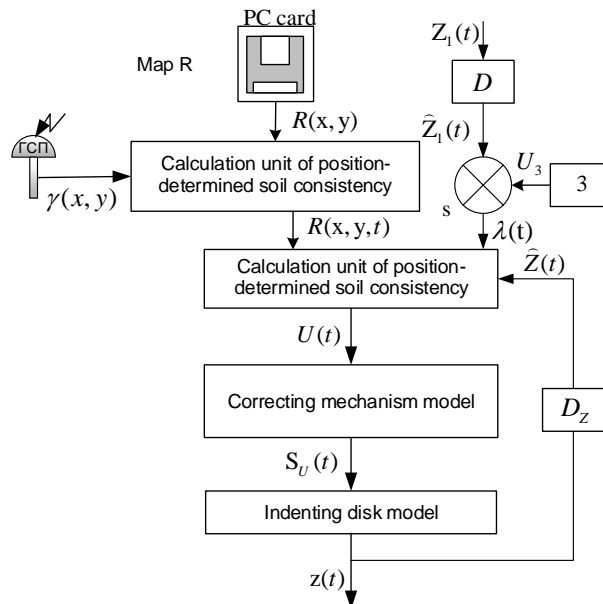
Fig. 2.4 - Scheme of an automated indenting disk correction system

The main task of the control system is the calculation of the optimum value of the control action $U(t)$, which is applied to the correction mechanism of an indenting disk position. The rod of a pneumatic drive S (see Fig. 2.3) adjusts the position of an indenting disk relative to a slot cutter depending on the set adjustments, the irregularities of the field surface and the value of soil resistance according to the coordinates of a seeding unit in the field and the value of an indenting disk running depth. As a result, at the output of the system a specific

position of an indenting disk *Z(t)*, as a signal function of the regulating action *U(t)* that comes from a pneumatic drive control module, is achieved.

A transfer function of an indenting disk model can be found by means of deriving a differential equation of an indenting disk movement. In order to formulate a dynamic equation of a coulter system motion along the irregularities of a field surface, let us apply Lagrange's dynamic equations of the second kind:

$$\frac{d}{dt}\frac{\partial T}{\partial \dot{q}_i} - \frac{\partial T}{\partial q_i} + \frac{\partial \Pi}{\partial q_i} + \frac{\partial \Phi}{\partial \dot{q}_i} = Q_{q_i} \tag{2.1}$$

where *T* and *Π* – kinetic and potential energy, respectively; *Φ* – dissipative function;

q_i – generalized coordinates; Q_{q_i} – generalized force.

Having determined the necessary components with their substitution in the dynamic equation (2.1) and having performed the necessary transformations, a dynamic equation of a coulter system motion along the irregularities of a field surface is obtained:

$$\ddot{z}\left(\frac{I\tan(\beta^2)}{R^2} + M\left(1 + \tan(\beta)^2\right)\right) + \dot{z}\frac{(dm + ld_3)}{l} + z\left(\frac{cm}{l} + \frac{n^2\sin(\beta)^2 c_U}{l^2}\right) - Q_U = S_U\left(\frac{n\sin(\beta)c_U}{l}\right) \tag{2.2}$$

A transfer function of the model of an indenting disk of a coulter system is of the following form:

$$W_{vd} = \frac{A_4}{A_1\tau^2 + A_2\tau + A_3} \tag{2.3}$$

where $A_1 = \frac{I\tan(\beta)^2}{R^2} + M\left(1 + \tan(\beta)^2\right)$; $A_2 = \frac{(dm + ld_3)}{l}$; $A_3 = \frac{cm}{l} + \frac{n^2\sin(\beta)^2 c_U}{l^2}$; $A_4 = \frac{n\sin(\beta)c_U}{l}$ τ – symbol of time differentiation.

A transfer function of the model of a servo-mechanism of an indenting disk position correction is of the following form:

$$W_{np} = \frac{K_k}{T_k^2\tau^2 + 2T_k\xi_k\tau + 1} \tag{2.4}$$

where K_k, ξ_k, and T_k – coefficient of amplification, a damping coefficient and the time constant of a position correction mechanism, respectively.

A transfer function of the sensor model of an indenting disk position is of the following form:

$$W_d = \frac{A_d}{T_d \tau + 1} \tag{2.5}$$

where $A_d = 1 + \Delta_d(t) + \xi_d(t)$; $\Delta_d(t)$ and $\xi_d(t)$ – systematic and random components of the relative error of sensor performance; T_d – sensor time constant.

The equations (2.4), (2.5) make a functional model of a two-phase coulter system. The analysis of such a model makes it possible to choose the structure and the parameter values of the control action $U(t)$ (law of control), which can provide process stability of the system as well as its operation at the permissible error values when keeping track of the goal achievement.

In order to determine the ability of a two-phase coulter system to operate a specified working mode, if such operating parameters as, for example, the amplitude and the frequency of irregularities entering a coulter system, the mass of a slot cutter and an indenting disk, a damping coefficient ξ, an amplification coefficient K etc. are changed, given that there are systematic and random errors of measuring and control elements, simulation modelling has been conducted.

At the first stage of the simulation modelling, the influence of systemic and random errors on the performance of the position sensors of a slot cutter and an indenting disk, without taking into account a soil reaction component, was analyzed. As a result, it has been determined that it is necessary to apply sensors with the minimum values of systematic and random performance errors for high quality covering of seeds at the set depth.

The next step of simulation modelling was the evaluation of the influence of soil consistency (the main component of soil reaction on a slot cutter) on the quality of an indenting disk performance. This influence is difficult to explain, since, as a result of the laboratory-field investigations on measuring soil consistency at the seeding depth in the field conditions, this value was determined to be within the range of 100…1300 kPa.

In order to conduct laboratory-scale and laboratory-field investigations, a laboratory-field plant has been designed and developed (Fig. 2.5).
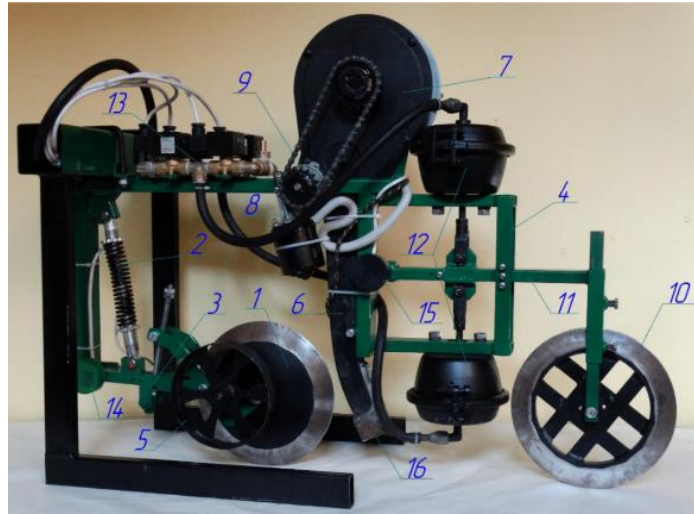
Fig. 2.5 - General view of a laboratory-field plant

1 – slot cutting disk; 2 – shock absorber; 3 – drawbar; 4 – a frame;

5 – supporting-running wheels; 6 – seed line;

7 – seed-feeding unit; 8 – electric motor reductor; 9 – chain drive;

10 – indenting disk; 11 – hanger; 12 – pneumatic cylinders;

13 – valve actuating gear; 14, 15 – position sensors of hangers; 16 – inductive

sensor

The laboratory-field plant is a two-phase coulter system consisting of a slot cutting disk *1*, which is hinged to a frame *4* via a drawbar *3*, which is spring-loaded by a shock absorber *2*. The running depth of a slot-cutting disk is regulated by means of supporting-running wheels *5*. There is a seed-feeding unit *7* with a seed line *6* arranged lengthways in series. An indenting disk *10* is arranged on a hanger *11*, which is hinged to frame. A seed-feeding unit is actuated by means of electric motor reductor *8* through an electric chain *9*.

The two-coulter system has an automated position regulation and control system of an indenting disk, which, in its turn, consists of two pneumatic cylinders *12*, a valve actuating gear *13*, position sensors *14* and *15* of hangers, an external compressed air supply (it is not presented in the Figure) and Mikrol

MIK 121 controller that controls the operation of a seed-feeding unit as well. In order to record the moment when a seed enters the bottom part of a seed line, an inductive sensor *16* is installed.

In the course of conducting laboratory-field investigations, the suggested coulter system was mounted on a 16-row John Deere 7000 planter (Fig. 2.6), which was utilized with John Deere 8400 tractor, instead of its commercial thirteenth row unit. Seeding units were the same on all the planter units (pneumatic, vacuum-type, equipped with an individual electric drive) and set for the same seeding rate.

Fig. 2.6 - A two-phase coulter system on John Deere 7000 planter

All the investigations were conducted according to the standard complete factorial procedure. The defined optimization criteria included the following: the uniformity of seed dropping distance along a row, the uniformity of seeding depth, soil consistency in the area of seed location and seed germination capability. Experimental data processing was conducted with the use of Statistica application sorfware package.

An investigation on the quality of seed covering by means of a two-phase method and on determining the nature of the soil area firmed by an indenting disk has been conducted in a tillage bin. Soil moisture content at the moment of

conducting the research was brought to 20±2 % and controlled by means of FIELDSCOUT TDR 300 Soil moisture tester.

With the help of the developed laboratory-field plant, the difference in the running depth Δh of a slot cutter and an indenting disk, which was necessary to provide soil consistency Q in the area of seed depth within the limits of 1,1…1,3 g/cm^3, was determined in a tillage bin. Before the beginning of the experiment soil moisture was brought to 20±2 % and the soil was tilled to reach the average consistency of 1 g/cm^3. The consistency formed at the seed depth was determined according to Kachynskyi method, however, a specially designed sampler 8 cm^3 in size was applied.

Parameter Δh was changed at three levels: 1 cm, 2 cm and 3 cm.

On condition that all the above mentioned values of the dynamic parameters of a two-phase coulter system are applied, the result of solving the process of its functioning according to the structural diagram of the automated correction system of an indenting disk position is presented in Fig. 7.

Fig. 2.5 shows that the functioning mechanism of an indenting disk (Z(t) coordinate) has the transient process of 0.35 s at the beginning of its operation. Besides, there is a phase displacement of 0.27 s in copying field surface irregularities that, for example, in case of the running speed of a planter being 2 m/s, corresponds to the copying with the displacement of approximately 0.54 m. In addition, the set amplitude of an indenting disk oscillations is not maintained. For example, from the 3rd to the 9th second time period, the amplitude of irregularity oscillations is equal to 9.8 cm, while the amplitude of an indenting disk oscillations within the same time period is only 7.5 cm. However, the most significant moment is the negative influence of soil reaction Rg on the process of copying irregularities. As it can be seen in Fig. 2.7, the raising of an indenting disk takes place with the failure of the copying process up to 1.8 cm.
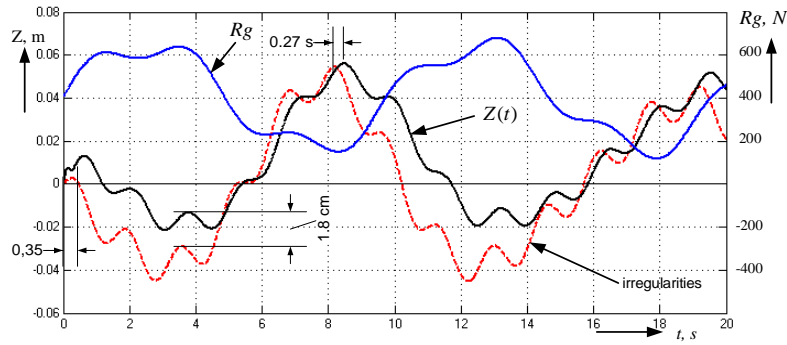
Fig. 2.7 - Representation of the operation process of the two-phase coulter system

Z(t) – coordinate of an indenting disk position;

Rg – value of soil resistance force
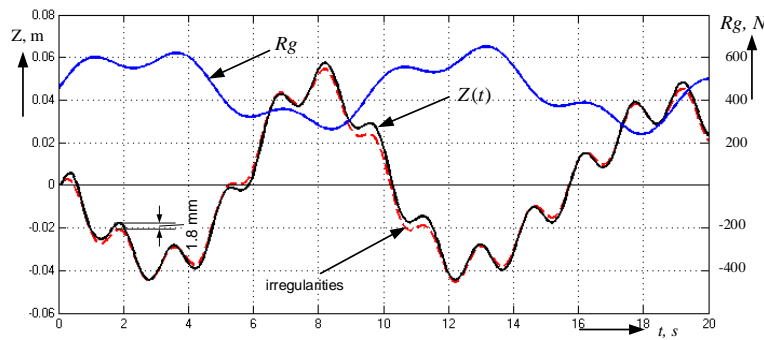
Fig. 2.8. Presentation of the operation process of the improved two-phase coulter system:

Z(t) – coordinate of an indenting disk position;

R_g – value of soil resistance force

It is to the point to have a system with steady and set modes of copying field surface irregularities, which is invariant with respect to the effect of soil reaction on an indenting disk. Computer simulating modelling made it possible to determine the influence factors for the achievement of the set goal. The main factors include spring stiffness c_U (see Fig. 2.3), the decrease of damping coefficient d as well as a time constant, the decay coefficient and the amplification coefficient of the control module of a pneumatic drive. Fig. 2.8

27

presents the operation process of the system at the values of c_U=360 kg/cm, d=120 N s/m, t=0.1 s, ξ=0.1, K=4.9.

The measure of inaccuracy *I* in evaluating the running depth of an indenting disk relative to the set one during the standard operation period *T* of a coulter system was equal to 1.5×10^{-4}.

In general, the achievement of the goal of maintaining the set running depth of an indenting disk of a two-phase coulter system is satisfactory. The dynamic parameters of the system are chosen in such a way that the changes in position determined soil consistency (by means of the parameter *Rg*) do not have a significant influence on the running stability of an indenting disk, its raising is reduced to a minimum and does not exceed 1,8 mm. In addition, there is no phase displacement in copying field surface irregularities.

The conducted research shows that soil consistency in the filed area, which is cultivated for planting crops, varies widely (up to 1300 kPa) and does not have the dominant variation frequency along the run of cultivated land. These results were taken into account when determining the post-conditions of the simulation modelling of the operation process of a two-phase coulter system.

On the surface of the soil a slot was made by means of a slot cutting disk and a seed was fed to it. Afterwards, an indenting disk was pulled along the slot. It cut the soil from the furrow walls and covered the seed (Fig. 2.9 *a*). As it can be seen, after the pass of an indenting disk, there was an area of firmed soil formed (Fig. 2.9 *b*) – top view and cross-sectional view (Fig. 2.9 *c*).

Parameter *v* was changed at three levels: 1 m/s, 1.7 m/s and 2.4 m/s.

Simultaneously, the influence of the running speed *v* of a two-phase coulter system on the optimization parameter of ρ was evaluated.

a)   *b)*   *c)*
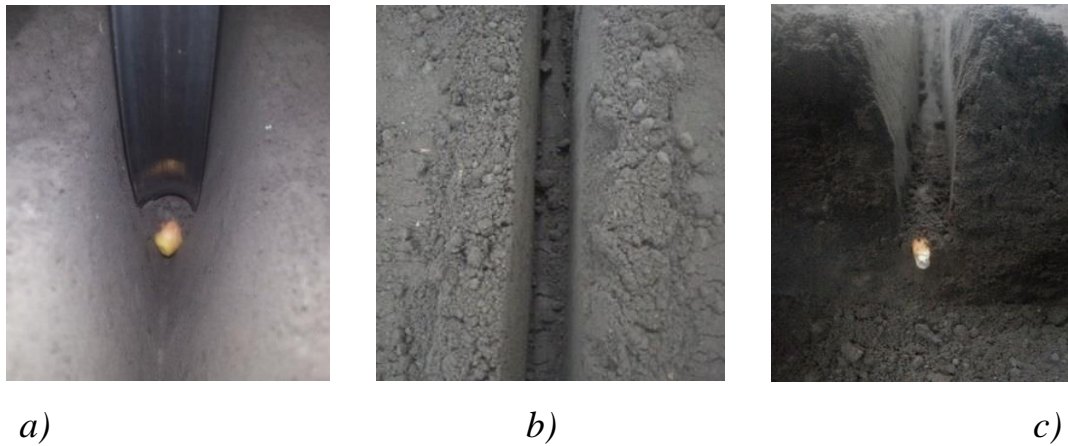
Fig. 2.9 - Representation of the implementaion of a two-phase method of seed covering

a – indenting disk operation; b – firmed soil area (top view);

c – soil cross-sectional view

The response surface of the change in soil consistency ρ depending on the parameter Δh and the running speed v of a two-phase coulter system has been built (Fig. 2.10).
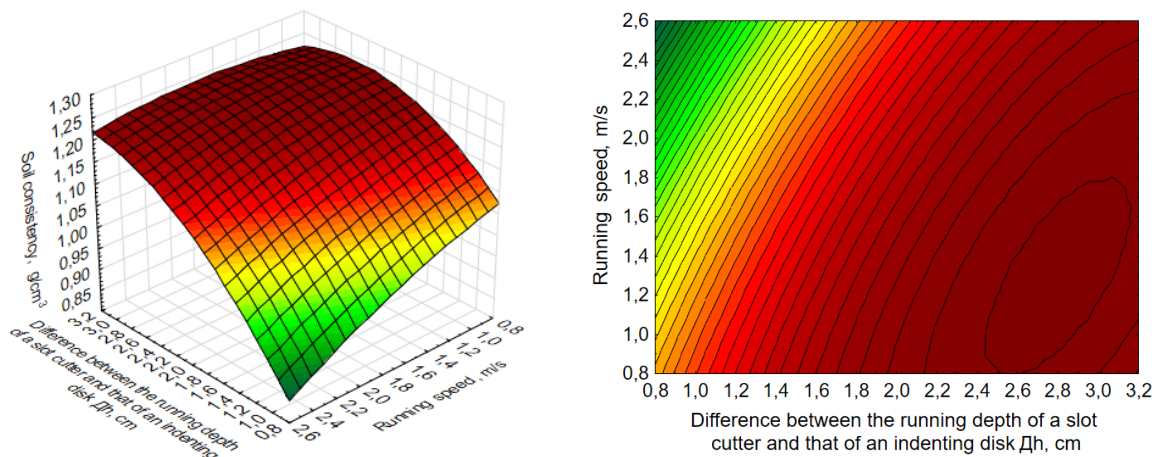
Fig. 2.10. Response surface of the change in soil consistency ρ depending on the parameter Δh and the running speed V

As a result of the conducted complete factorial experiment 3^2, a regression equation in natural values has been obtained.

The obtained regression equation determined the dependence between the optimization parameter of ρ and the following parameters: running speed of a coulter system V and the difference in the running depth Δh of a slot cutter and that of an indenting disk, which is the most influential parameter. According to the defined conditions the optimal values are the following Δh_{opt}=2.802 cm, V_{opt}=1.29 m/s.

Laboratory-field investigations aimed at determining the change in the variation coefficient of seed covering depending on the running speed of a planter and the running depth of a coulter, have been conducted. The investigations were conducted in field № 6 of Agronomic Research Station during corn planting. The soil was low-humic typical chernozem and its moisture content ranged within the limits of 18…22 %. The depth of seed covering was determined after the germination by means of measuring the ethylated part of a plant. The test was conducted with two factors at three levels. The running speed of a planter v was set at three levels: 1 m/s, 2 m/s and 3 m/s, coulter running depth h was set to be 3 cm, 5 cm and 7 cm. As a result of the obtained data processing, a response surface has been plotted (Fig. 2.11).

The regression equation that determines the dependence between the optimization parameter of W and the following parameters: the running velocity v of a coulter system and the depth h of seed covering. In this case, the speed h is the most influential factor.

In order to obtain comparative evaluation of a two-phase coulter system operation in the field conditions, variation coefficients of seed covering depth, the distance between the plants in a row, field germination capability of seeds and the average soil consistency in the area of seed location have been determined. All the indices were determined after the germination by means of measuring thirty sequentially placed plants in five different areas. The thirteenth (a two-phase coulter system) and the fourteenth rows of a planter have been compared. Fig. 2.11 represents the processed data of the measurements.
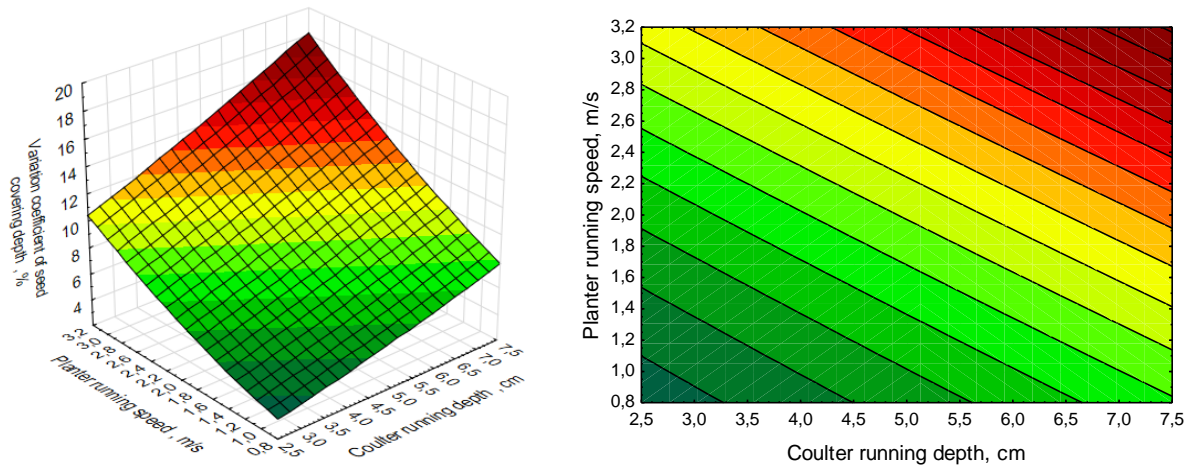
Fig. 2.11 - Response surface of the variation coefficient of seed covering depth *W* depending on the running speed of a planter *V* and the set running depth of a coulter *H*
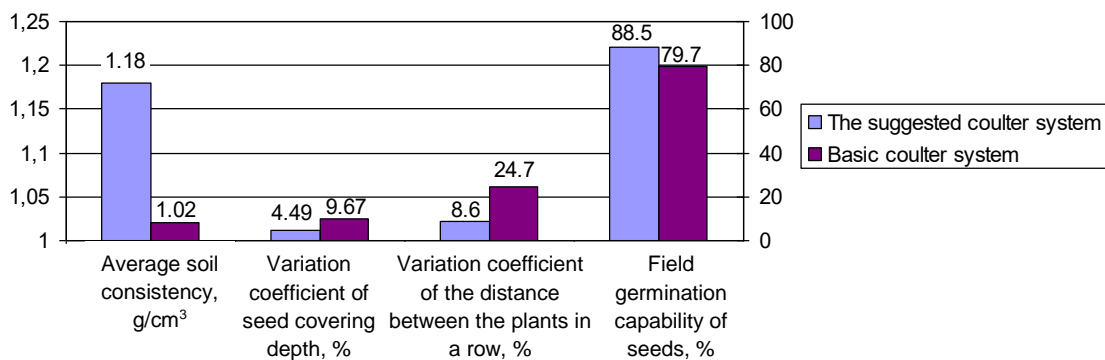
Fig. 2.12 - Value of the variation coefficient of seed covering depth, %; variation coefficient of the distance between the plants in a row, %; field germination capability of seeds, %; and the average soil consistency in the area of seed location, g/cm³

Fig. 2.12 shows that the variation coefficient of seed covering depth decreases in 2.1 times, the variation coefficient of the distance between the plants decreases in 2.9 times and field germination capability increases in 8.8 %. Here, the value of the average soil consistency in the area of seed location increases from 1.02 g/cm³, when planting is performed by means of a basic coulter system, to 1.18 g/cm³, when sowing is realized by the suggested coulter

31

system, which is within the range of optimal values 1.1…1.3 g/cm^3.

Conclusions to chapter 2

1.   The advanced way of the improvement of the process of sowing by means of applying a two-phase coulter system has been substantiated based on the conducted analysis of the existing ways and the facilities for sowing tilled crops.

2.   A mathematical functional model of a two-phase coulter system for row-crop planters has been developed and the simulation modelling of its operation has been conducted, which has made it possible to determine the influential factors for the set goal achievement. These main factors include the spring stiffness c_U=360 kg/cm, the damping coefficient d=120 N s/m, the time constant T=0.1 s, the decay coefficient ξ=0.1 and the amplification coefficient K=4.9 of a pneumatic drive control module.

3.   Theoretical and practical analysis of the interaction of the operating elements of a two-phase coulter system and the soil as an integral dynamic system has been conducted and the interrelation of a slot cutter and an indenting disk operation process has been substantiated. The optimal value Δh_{opt}=2.802 cm of the difference in the running depth of a slot cutter and that of an indenting disk, which is necessary for the formation of soil consistency within the limits of 1.1…1.3 g/cm^3 in the area of seed location, has been determined.

4.   Experimental investigations on the influence of the substantiated design parameters of a two-phase coulter system on seed distribution in the soil show that there is a decrease in the variation coefficient of seed covering depth in two times (up to 4.49 %), a decrease in the variation coefficient of the distance between the plants in almost three times (up to 8.6 %), an increase in

seed germination capability in 8.8 %, an increase in the average soil consistency in the area of seed location from 1.02 to 1.18 g/cm^3 compared to a basic coulter system.

CHAPTER 3. ENGINEERING MANAGEMENT OF TILLAGE EQUIPMENT WITH CONCAVE DISK SPRING SHANKS

The programme and the procedure of the experimental laboratory and field investigations of the shank parameters and the interaction process of a concave disk spring shank and a soil medium under ballast operating element loading, if there is a change in the travelling speed of a unit, have been developed. Estimation of the measurement results has been conducted based on the uncertainty concept. Under ballast loading (optimal reduced mass), the influence of the random components of a draft force on the process of interaction of a concave disk on a spring shank and the soil is at least one and a half times less. According to the results of the experimental studies, the dependences that show the influence of a unit speed and an operating element reduced mass on the drag force (energy indicator) and the elastic deflections of a shank (an agro-technical indicator) have been determined. Technical and economic assessment of the operating efficiency of tillage equipment according to the operating cost structure and based on practical implementation has been conducted.

There are significant quality changes taking place in modern agricultural production engineering caused by intensification of production processes together with efficient use of resources (*Vlăduţ D.I. et al, 2018*). According to these changes, it is necessary to improve agricultural equipment in order to provide their optimum process conditions with minimum energy consumption and improve reliability of individual parts and units (*Xiong P. et al, 2018*). The accomplishment of these tasks is of great importance for soil-tilling equipment, namely for disk headers, since they provide 60–80% of soil pre-treatment and basic cultivation (*Razzaghi E. & Sohrabi Y., 2016; Srivastava A.K. et al, 2016*).

The non-market harvest part left on the surface of a field is the determining factor for further performance of technological operations and developing requirements for operational devices, namely, for the development of disk tillage equipment with new design and technical characteristics in order to provide quality stubble cleaning, the decrease of energy consumption and the increase of operational reliability (*Vlăduţ V. et al, 2018*). The experience of using spring shanks of cultivator operating elements and their positive assessment opens up fresh opportunities for the improvement of disk tillage equipment reliability (*Dewangan A. et al, 2017*).

Operating elements arranged on spring shanks oscillate due to the irregularity of soil drag forces (*Gheorghiţă N.E. et al, 2018; Badegaonkar U.R. et al, 2010*). As a result, soil breakdown takes place with less energy consumption that decreases the rate of fuel consumption by tillage equipment *(Klendii M.B. & Klendii O.M., 2016*). A disk header with spring shanks can be better adjusted to a field surface texture and, thus, can provide the required quality of soil cultivation (*David A. et al, 2014*).

Thus, a relevant applied scientific task is the substantiation of the dynamic characteristics and the design parameters of the spring shanks of the disk operating elements of soil-tilling equipment *(Hevko B.M. et al, 2018; Hevko R.B.et al, 2017*).

The aim of the research – is to improve the operating efficiency of disk tillage equipment by means of substantiating their design parameters and the dynamic characteristics of operating element spring shanks.

The general research technique provided the use of modern methods of theoretical and experimental investigations, the theoretical substantiation was conducted with the help of the methods of mathematics, theoretical mechanics, oscillation theory, differential and integrated calculation (*Asejeva A. et al, 2013*). The experimental research was conducted in the field environment based on standard practices and the specific techniques developed by the author. The

procedure of measuring elastic deflections of the operating elements provided for the use of the information and measurement system and the method of strain measurement (*Tutunaru L.F. et al, 2014*). The research data processing was conducted with the help of mathematical methods of statistics. The method of regression analysis was applied.

The design and engineering characteristics of disk tillage equipment are improved in case of the arrangement of disk operating elements on spring shanks due to their oscillations. Substantiation of the design parameters and the dynamic characteristics of shanks as a system "soil – disk – spring shank" allows for improving the efficiency of equipment operation in terms of operational reliability and energy consumption.

The analysis of the existing scientific research suggests that the significant influence on the operation process of a tillage unit on a spring shank is characterized by the models that take into account the influence of empirical factors and design parameters with coefficient matrices. The application of complex models makes it almost impossible to solve the problem of the description of a spring shank with a concave disk movement (*Barwicki J. et al, 2012*).

Thus, it is necessary to solve the applied scientific task – substantiate the dynamic characteristics and the design parameters of a spring shank of disk tillage equipment (*Constantin N. & Cojocaru I., et al, 2012*).

The programme of the experimental investigation on spring shanks of concave disks allowed for:

- substantiating the measuring diagram and estimating the dynamic characteristics of a concave disk spring shank;

- determining the design parameters and the dynamic characteristics of a spring shank;

- investigating the influence of the dynamic characteristics of an operating element spring shank on the efficiency of equipment, taking into account the randomness of soil reaction (field research);

- comparing the theoretical and the experimental data and their compliance.

The scheme of the measuring system, taking into account the information flow of the changes in soil properties, was substantiated (*Galat U.N. & Ingale A.N. et al, 2016*). There were KF-5P1 full-bridge strain gauge sensors arranged on a shank and they were connected through SPIDER-8 analog-to-digital converter with CatMan Express 4.5 software (*Trokhaniak V.I., et al, 2019*). The converter performed scanning with a frequency of 250 Hz, analog-to-digital signal conversion and digital array generation as a *.xls file (*Gheres M.I., 2014*). The sensors were cable connected to the equipment and protected from the effect of inferences (*Rogovskii I.L. et al, 2019*). In order to conduct experimental research (testing and assessment of spring shank performance), an experimental plant was developed (Fig. 1). The information obtained as a result of the laboratory experiments was presented in the form of calibration curves of "deflection" and "loading" (*Rogovskii I.L. et al, 2019*). Simulation of the change in spring shank dynamic characteristics was performed by applying lumped mass to an operating element mounting and bearing unit (impact factor at the following levels: reduced mass and mass plus added weight) (*Rogovskii I.L. et al, 2019*). The investigation was conducted with the use of a multilevel experiment (*Constantin N. & Cojocaru I., 2008*). The peculiarity and the advantage of this pattern is the most complete estimation of the investigation process (Table 3.1). The increase in the level of external impact (by means of increasing travelling speed) determines the level of influence on a spring shank and ballast loading determines the sublevel.
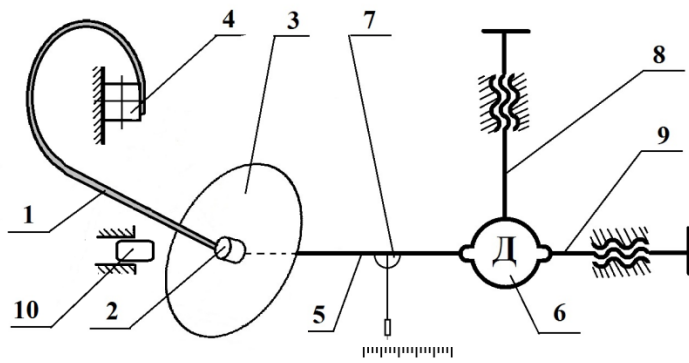
a)   b)

Fig. 3.1 - An experimental plant (technical equipment) for testing and evaluation of spring shank operation efficiency

a – structural diagram; b – general view; 1 – spring shank of a concave disk; 2 – bearing unit; 3 – operating element (concave disk); 4 – fixed base; 5 – wire rope; 6 – dynamometer; 7 – level; 8 – screw-type vertical regulator; 9 – screw-type horizontal regulator; 10 – percussive mechanism for disturbing shank equilibrium.

Table 3.1

Investigation Pattern

Impact factors				Optimization Parameters					
Travelling speed, v [km/h]		**Reduced mass, m [kg]**		**External impact / draft force, [N]**		**Deflection [mm]**		**Generalized coordinate [deg.]**	
Level (total levels)	Variability interval	Level (total levels)	Variability interval	Average value	Mean square deviation	Average value	Mean square deviation	Average value	Mean square deviation
1 (5)	2	30	0.5 (2)	F	F_{MSD}	δ	δ_{MSD}	λ	λ_{MSD}

Process parameters were recorded in real time in the course of unit operation rounds with the predefined sampling period. Recording areas under steady-state loading conditions were considered. The defined digital array obtained from the analog-digital converter contained several thousand values of the variable under study. If there are many observations, the "n" testing error is less than 0.5 – 1%. According to "loading" calibration curves, the digital array of the external impact values was processed and statistical process parameters were determined.

In order to process the experimental data, the methods of mathematical planning and mathematical statistics were used. The estimation of the research findings was performed on the basis of the uncertainty conception describing the dispersion of the values, which could be reasonably assigned to the variable to be measured.

a)   *b)*
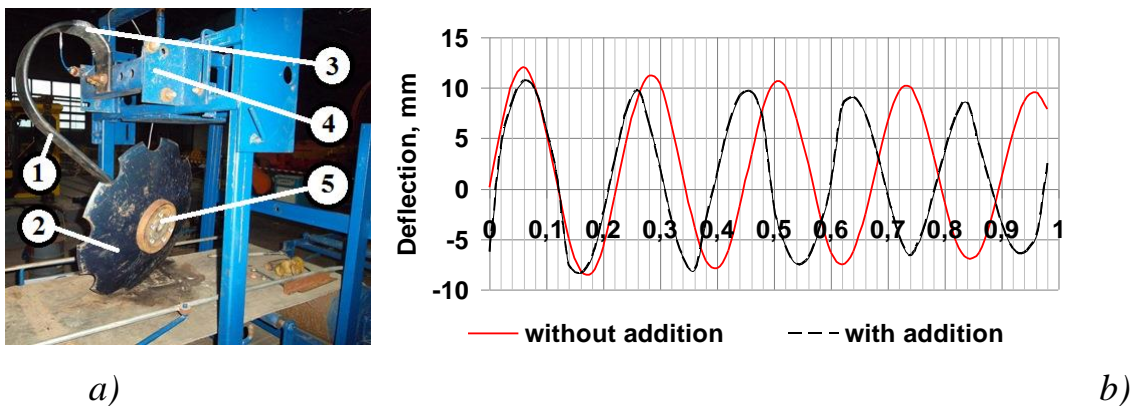
Fig. 3.2 - Realization of laboratory investigations: a – exterior of a spring shank with ballast loading while determining the reduced mass; *b* – free spring shank oscillations

1 – a spring shank of a concave disk; 2 – an operating element (a concave disk); 3 – resistive strain gauges on the surface of a spring shank; 4 – a fixed base; 5 – ballast loading.

The procedure of determining the design parameters and the dynamic characteristics of spring shanks was investigated using the suggested fabricated

and approved design of the experimental plant, the values of the reduced mass (Fig. 3.2, a) were determined, a load-deflection curve was defined and free spring shank oscillations were observed (Fig. 3.2, b).

a)   *b)*
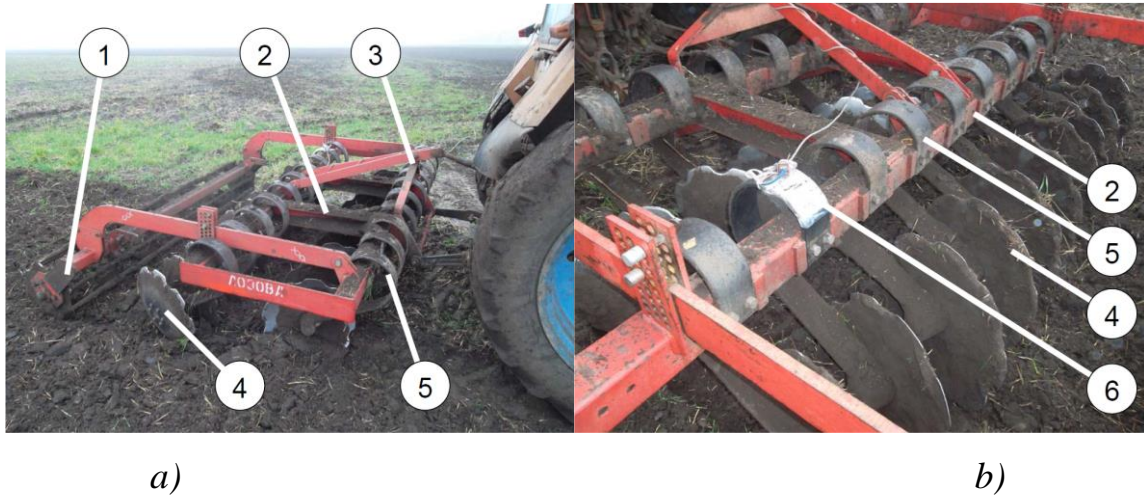
Fig. 3.3 - General view of a disk header with spring shanks

a – general view of the unit; b – spring shanks under study; 1 – roller; 2 – unit frame; 3 – hitch linkage; 4 – operating element (a concave disk); 5 – spring shank; 6 – resistive strain gauges on the surface of a spring shank.

Field experiments were conducted in the process of breaking grain crop fallen seeds germination (second de-husking). The experimental spring shank was attached to the frame of DL-2.5 unit (Fig. 3.3).

It was determined that the interaction process of a disk operating element on a spring shank and the soil is unsteady and its statistic performance varies

with time (Fig. 3.4). Process unsteadiness is caused by quick changing conditions of operation in a soil medium and the influence of meso- and micro-relief of a field surface.

The probability laws of the instantaneous indicator values of the interaction process of the soil and an operating element on a spring shank (Fig. 3.4, b) show two vertices in the distribution series, which proves the unsteadiness of the phenomenon under study, the degree of the distribution asymmetry is within the range from 0.1 to -0.1.

a) b)

c) d)
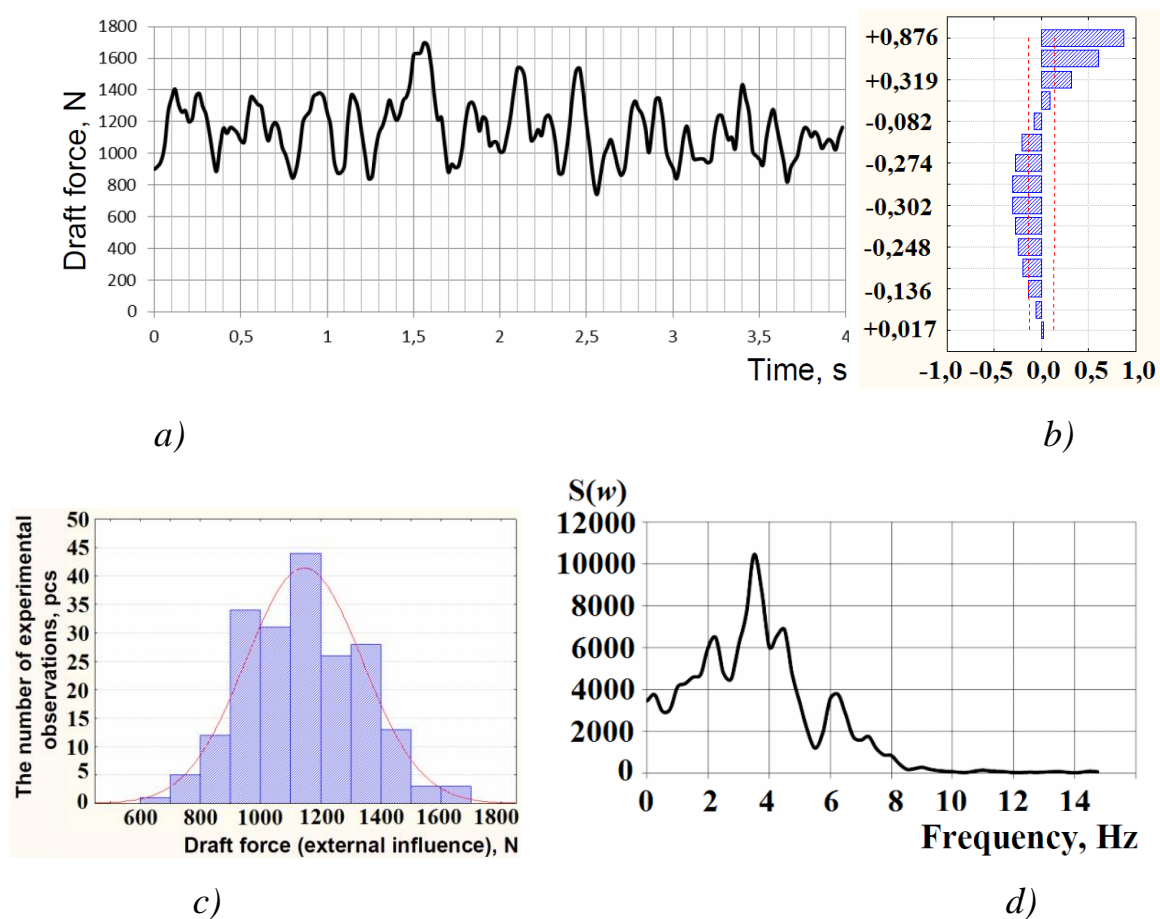
Fig. 3.4. Statistical characteristics of the interaction process of an operating element on a spring shank and the soil

a – behaviour of spring shank response to the external impacts; b – autocorrelation function; c – density of distribution; d – spectral analysis.

The shape of the correlation function (Fig. 3.4, c) meets a zero value that corresponds to the cycle of latent periodical vibrations; however, since the influence of random noise is significant, if there are considerable shifts, the value of the correlation coefficient tends to zero.

The conducted spectral analysis (Fig. 3.4, d) shows that shank oscillations is a mixed random process with a polyharmonic deterministic component.

The investigation results prove that there is a change of spring shank response to a soil medium under additional operating element loading. The increase of the draft force was $F = 1180 - 1300$ N of the device speed without additional operating element loading, which was equal to 17%, and under additional loading it was $F_{load} = 1170 - 1240$ N or 11%. If a unit travelling speed is 4 m/s, the difference between additional loading options is equal to 10% (Fig. 3.5, Fig. 3.6).

Vibroactivity $F_{MSD} = 180 - 290$ N of a spring shank without additional loading increases almost linearly and within the speed range from 1.9 to 4 m/s it increases for 78%, and under additional loading it increases for 136% – in 2.36 times. The increase of operating element vibroactivity influences a soil medium and decreases its resistance to breaking down, which explains the decrease of the drag force under additional loading.

Estimation of the process-dependent parameters of a disk header with spring shanks was conducted according to the statistical characteristics of elastic deflections in the process of interaction of an operating element and the soil (Fig. 3.7, Fig. 3.8).

Mean-square spring shank deflection describes the uniformity of tillage depth provided by an operating element, according to the reference conditions the non-uniformity is $\sigma = 15$ mm. That is to say, the increase of a unit's energy efficiency (draft force decrease) is limited by the qualitative process flow indicator at the speed value of 4 m/s.
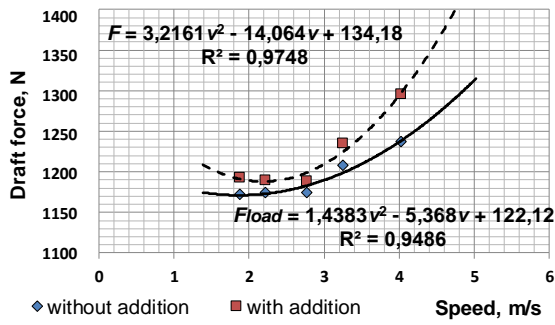
Fig. 3.5. Draft force-vs-unit travelling speed characteristic curve (according to calibration curves)
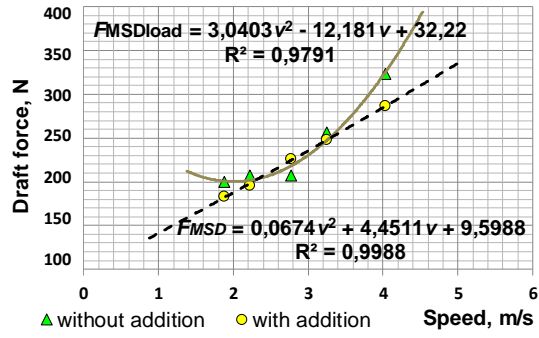
Fig. 3.6. Mean-square draft force deviation-vs-unit travelling speed curve
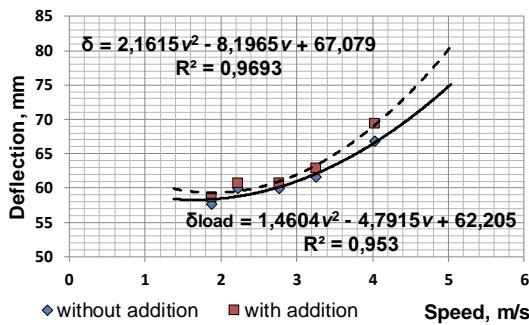
Fig. 3.7. Average deflection value-vs-unit travelling speed curve (according to calibration curves)
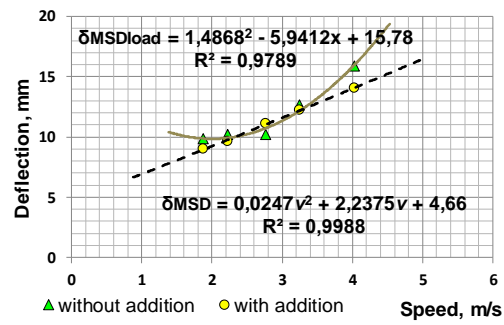
Fig. 3.8. Mean-square value of shank deflections-vs-unit travelling speed characteristic curve $\sigma = f(\delta)$

Based on the minimum draft force criterion, the aimed speed rate is 10 km/h, and the value of draft force is equal to approximately 12 kg per one shank.

When comparing the uncertainties of the measurements, it can be concluded that, if there is ballast additional operating element loading, the influence of random components on the interaction process of a concave disk on a spring shank and the soil is at least one and a half times less.

The theoretical and the experimental investigation results on the change of the generalized coordinate during process performance were compared (Fig. 3.9), the difference in the values under various unit speed rates increases with speed gain, the decrease rate at the speed of 4 m/s is by 1.33% greater

compared to the theoretical dependence. The average deviation of the experimental data (rate 2.77 m/s) from the theoretical ones is equal to 0.164 deg., which does not exceed the expanded measurement uncertainty.

a)   *b)*
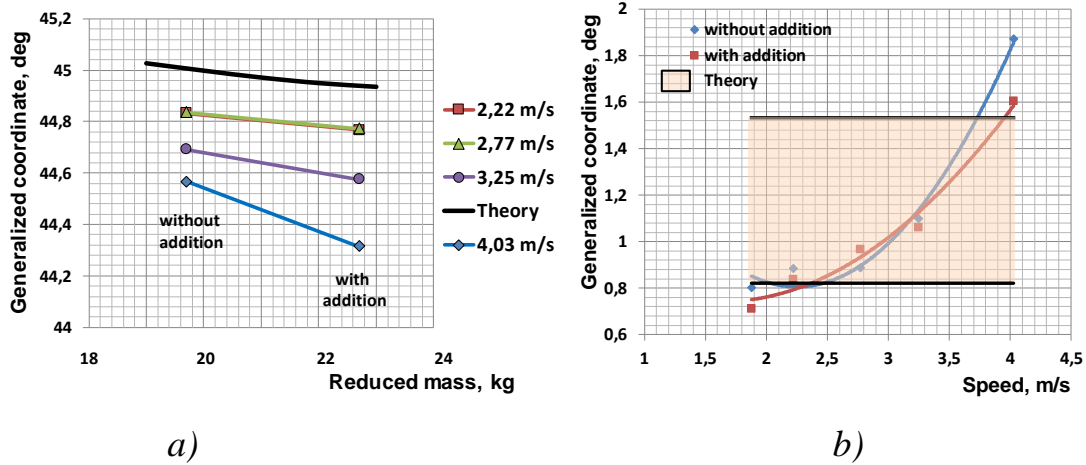
Fig. 3.9. Comparison of the theoretical dependences and the experimental data

a – generalized coordinate value in dynamic equilibrium;

b – generalized coordinate value as a mean-square deviation from dynamic equilibrium.

When comparing the theoretically obtained dependences of the generalized coordinate deviations and the mean-square values from the experimental data, it is obvious that there is their significant compliance according to the range of values. The lower limit to the range of values obtained theoretically (Fig. 3.9, b) approximates the experimental data at the rate of 2.22 m/s, the upper limit approximates at the rate of 3.25 m/s, here, the value deviations exceed the uncertainty of measurements by 4.3 and 1.7 times, respectively. Thus, it can be concluded that deviations from the dynamic equilibrium are determined by the influence of a soil medium, however, if the reduced mass is increased, the uncertainty decreases – the interaction process of a concave disk on a spring shank and the soil acquires 2.5 times better controllability.

Conclusions to chapter 3

1. The dependences obtained from the experimental investigations prove that there is a change in the interaction characteristics of an operating element on a spring shank and a soil medium on condition of the reduced mass change. While in operation, the increase of the draft force produced by the change of the speed from 2 to 4 m/s is equal to 17% for a unit equipped with typical spring shanks and it is equal to 11% in case of the shanks with the substantiated reduced mass indicators, which proves the weightage of the reduced mass influence on process performance. If a unit speed is 4 m/s, the advantage of the spring shanks with the substantiated parameters makes the difference of 5%, or 60 N per each shank.

2. Due to the use of the improved procedure of estimating measurement results it has been determined that the influence of random components on the interaction process of the system "soil – disk – spring shank" is at least one and a half times less in case of the operating elements with the substantiated reduced mass. The mean difference of the experimental and the theoretical data according to a shank deflection parameter is equal to 0,164 deg. (speed rate 2.77 m/s), which does not exceed the permissible measurement uncertainty.

3. The recommended rational parameters of spring shanks, which have been determined according to the investigation results, are the following: the rigidity (20 – 40 kN/m), the reduced mass (10 – 30 kg), the frequency (1.6 – 4 Hz and 3.5 – 7 Hz) and the amplitude (1 – 9 deg. and 2.5 deg.) of oscillations. It has been determined that the use of spring shanks with the defined parameters allows for decreasing energy consumption in the process of soil tillage by a disk operating element by 7% without degrading the quality of process performance, compared to a typical spring shank with the parameters that are substantiated only in terms of the functional need to protect an operating element from overloading.

CHAPTER 4. EXPERIMENTAL STUDY ON THE PROCESS OF GRAIN CLEANING IN A PNEUMATIC MICROBIOCATURE SEPARATOR WITH APPARATUS CAMERA

In the article the analysis of existing designs of flat-row separators is carried out. Hypotheses are put forward, which allow to eliminate existing disadvantages of constructions. Their essence is reduced to the feeding of grain perpendicular to the direction of air flow. This is provided by the slope of the walls of the aspiration canal at an angle close to 45°, so that the aspiration channel acquires the shape of a truncated hollow cone, coaxially inside a scattered installed, in the form of a truncated cone, which is turned with a larger base upward. The equation of regression of efficiency and clarity of the process of pneumatic separation from the regime parameters of the aspiration chamber is obtained. The regression equation of the purification and precipitation of light impurities has been obtained by an improved aspiration chamber.

In today's conditions of a market economy of Ukraine, there has been a tendency to change the ownership of land and change the structure of crop areas [1]. This contributed to the emergence of farms that cultivate small areas of grain crops [2]. For the processing of cereal streams coming from these crops, farms use mobile grain cleaning machines that perform preliminary and basic purification [3]. It is mainly mobile flat-panel machines with productivity from 10 t/h to 30 t/h [4].

The disadvantages of their work include the allocation of grain dust and light impurities in the working space around the machine, which complicates its operation and worsens ergonomic performance [5]. Therefore, the search for new technical solutions for the utilization of grain dust and light impurities on mobile flat-panel machines is an urgent task. Universal pneumatic centrifugal grain separators are widely used in farms of Ukraine as machines of preliminary

and primary purification due to their high specific productivity and insignificant specific material content. Their use allows to reduce the need for production space three times as compared with traditional separators. As a rule, universal pneumatic centrifugal separators consist of two parts: pneumatic centrifugal and vibration center-resonator. With high productivity and compactness, the work of these separators showed an inadequate purification of the grain mixture from light impurities (floor, parts of stems, etc.), which is due to the disadvantages of the design of the pneumatic centrifugal part. Therefore, the actual scientific and technical task is the further technical improvement of the pneumatic centrifugal part of the pneumatic centrifugal grain separator.

Most foreign firms (Miag (Germany), Buhler (Switzerland), Hept-Carter (USA), etc.) do not install aspiration chambers on their separators, and the separation and concentration of light impurities from separators are performed centrally in a separate device. With such a system, it is difficult to tailor the isolation individually to each separator [6]. In addition, this allocation system is possible when the farm has a certain system of cleaning machines, which in the conditions of the farm is not always acceptable.

Aspiration chambers of two types are most often installed on mobile flat-row separators: in the form of a bunker with a partition for changing the direction of air flow – a chamber of gravitational type; centrifugal chamber with a central tube and a spiral or inclined cavity for the east of the isolated admixtures. Studies have shown [7] that chambers of the centrifugal type have the same efficiency with cameras of gravity type and when installed on mobile grain cleaning machines shift the center of gravity, which increases the probability of a turning over when driving. No significant studies have been carried out on the use of gravity aspiration chambers on mobile flat-row separators, which makes the research relevant.

Studies [8] found that the reason for poor cleaning of the grain mixture from light impurities is the inappropriate feeding of grain into the ascending air

flow by the spreader. During the process, the spreader feeds the grain mixture with a dense layer in the air stream [9]. Since the blades are installed in the lower part of the serial spreader, this contributes to the uneven (perimeter) feeding of the grain to the aspiration channel due to the fact that the blades guide the grain in the form of "jets", thereby providing zones with increased grain density [10]. Another disadvantage of the pneumatic separating part of the pneumatic centrifugal separator is the swing in the duct connection zone with the upper cylindrical part of the aspiration chamber, which reduces the air flow velocity in certain areas of the chamber.

In [11], hypotheses were put forward to eliminate these shortcomings. Their essence is reduced to the feeding of grain perpendicular to the direction of air flow [12]. This is ensured by the slope of the walls of the aspiration channel at an angle close to 45°, so that the aspiration channel acquires the shape of a truncated hollow cone, coaxially inside a scattered installed, in the form of a truncated cone, which is reversed with a larger base upward [13].

Theoretical studies [14] substantiated the basic parameters of the operating mode of the pneumatic separating part of the pneumatic centrifugal separator. However, most provisions require experimental confirmation [15].

The purpose of the research is to detect and evaluate the influence of the regime parameters of the improved air separation part on the qualitative parameters of purification of the grain mixture.

According to the hypotheses and the theoretical propositions put forward in [7], there were developed 2 clatterers (Fig. 1 a, b). The first one is a truncated cone, which is backed up by a larger base, up to a diameter of 720 mm. Moreover, much of the side surface of the spreader is made of rubber and has a distribution cone in the center (Fig. 4.1a). The second spreader, unlike the first one, has a narrow rubber upper part of the lateral surface, which is attached to a conical metal part having a blade (Fig. 4.1 b) but does not contain a distribution cone in the center. The third spreader is similar to a serial design

(Fig. 4.1 c).

Experimental studies of the described scatterers were carried out in an improved aspiration chamber (Fig. 2 a).

| *a* | *b* | *c* |
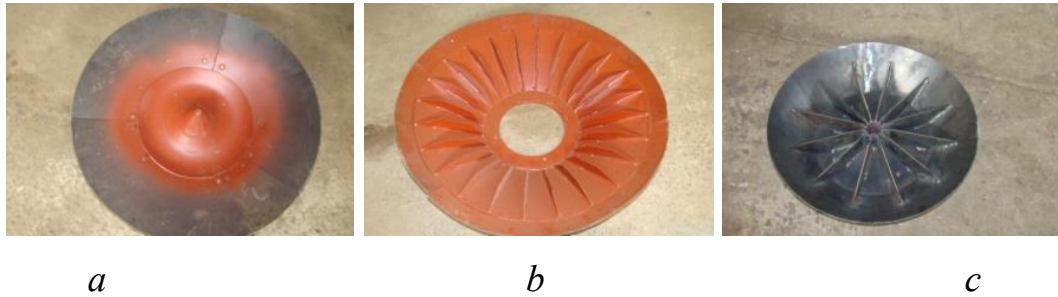
Fig. 4.1. The general view of the spreaders, which carried out experimental research:

a – conical scoop without blades; b – conical spreader with shoulder blades;

c – serial spreader

| *a* | *b* |
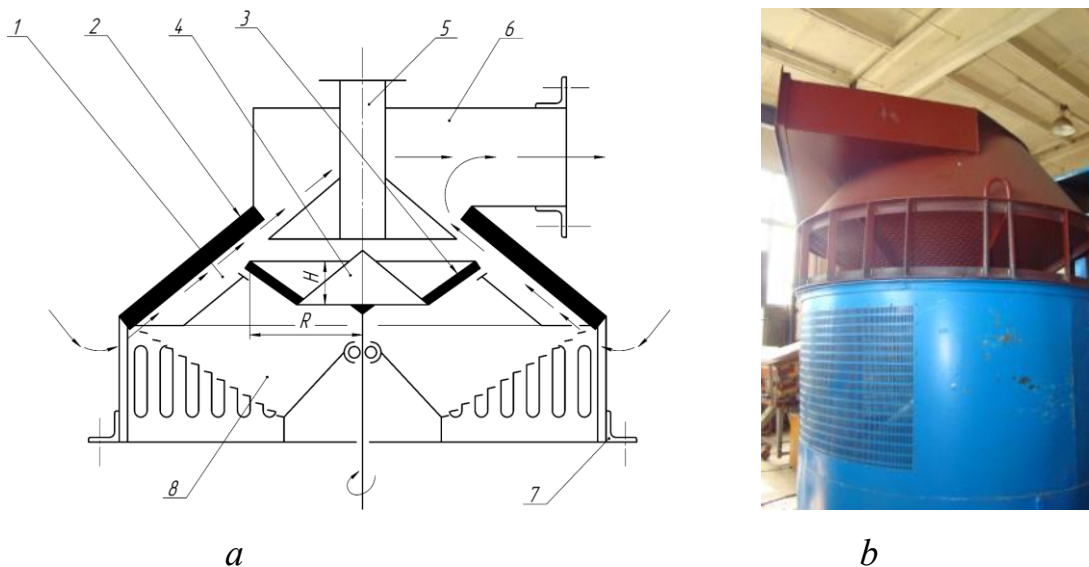
Fig. 4.2. The design scheme is suited to the aspirating camera (a) and the illegal camera at the warehouse of the experimental installation (b):

1 – ring channel; 2 – internal channel surface; 3 – the inside of the grain spreader; 4 – grain spreader; 5 – dispenser; 6 – pipe; 7 – flange;

8 – aero-cleansing

It is a designconsisting of a ring channel *1* formed by two conical walls (Fig. 4.2 a). In the center of the aspiration chamber there is a spreader *4* over

which the dispenser *5* is located (Fig. 4.2 a). The connector *6* is connected to the upper part of the ring channel *1*. A flange *7*, representing a cylindrical ribbed surface and an air gap *8*, representing the louvre cone, is attached to the bottom of the annular channel.

To carry out experimental studies, the aspiration chamber was improved on an experimental installation (Fig. 4.2 b).

Technological process on the advanced aspiration chamber is as follows. Grain material is fed through the dispenser *5* to the spreader *4*, where, under the action of centrifugal force, it moves to the edge of the inner surface of the grain thrower *3* and is introduced at an initial rate into the air stream passing through the annular channel *1*. Light impurities, under the influence of aerodynamic force, are captured by air flow and through the air line 6 are removed outside the aspiration chamber. The purified grain, reflecting from the inner wall of the channel *2*, falls on the aerosol hole *8*. When leveled along the air deflector *8*, the grain is further purified by air jets blowing from the louver openings and supplied for additional purification.

Experimental studies were carried out on the subject of the influence of the regime parameters of the aspiration chamber: q – supply of grain material; v – speed of ascending air flow; n – frequency of rotation of the spreader on qualitative parameters of air separation: efficiency of separation E and clarity of Z separation.

The efficiency and clarity of separation of the improved aspiration chamber were determined by the degree of discharge of garbage impurities, that is, the relative content of the passage fraction. To achieve the determination of the influence of the above-mentioned regime parameters on qualitative parameters of air separation, the method of a multivariate experiment was applied. A three-factor experiment was conducted on the D-optimal Boxx-Benick plan. Guided by the earlier theoretical studies of the process of air separation of grain, it is possible to establish the most influential factors and

determine the limits of their variation. These factors include: the rate of ascending air flow v, the grain supply q, the spin speed n. The values of the proposed factors are given in Table 4.1.

Table 4.1

Levels of independent factors of experimental research

Name, designation and dimension of influential factors	Levels of variation of factors			Variable interval
	Upper (+1)	Zero (0)	Lower (-1)	
The rate of ascending air flow, v, m/s	9	7	9	2
Feeding grain material, q, t/h	25	15	5	10
Frequency of rotation of the spreader, n, rpm	160	130	100	30

For the optimization parameter, the efficiency of separation in percent E and the clarity of the pneumatic separation Z are accepted. Experimental studies were carried out on wheat grains.

In order to improve the effect of purification from light impurities and their concentration for an experimental flat-line separator, an aspiration chamber was created as a result of research carried out, the general appearance of which is shown in Fig. 4.3. It is a structure consisting of hull, a bunker, pit latches, guiding channels, a siege chamber, shells, cleaning shelves, a fan, a screw and output channels.

a   *b*

Fig. 4.3. Design of the modernized aspiration chamber of the flat-radiator separator and its general appearance (a, b).

The camera was installed above the lattice states of the experimental sample of the flat-line separator.

The technological process of work on it was carried out as follows. Grain mixture was driven from the bunker to pods.

Slipping down the shelf, the grain with light impurities falls into the sloping air flow created by the fan. Due to its weight and small coefficient of aerodynamic resistance, the grain falls down to the subsequent purification by sieve, and light impurities captured by air flow, due to a higher coefficient of aerodynamic resistance, are fed along the guide channel to the siege chamber.

In the siege chamber there is a turning of the air flow due to the shape of the shell, resulting in a decrease in the flow rate in the zone of rotation of the air stream. When the speed of air flow decreases, aerodynamic force decreases, therefore, light impurities are deposited and collected in the harvesting shelves to the screw, which they are transported to the outlet channel.

To verify the operation of the aspiration chamber, a one-factorial experiment was conducted on the effect of the performance of the flat-panel

separator q on the efficiency of purification *E*, % and precipitation *Ek*, % of light impurities.

An overweight of 60 kg with litter with light impurities of 3% was passed through an aspiration chamber. The valve on the bunker regulated the productivity of the flat-rust separator in the range of 0.4-9.6 t/h. To account for the light impurities that were captured by the fan impeller, a 2-meter-long sack was put on the fan feed line.

The efficiency of cleaning E was calculated by the formula:

$$E = \frac{m_1 + m_2 - m_3}{m \cdot \varepsilon} \tag{4.1}$$

where *m* – a lot of weightlessness, kg; ε – turbidity, %; m_1 – mass of light impurities allocated aspiration chamber, kg; m_2 – mass of light impurities in the bag, kg; m_3 – the mass of grain in the segments separated by a bag and aspiration chamber, kg.

The efficiency of precipitation of light impurities *Ek* was calculated by the formula:

$$Ek = \frac{m_1}{m_1 + m_2} \tag{4.2}$$

The plan for implementing the experiment is presented in Table 4.1.

After analyzing the significance, reproducibility and adequacy, the following regression equations for efficiency and clarity of pneumatic separation for the 3 types of spreaders were obtained.

Equation for separation efficiency (4.3, 4.4):

$$\begin{aligned} E1 &= -68.79 - 0.2 \cdot n - 2.29 \cdot q + 44.6 \cdot v + 0.063 \cdot q^2 - 2.56 \cdot v^2 \\ E2 &= 22.38 + 7.38 \cdot v - 0.011 \cdot q \cdot n + 0.027 \cdot q^2 \\ E3 &= -49.75 - 0.43 \cdot n - 0.41 \cdot q + 36.45 \cdot v + 0.053 \cdot n \cdot v - 2.53 \cdot v^2 \end{aligned} \tag{4.3}$$

$$\begin{aligned} Z1 &= 73.83 + 9.31 \cdot v - 0.83 \cdot v^2 \\ Z2 &= 68.9 - 0.49 \cdot q + 11.49 \cdot v + 0.083 \cdot q \cdot v - 1.07 \cdot v^2 \\ Z3 &= 72.12 + 0.285 \cdot n - 0.001 \cdot n^2 + 3.64 \cdot v - 0.006 \cdot n \cdot v - 0.27 \cdot v^2 \end{aligned} \tag{4.4}$$

Analysis of the data of the regression equations shows that the rate of ascending air flow v has a significant effect, less importance is the supply of grain q and the influence of the spin rotation frequency n is negligible.

On the basis of the regression equations (4.1) graphic dependences (Fig. 4.4) of separation efficiency E from the air flow velocity v (at $n = 130$ rpm, $q = 15$ t/h) and from the feed grain material q (at $n = 130$ rpm, $v = 7$ m/s).

| a | b |
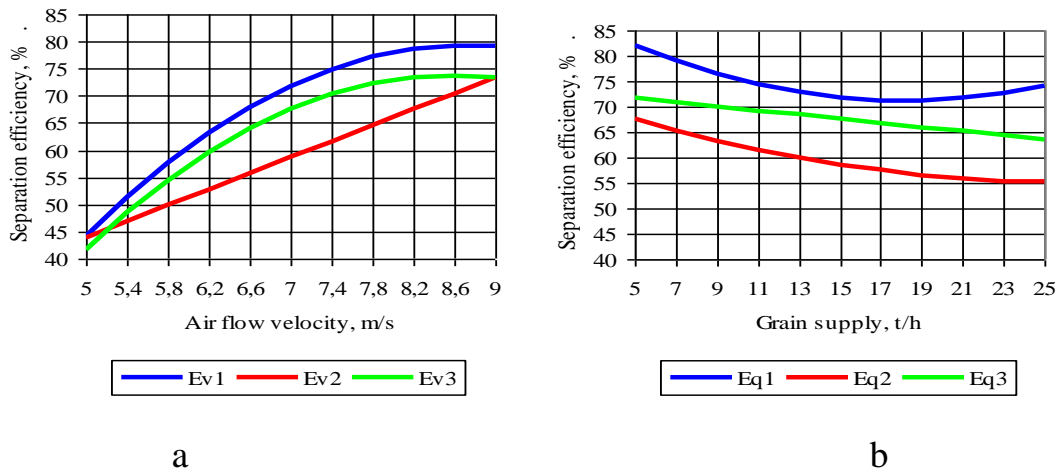
Fig. 4.4. Graphic dependences of separation efficiency E on air flow velocity

v (a) and grain supply q (b):

1 – conical scatterer without vanes; 2 – conical spreader with shoulder blades;

3 – serial spreader

The analysis of dependency data shows that the increase in the air flow rate v increases the efficiency of the process of pneumatic separation E (Fig. 4.4 a) and reduces the efficiency of the process of pneumatic separation E with an increase in the supply of grain q. The greatest efficiency is achieved when using a conical spatula without blades. This is due to the fact that this spreader does not create so-called "jets" zones of local grain condensation. Thus, this is confirmed by theoretical hypotheses. The highest efficiency of 80% is achieved at an air flow velocity of $v = 8.7$ m/s and a feed of grain material $q = 6$ t/h by a conical scoop without blades. The serial spreader showed the

lowest efficiency, since it does not provide perpendicular input of grain into the air stream.

On the basis of the regression equations (4.2) graphic dependences (Fig. 4.5) of the separation Z on the air flow velocity v (at $n = 130$ rpm, $q = 15$ t/h) are constructed.
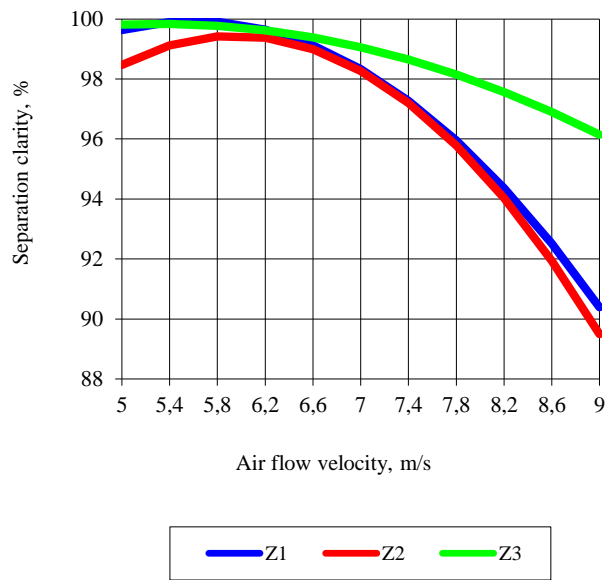
Fig. 4.5. Graphic dependencies of separation clarity Z on air flow velocity υ:
1 – conical scatterer without blades;
2 – conical spreader with shoulder blades; 3 – serial spreader

These dependences show that with increasing airflow separation υ decreases clarity Z greatest clarity separation shows conical spreader with blades. This is due to the fact that the spreader with a significant diameter 720 mm and thanks to the effect of "jets" that cause the conditions set blades capture airflow grain particles much worse than when grain is introduced into the airflow serial spreader (smaller diameter 540 mm) or conical scoop without blades (Fig. 4.1).

Summarizing the graphic dependencies shown in Fig. 4.4-4.5, we can conclude that the most rational design is a conical scraper without blades. In order to establish a rational velocity was built comparative graph, which built on

two axes *Z* clarity and separation efficiency *E* for *n* = 130 rpm, *q* = 15 t/h (Fig. 4.6).
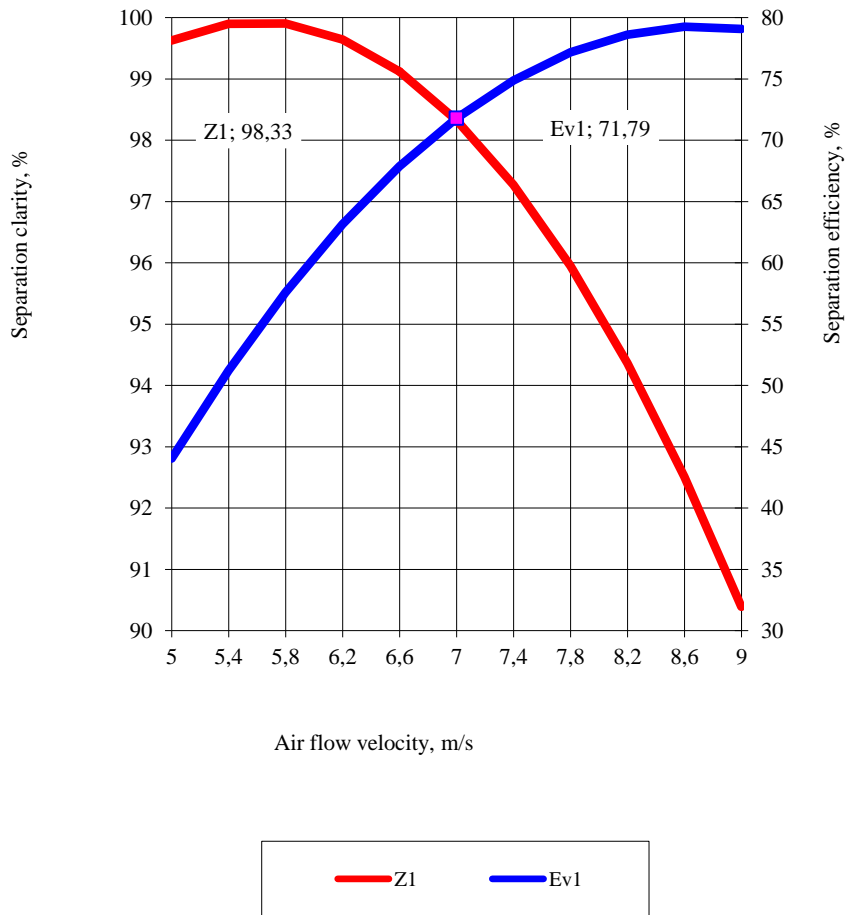
Fig. 4.6. Comparative graph of Z-resolution and separation efficiency E from the air flow velocity υ for a conical scoop without blades.

As a result, the intersection of the *Z*-graphs and the separation efficiency *E* gives the optimum point, which has the highest efficiency and the highest degree of separation. The highest separation efficiency *E* = 71.8 % and the highest separation clarity *Z* = 98.3 % can be achieved simultaneously at air flow velocity *υ* = 7 m/s.

The experimental data of the modernized aspiration chamber were amalgamated by a polynomial of the second degree. The equation of regression

for the efficiency of cleaning E and the efficiency of precipitation of light impurities by an aspiration chamber from the performance of a flat screen separator q took the form:

$$E = 72.223 - 7.1473 \cdot q + 0.2641 \cdot q^2 \qquad (4.5)$$

$$Ek = 68.473 + 3.9712 \cdot q - 0.5033 \cdot q^2 \qquad (4.6)$$

On the basis of equation (4.5) and data Table 4.2 a plot of the dependence of the purification efficiency from light impurities E on the separator q efficiency (Fig. 4.7) was constructed.

Table 2

Levels of independent factors of experimental research

Separator productivity, t/h	Efficiency of cleaning from light impurities,%	Efficiency of precipitation of light impurities,%
0,4	69,3	70,0
4	49,6	76
4,4	44,2	76,5
9,6	28	60,2

The graph shows that with increasing productivity q the effectiveness of pneumoconference is reduced, which is explained by the deterioration of the conditions for the allocation of light impurities. The maximum separation efficiency of 70% can be achieved with minimum performance values.
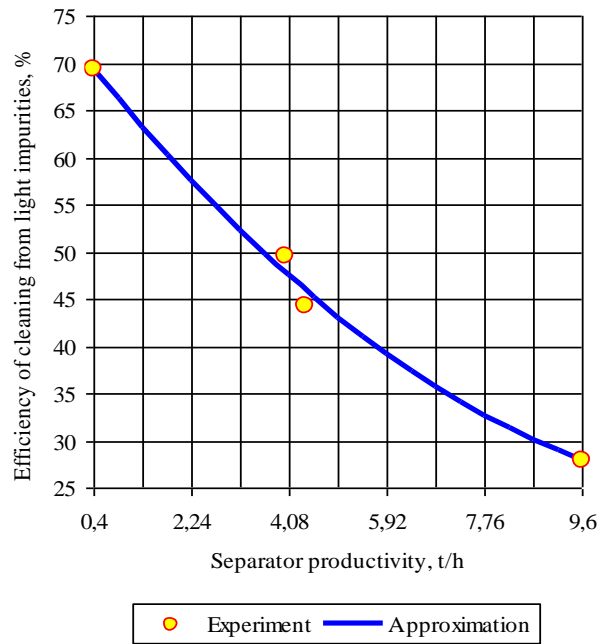
Fig. 4.7. Graph of the dependence of the technological efficiency of the air separation E, % of the modernized aspiration chamber on the performance of the separator q
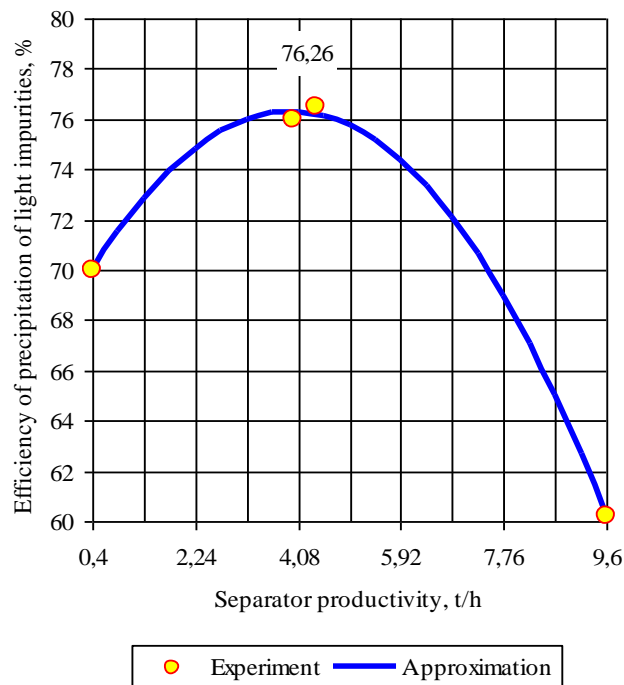
Fig. 4.8. Graph of the dependence of the technological efficiency of precipitation of light impurities Ek, % aspiration chamber of the flat-line separator on the efficiency of the separator q

On the basis of equation (4.6) and data Table 4.2 a plot of the dependence of the precipitation efficiency of the light impurities *Ek* on the separator productivity *q* (Fig. 4.8) was constructed.

An analysis of this graph shows that the function has an extremum at 3.95 t/h. This value of productivity corresponds to the highest value of precipitation efficiency of 76.26 %.

This zone can be explained by the fact that when the productivity of the flat-line separator q increases, the amount of isolated light impurities is decreased, that is, their concentration (Fig. 4.8).

Reducing the concentration of light impurities improves the conditions of deposition, but with increased concentration of light impurities in the air stream, the air flow velocity between the particles increases and as a consequence of the decrease of the air flow rate at the turning in some zones is inadequate. Further lowering of the concentration of light impurities in the air stream also negatively contributes to precipitation, as at a small concentration of light impurities in the air stream, the dynamic pressure, which limits the lower boundary of the air flow velocity at the turning point, increases.

Conclusions to chapter 4

The experimental researches of the advanced aspiration chamber using various types of scatterers have been confirmed by theoretical researches and hypotheses. New equations of regression of efficiency and clarity of the separation process, as well as their graphical interpretation, are obtained. The rational use of a conical spatula without blades has been proved experimentally. It was established that the optimal mode parameters of the aspiration chamber, which increase the separation efficiency (76-78 %) and the separation severity (98,0-98,8 %), are within:

-   air flow velocity $v = 7.2\text{-}7.4$ m/s;

- grain delivery q = 6-7 t/h;

- frequency of rotation of the spreader n = 100-130 rpm.

As a result of the experimental research of the modernized aspiration chamber of the flat-line separator, the regression equation of the efficiency of purification and deposition of light impurities and their graphical interpretation was obtained. It has been established that maximum purification efficiency can be achieved with minimum productivity values and maximum efficiency of precipitation of light impurities 76.26 % – at a productivity of 3.95 t/h.

CHAPTER 5. RESEARCH OF VIBROACOUSTIC DIAGNOSTICS OF FUEL SYSTEM OF ENGINES OF COMBINE HARVESTERS

To determine the diagnostic parameters of fuel system of engines of grain harvesters, technological and structural parameters of technical condition were considered. The authors investigate the structural schemes of indicator connection of purpose (performance) of fuel system of engines and parameters of technical state of its structural elements. For example, we consider the modal structure diagram, which characterizes the fuel system of grain harvesters engines and parameters of the technical state of its structural elements. For example, we consider the modal structure diagram, which describe the fuel system of the engines. At the highest level there are parameters that describe the process of fuel supply and directly determine the characteristics of injection, or the law of fuel supply. On the lower levels there are parameters that characterize the technical state of the most important elements of fuel equipment. They are used for elemental diagnostics. Experimental studies of vibration characteristics of nozzles of diesel engines have shown that the energy vibration nozzles manifested most actively at frequency from 5 kHz to 10 kHz. Application Hilbert's conversion to vibration analysis has made it possible to use the ability to control the identity of nozzles and identify defects such as breakage of nozzles and spray gun hangs. When the injection pressure changes from 27.0 MPa to 8.0 MPa signal duration, which is measured between the front and rear fronts with maximum amplitudes, decreases 2 times. Application of technological cards together with diagnostic means will allow in 1,5 times to cut down the technical equipment due to technical problems at expense of prevent bursts and reduce fuel consumption by 5-10%. The range of sensors for diagnostics of diesels, the basic electric circuit of tool for measuring the angle is

developed the advance of fuel supply, the requirements for computerized system for bench diagnostics of fuel equipment.

Technical diagnostics of the fuel system of the engine is an important link in the system for controlling the reliability of combine harvesters [1]. Knowledge of the technical state of the fuel system of the combine engine at any time allows it to be used with the highest efficiency, to determine the amount of work during maintenance and repair [2].

To do this, first of all, diagnostic tools and diagnostic technology are needed, taking into account new combine harvester models [3].

Creation of a database of diagnostic tools should be carried out on the basis of dynamic diagnostic methods [4], which allow to use for diagnostics the parameters of working processes that directly characterize the state of the object, electronic diagnostic tools are developed [5]. This is especially true with simultaneous work in the direction of mutual adaptation of the means and combines to the diagnosis [6]. This requires the appearance of combines equipped with on-board diagnostics based on built-in sensors and electronic equipment [7].

The urgency of the work is to increase the technical readiness of combines, reduce fuel consumption and engine power losses due to timely diagnostics of the fuel system of the engine and troubleshooting [8].

To examine the mechanisms of vibroacoustic processes arising in the nozzle during fuel injection, two main factors were determined: shock effects of the needle of the sprayer during its lifting and landing and hydrodynamic phenomena; the fuel supply process was analyzed in the outlet section of the fuel line near the nozzle [9].

In the analysis it was taken into account that in the process of fuel supply from the pump to the nozzle with the speed of sound passes the primary pressure wave, and the jump-like transition of the section of the injection fuel to the passage sections of the spray holes leads to a hydraulic impact [10]. At the time

of fuel injection through spray holes, the fuel flow had a turbulent character [11]. This caused a pulsation of both the flow velocity and the pressure that had a fairly wide range of amplitudes [12]. In the analysis of processes, we take into account the developments [13]. In general, the results of the analysis revealed the possibility of diagnosing injectors on a diesel engine by vibroacoustic characteristics, obtaining initial data for the selection of measuring and recording equipment, and developed a method of experimental research [14].

It should be pointed out that the state of the plunger pairs of the high-pressure fuel pump affects the nozzle processes. The valve in the closed position has greater impact on the signal, however, that impact is still minimal. Firstly, the engine is V-shaped. Secondly, the frequency of the valve closure has a lower oscillation frequency (approximately 6-8 kHz).

Vibroacoustic diagnostics showed that the neighboring injectors don't affect the nozzle operation signal because of the wave velocity. The injectors don't actuate simultaneously. In addition, the speed of ultrasound propagation in steel is about 5.8 km/s. Taking into account the construction and placement of the injectors on the engine and the time among pulses of neighboring injectors, the signal will go this distance for about 100 times.

The experimental installation for research of vibration characteristics of diesel nozzles was created on the basis of a computerized measuring device. Signal processing programs, a nozzle testing device and a bench for adjusting fuel equipment with a stand fuel pump and a set of fuel lines. The vibration accelerator sensor was mounted on the nozzle with a special clamping device.

The experimental installation ensured the creation of the required high-speed mode and measurement of fuel supply with an injector. The program of signal processing carried out on the computer record of the signal from the accelerator sensor and its processing in the mode of spectral analysis of oscillations [15].

At the first stage of experimental research, an injector with an accelerometer was installed on a bench for adjusting the fuel equipment. The signal from the sensor was fed to the input/output board of the L-1250 signals. Signal registration was carried out at band-filtering with a 9 kHz bandwidth filter, focusing on the range of vibration of the jet from 7 to 16 kHz. The signal was recorded to the computer's memory buffer.

With the help of spectral analysis of the vibration of the nozzle, the range of frequencies was specified, in which the energy of vibrations is most actively displayed. In the course of research, the speed of the camshaft of the fuel pump varied from idle speed to nominal, and the injection pressure was in the range of 13 to 25 MPa. In the processing of the input signal, the influence of the nozzle defects on the amplitude and the phase parameters of the signal, as well as on the vibration spectrum of the nozzle, was analyzed.

At the second stage, research was conducted on the engine of the «Slavutich» combine harvester using a vibration accelerator sensor and a computerized system. The processing of signals was carried out in accordance with the method used for bench testing. The signal recording was carried out at the nominal value of the injection pressure and in the simulation of such defects as breakage of the spring and freezing of the spray needle in idle mode. Particular attention was paid to filtering the signal to provide diagnostic information. For the analysis of vibration signals, the transformation (transformation) of Hilbert was used and an option was chosen that allowed the localization of the component of the spectrum containing the diagnostic information.

The nozzle is one of the main elements of the fuel equipment, which affects the formation of the injection characteristics, and especially its final phase. Therefore, estimating the efficiency of nozzles directly on the diesel engine will allow to timely prevent the violation of the fuel supply process. One of the possible directions of searching for diagnostic methods is the use of

vibroacoustic processes that occur in the nozzle when fuel is injected. The main factors that cause such processes are the impact of the needle spray when it is raised and lowered and hydrodynamic phenomena in the process of fuel supply. Consider the mechanism of occurrence of these vibroacoustic processes.

After the pressure wave generated at the pump runs through the fuel line, the pressure in the cavity of the sprayer rises. As soon as this pressure begins to exceed the pressure of the beginning of the needle lift, it separates from the saddle. From that moment on the pressure acts on that part of the needle, which until the lifting of the needle was closed saddle. This leads to a sharp increase in the speed of needle lift from 1.6 to 2.2 m/s. Moving the needle with such a speed and the shock nature of its lifting and landing cause intense coincidence and vibration of the nozzle body.

Using the method of hydrodynamic calculation of the fuel supply process and considering the equation of the boundary conditions for the initial cross section of the fuel line (near the nozzle), you can write the equation of motion of the needle spray in this form:

$$m_g \frac{d^2 h_g}{dt^2} = \left(f_g - f_g^{'} \right) \left(P_f - P_{fo} \right) - \delta_{pr} \left(h_g - h_{pr} \right) + f_g^{'} P_f^{'}, \tag{5.1}$$

where δ_{pr} – the stiffness of the spring, N/m;

m_g – needle weight, kg;

h_g – needle lift, m;

h_{pr} – preliminary compression of the spring, m;

f_g – cross-sectional area of the needle, mm^2;

$f_g^{'}$ – the area determined by the seat diameter of the needle cone, mm^2;

P_f, P_{fo} – fuel pressure in the cavity of the sprayer above the stop cone current and at the moment when the needle is started, MPa;

$P_f^{/}$ – pressure between the shutter cone and spray we spray nozzles (counter pressure), MPa;

t – time, s.

From the above equation (1) it can be seen $m_g \dfrac{d^2 h_g}{dt^2}$, that the value that determines the intensity of the needle's impact upon reaching the stop will depend on the effort of the previous tightening of the nozzle spring $P_z = \delta_{pr} h_{pr}$.

Thus, the oscillatory processes in the nozzle, which are caused by the shock effects of the needle, are due to the tightening force of the spring of the nozzle. Therefore, the change in P_z during the operation will directly affect the parameters of the vibration signal.

Analysis of works in this direction [7; 14] shows that the energy of vibration of nozzles most actively manifests itself in the frequency range from 12 to 18 kHz. The frequency of intrinsic vibration of the nozzle is in the ultrasonic frequency range. However, the authors are ambiguous in the impact of the impact of the needle spray on the vibration characteristics of the nozzle. The most practical, from a practical point of view, is the use of the vibration characteristics of the nozzles to assess the identity of their operation on the diesel engine, to determine the angle of advance of the start of the injection, to detect such failures, such as breakage of the nozzle spring and freezing of the spray needle.

The research was conducted to use vibration characteristics to assess the technical condition of nozzles. For this purpose an experimental installation was prepared (Fig. 5.1).

Fig. 5.1. Experimental installation and the stand of vibroacoustic diagnostics

The study used a standard diagnostic kit for diesel engines, namely: two ultrasound transducers and a low-pass sensor mounted on the engine head; a sensor of a "diesel" binder and a high frequency sensor mounted on each high pressure fuel line and nozzle, respectively. The aim was to determine the dynamic performance indicators of the fuel pump plunger and the operation of the nozzle of the selected section. Experiments were conducted for each engine cylinder separately, which made it possible then to compare the results between them.

The general picture of the performance indicators of the first section of the fuel pump and the first engine cylinder jet is shown in Fig. 2.

For a more detailed analysis of the results, we have identified and left on the screen only those sensor values that are needed for the study, which can be seen in Fig. 5.3.

According to the results of the taken indices, estimated tensile time of fuel spray nozzle, which was on average 1.5...2 ms. depending on the operating mode of the diesel engine. The time of transfer of pressure from the plunger to the nozzle is 0.47 ms.
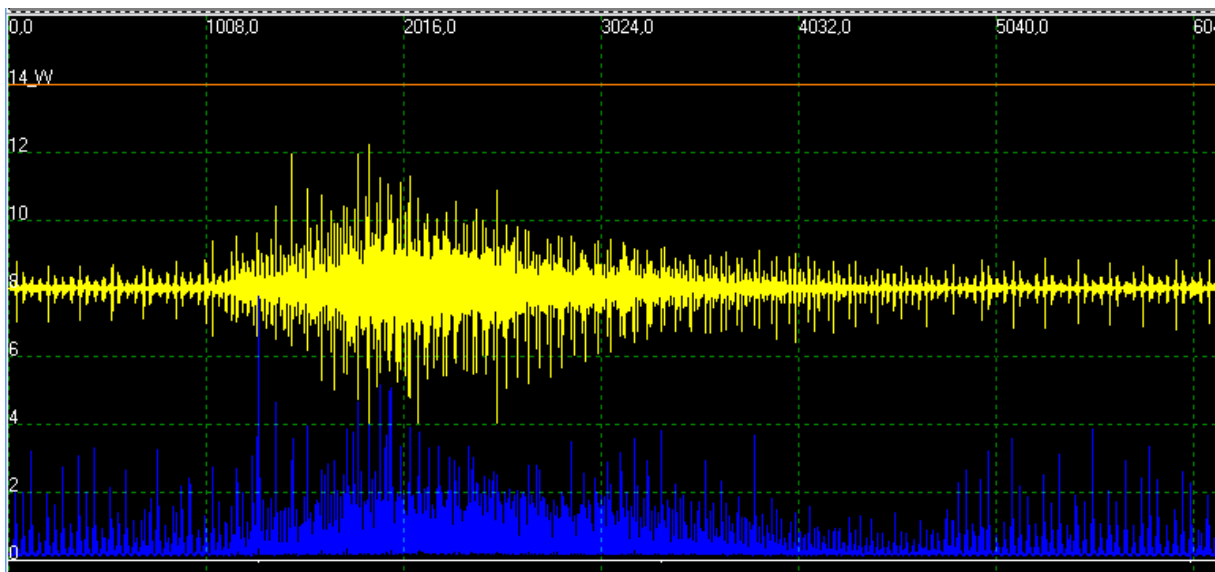
Fig. 5.2. Indicators of operation of the first section of fuel pump and the first cylinder engine jet
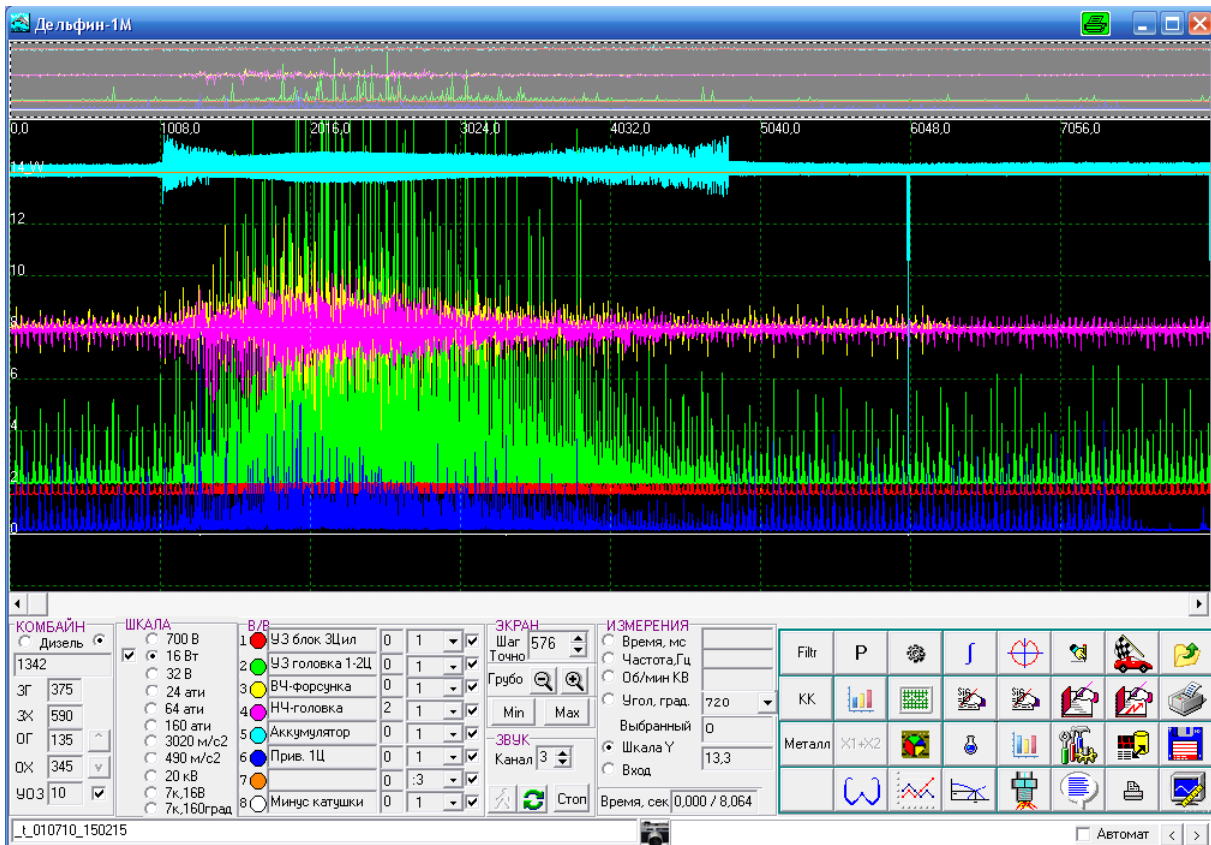
Fig. 5.3. Indicators of sensors for binding the diesel (bottom) and high frequency sensor (on top)

Having removed the figures from the fuel system of the diesel engine came the following conclusions. The shut-off valves of the fuel pump plunger are not in the best condition, this is said to be uneven sensor displays. This indicates that the valves already have certain deposits. It is also possible to say with certainty that the valve status is closely linked to the quality of modern diesel fuel. The spray nozzles have a marked cramming of seats, which is reflected on the oscillogram in smoother features of the opening and closing of injectors, when the new features are as sharp as possible.

More thorough research was carried out on the diagnostic parameters of the engine nozzles. Analyzing the operation of the nozzle according to t the high frequency sensor, it is evident that when the nozzle opens, it behaves rather quietly, moving components (needle) do not have shock contacts with other details of the design. Such work is provided primarily by countering the nozzle spring and centering the spray needle with the pressure of the injected fuel. After

the characteristic fuel injection into the combustion chamber, an injector closes, which is characterized by a powerful splash of the high-frequency components of the indicators. This is due to the very essence of the injection at the moment. The nozzle should maximally sharply complete the injection process, depending on which flow of fuel in the sprayer. If the nozzle does not close quickly enough, the fuel remains in the spray gun, which in the future will affect the coke of the spray, which leads to a violation of the spark ignition and burning of fuel. As a result, the toxicity of the exhaust gases of the engine increases. These all factors entail a loss of powerful characteristics and increased fuel consumption by the engine, which in the future will necessarily affect the cheap repair of fuel equipment.

Having examined the work of the nozzles of the second cylinder, found a defect, namely: coking a seat of the needle sprayer. This is evident from the oscillogram depicted in Fig. 5.4: the absence of sharp bursts of closure of the nozzle marks the difficult movement of the spray needle and the unclear completion of the process of fuel injection into the combustion chamber.

Fig. 5.4. Work of the second cylinder nozzle

Characteristics of the third cylinder nozzle are shown in Fig. 5.5. The nozzle has somewhat overestimated closing energy by the high frequency signal of the sensor, indicating that the needle is pinched and its seat is activated.
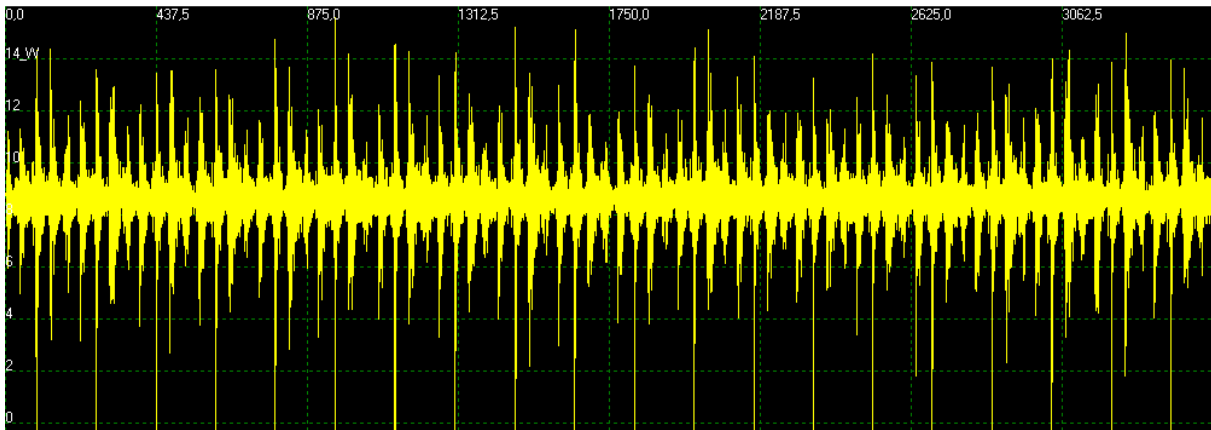
Fig. 5.5. Work of the third cylinder jet

On the sensor signal, as in the Hilbert transform, there are clearly two characteristic vibro-pulses that correspond to the lifting and planting of the spray needle. With an increase in the frequency of rotation in 2 times the amplitude of the first vibration impulse increases. At the next stage, the failure of the spring of the nozzle was imitated by a decrease in pressure P_f from 27.0 MPa to to 8.0 MPa. The position of the rail of the pump remained unchanged. In the mode n = 300 min^{-1}, the amplitude of the second vibrational pulse decreased by 1.5 times. With an increase in the frequency of rotation at such a defect, the amplitude of the first vibration impulse increases by 6 times, and the second vibrational pulse disappears, even visually reflecting such a malfunction of the nozzle.

One of the implementations of vibration of the nozzle during the hole of a spray needle. The tightness of the sprayer is unsatisfactory; the cyclic feed has decreased to 8.7 mm^3/cycle. Such a defect results in significant changes in the signal of the vibration sensor. Its duration increases 3 times, and the amplitude decreases by 4 times. These changes also reflect Hilbert's conversion. The decrease in the amplitude of the vibration signal is due to the fact that when the needle is in a stale state, the fuel enters the spray holes without delay. As a result, the pressure decreases before the spray holes, which reduces the velocity of the turbulent motion of the particles of fuel, which also determines the energy

of the vibration of the nozzle. A similar phenomenon is observed in the case of a weakening of the tightening of the spring due to its breakdown. Fuel, practically, freely passes through the sprayer. With an increase in the speed of a sharp increase in fuel pressure, which increases the intensity of vibrations.

In general, the results of conducted experiments indicate the possibility of assessing the identity of the nozzles and detecting such defects as breakage of the spring and freezing of the needle spray vibration acoustic parameters.

On the basis of consideration and analysis of existing diagnostic technologies, a list of diagnostic parameters of the technical condition of diesel fuel equipment, which are given in Table 5.1.

Table 5.1

Diagnostic parameters of the technical state of the fuel system

Fuel system and its components	Parameter name
Fuel pump	Bulk fuel consumption. Setting angle of the beginning of injection (supply) of fuel. The starting angle for fuel injection
Revolutionary regulator	Frequency of rotation of the crankshaft (minimum, maximum). Uneven frequency of rotation of the crankshaft
Automatic fuel outflow coupling	Change the starting angle of the fuel supply
Plunger pair	Pressure that develops a plunger pair at the starting speed
Pressure valve	Tightness
Nozzle	Injection pressure
Fuel is a suction pump	Pressure before the filter of fine fuel cleaning during crankshaft scrolling of the launcher and off fuel feed. The maximum pressure that the pump develops with the running outlet
Filter for fine fuel cleaning	Pressure at the inlet to the filter when the fuel is fed manually by a suction pump and an open outlet from the filter

The sequence of diagnostics of the fuel system of combine engine engines depends on specific production conditions, accepted organizational forms of maintenance, availability of diagnostic tools and other factors. In general, the diagnostic process is constructed in such a way as to avoid performing unnecessary work and unnecessarily loading the process with simple prophylactic operations. The basic principle is that a deep check of the state of the components of the machine must be performed only in the case of a real need. Otherwise, they are limited to a general check of the quality of the functioning of the components and the state of adjustment of parameters.

The computerized diagnostic system of the combustion engine fuel system includes the following requirements:

a) analog input and I/O of digital information via a L-1250 type card;

b) bit 12 (16) bit;

c) number of input channels – 16;

d) the range of input voltages – from 0.1 V to 10 V;

e) the presence of sensors for receiving pressure signals in the fuel supply system, the provisions of the top dead point of the camshaft pump, vibration sensors for information on the phase parameters of the fuel supply;

f) recording and displaying on the monitor the characteristics of the pressure change in the fuel line;

g) the presence of amplifiers, signal switches, the ability to synchronize signals;

h) the signal processing program should provide digital filtering, signal integration, spectral analysis of signals from vibration detectors based on Hilbert's quick conversion.

The composition and number of sensors are determined by a set of diagnostic parameters that are measurable, taking into account a number of technical requirements.

Electronic resources, in our opinion, should be used, first of all, to measure the diagnostic parameters that characterize the workings of the diesel system.

The diagnostic parameters that reflect the working processes, such as the characteristic of pressure change in the fuel line of high pressure, contains several diagnostic features. Thus, the residual pressure in the fuel line characterizes the state of the pressure valve and the needle of the sprayer; the velocity of pressure increase in the fuel line depends on the state of the plunger pairs. The maximum pressure determines the tightening pressure of the nozzle spring.

At the same time, the characteristic of pressure change in the fuel line contains signs of too different levels. So the residual pressure and the maximum pressure in the fuel line can differ in 5-10 times, which imposes rigid requirements on the sensors for accuracy and overload capability.

Frequency range of change of diagnostic parameters of vibroacoustic processes in diesel jet nozzles is 10-20 kHz, parameters of working processes of 5-10 kHz. The oil pressure in the lubrication system has a pulsating pattern relative to the average level with a pulsation frequency of up to 40%.

The sensors must have a sufficiently high output signal, the linearity of the output characteristics throughout the operating range, (1.5-2.0) – double load capacities and the stability of the output characteristics.

In addition, the sensors demand interchangeability. This is especially necessary in the analysis of the identity of processes, such as the characteristics of pressure change in the fuel line along the lines of injection.

Conclusions to chapter 5

1. Investigation of the vibration characteristics of the nozzles of diesel engines showed that the energy of the vibration of the nozzle is most actively manifested at a frequency from 5 kHz to 10 kHz.

2. The use of Hilbert's conversion to analyze the vibration signal enabled it to be used to control the identity of the nozzles and to identify defects such as breakage of the nozzle spring and freezing of the spray needle. When the injection pressure is changed from 27.0 MPa to 8.0 MPa, the signal duration, which is measured between the front and rear fronts with maximum amplitudes, is reduced by a factor of 2.

CHAPTER 6. EXPERIMENTAL STUDIES AND NUMERICAL SIMULATION OF SPEED MODES OF AIR ENVIRONMENT IN A POULTRY HOUSE

Due to the range of indeterminate factors that influence energy consumption and quality indicators of the air medium while providing the necessary conditions for poultry management, the use of analytical methods for determining the patterns of heat-, mass- and energy-exchange processes happening there is not sufficient enough and additional experimental research is required.

For that purpose, numerical simulation and experimental investigations on the performance of the environment support system in a typical poultry-broiler house according to technological conditions have been conducted. In the course of the experiment, quality indicators of the air medium and the process energy performance have been determined.

Papers *(Blanes-Vidal V., et.al., 2008; Bustamante E., et.al., 2017)* cover computational fluid dynamics (CFD) simulation of the flows of air and heat-mass exchange in a poultry house, where there is side system of ventilation used. The authors *(Blanes-Vidal V., et.al., 2008; Bustamante E., et.al., 2017)* believe that the method of side mechanical system of ventilation is more effective compared to other methods and make it possible to reduce heat stress and increase productivity of summer poultry raising. As a result of numerical simulation presented in *(Blanes-Vidal V., et.al., 2008; Bustamante E., et.al., 2017)*, the distribution of velocities, pressures and temperatures of the air flow in poultry houses for a side system of ventilation have been obtained. The results of numerical simulation have been compared to the data obtained from experimental studies, here the difference between them does not exceed 12%.

The paper paper *(Zajicek M. and Kic P., 2012)* presents the CFD solution of miscellaneously improved cases for the various flow and shape configurations of the broiler house. Effects of the transversal and longitudinal ventilation are combined with the changes of inlet air streams directions and also with the different cross-section shaping obtained using curtains.

Papers *(Gorobets V.G. et al. 2018; Gorobets V.G. et al. 2018).* cover the system of cooling the outside air with the help of heat exchange apparatuses of special design *(Gorobets V.G. et al. 2019)*, in which water from subterranean wells is used as a cooler. Mathematical simulation of the processes of heat and mass transfer during air ventilation in the poultry houses, where the location of ventilation equipment is changed height wise, has been conducted. As a result of numerical simulation, the fields of velocities, temperatures and pressures in a poultry building have been obtained.

The developed CFD model *(Fidaros D. et al. 2018)* is validated against measurements of temperature (16 points) and air velocity (6 points). According to the simulation results, it is drawn that the vertical temperature gradient should be taken into account when the operational sensors for the cooling devices are positioned inside the chamber since there is a deviation higher than 2 °C between the air content above and among the birds. Also various combinations of the available five fans, operating in two possible modes of the examined poultry chamber are studied in order to assess their effect to the internal microclimate. The operation of two or three central fans are proven to be the optimum choice in terms of temperature, ventilation and air velocity. The operation of only one fan fails to preserve the required temperature, while the operation of more than three fans does not improve the ventilation rates.

Based on the conducted analysis, the main drawbacks of numerical simulation in greenhouses have been determined *(Trokhaniak V. and Klendii O., 2018)*. Numerical simulation of the processes of hydrodynamics and heat-mass

exchange, that take place within the limits of commercial-scale greenhouses, has been conducted.

This work *(Pourvosoghi, N. et al. 2018)* focused on evaluation and numerical analysis of the influence of differential pressure (20, 30 and 40 Pa) and fan activation scenarios on indoor air velocity and temperature distribution in a poultry house. Results showed that air velocity tends to be maximum toward the centre of the cross-section of the house and minimum near the floor next to the side walls. Furthermore, it is elucidated that considerable thermal discomfort for chickens is likely due to temperature variation at the proximity to the exhaust fans.

Maintaining proper environment in hen house by mechanical ventilation is essential for the production. In order to fully mix the cold inlet air in winter with room air, the free space beneath ceiling of hen house is normally large. However, in summer, such a design is not optimal for tunnel ventilation that air is drawn into one end of the house and exhausted at the other end, i.e., a large portion of the ventilation air would pass through the free space under ceiling instead of caged-hen occupied zone (CZ), which leads to reduced air speed in CZ as well as wind chill effect. To solve this problem, application of deflectors beneath the ceiling was investigated by CFD simulations. To assess the effect of deflectors *(Cheng, Q.Y. et al. 2018)*, the indoor air speed and distribution with deflectors were compared to those without deflectors. The effects of heights (0.4 m, 0.55 m, 0.7 m, 0.85 m and 1 m) and intervals (6 m, 9 m, 12 m, 15 m and 18 m) of deflectors on air speed and distribution in CZ were analyzed. The CZ was modelled as porous media in simulations to reduce mesh numbers.

The present work *(Rojano F. et al. 2019)* proposes a three-dimensional modelling tool that uses CFD. External and internal climate and the sensible and latent heat emitted by the hens were included in the model in accordance with the principles that govern heat and mass transport, momentum, and radiative energy. Experimental data were used in the proposed 3D CFD model to predict

the internal climate, considering a time series when wind blew perpendicular to the ridgeline. A period of 3h30min, occurring under a stable wind direction was replicated, resulting in an overall RMSE of 1 degrees C and 1 g [H_2O] kg [dry air] for temperature and absolute humidity, respectively. In addition, the coefficient of variation indicated that the experimental data pertaining to the internal climate showed less overall variability than did predicted data.

A method of calculation of the characteristics of compensated asynchronous machines taking into account the change of the magnetizing contour resistance is presented. The advantages of compensated asynchronous motors and compensated asynchronous generators are determined. Recommendations as to their effective practical use are given *(Mishin V.I. et al. 2016)*.

To ensure stable joint operation of asynchronous machines in an autonomous system under extreme conditions, separation of excitation capacitances and their distribution between branches of a unified electric circuit that are separate for the motor and the generator and not interrelated by the condition of the voltage resonance are proposed using an isolated induction generator with internal capacitive excitation *(Mishin V.I. et al. 2013)*.

The investigations were conducted on one of the poultry farms in Ternopil region (Public Company "Ptakhofabryka Ternopilska", Company "Skalat-Produkt") in a poultry building for raising broiler chicken (10 thousand heads) with floor housing on a deep wood chips litter during a transient period (February-March).

In order to determine the behaviour and the dynamics of temperature change in a poultry building, the measurement of the indicated parameters was conducted immediately during the technological process. During this period the average temperature of the atmospheric air was +4 $^\circ$C, the value of ventilation air exchange was 0.8–1.1 m³/h per 1 kg bird body weight.

In a standard building (12×76 m) there are 5 rows of technological equipment located. The investigations were conducted during the operation of heating-ventilation system. The maintenance of the predetermined temperature was conducted by means of the equipment set of "Climate-4" type (Airstream Ventilation Systems, Big Dutchman) (with 10 extractor type fans (VO-7.1) and 5 fresh air fans (VO-5.6) with electric motors P = 0.37 kW.

Spatial temperature distribution was investigated at the level of bird location (0.3 m from the floor level) at 27 points of the building (Fig. 6.1).
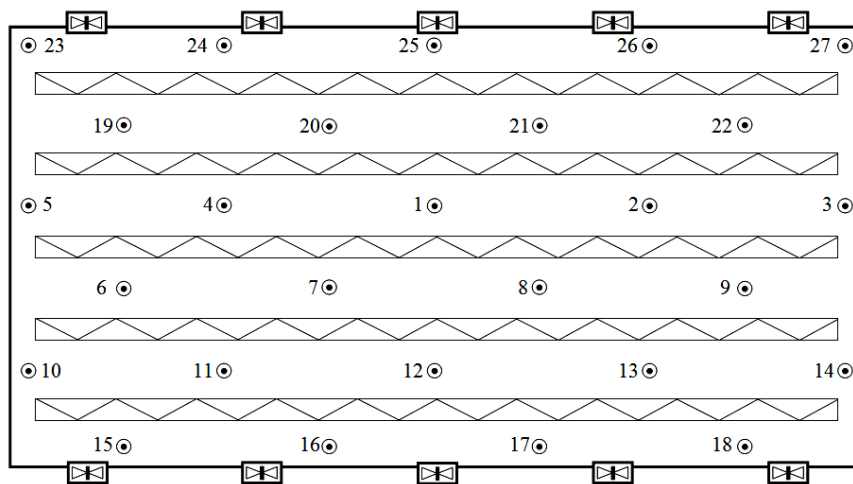
Fig. 6.1. Location schematic of the points of experimental measurements

Mathematical simulation of hydrodynamic processes and the processes of heat transfer in a poultry house was conducted. For this purpose, the CFD based on ANSYS Fluent software package was used. The mathematical model is based on Navier-Stokes equations *(Khmelnik S.I., 2018)* and energy transfer equation for convective currents. Spalarta-Allmarasa turbulence model *(Spalart P.R. and Rumsey C.L., 2007; Allmaras S.R. et.al., 2012; Bailly C. and Comte-Bello G., 2015)* and Discrete Ordinates radiation model (DO) *(ANSYS, 2017)* were used in the calculations.

Fig. 6.2 a presents boundary conditions at the "inlet" and the "outlet" and Fig. 2 b shows "symmetry" and "wall", which were predetermined for conducting numerical simulation in a poultry house.
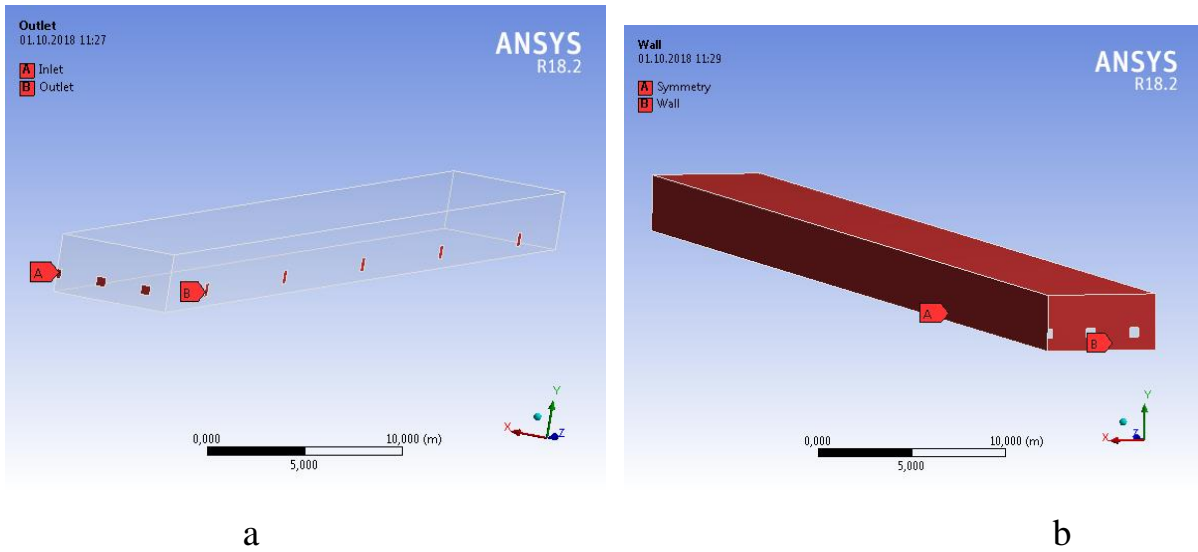
Fig. 6.2. Boundary conditions in a poultry house:

a – "inlet" and "outlet"; b – "symmetry" and "wall"

At the boundary "inlet" the mass air flow was predetermined to be 5.555 kg/s with the temperature of +4 ℃. The walls and the floor were made of keramzite concrete 0.4 m in thickness. At the boundary "wall" the temperature of the outside air was preset to be +4 ℃, taking into account DO radiation model. In the poultry building there were birds kept with floor housing, which is the source of heat generation of +41 ℃.

According to the investigation results, temperature fields (Fig. 6.3) that present the pattern of its distribution in a poultry house during a raising cycle have been built. The significant extremums presented in the graphs (30 and 21 °C, see Fig. 3) indicate the exceedance of zoo-hygienic norms for the parameters of the air medium (26 – 28 °C at the beginning of a cycle and 16 – 19 °C beginning from the 5th week) generated by the presence of heat sources (birds' heat production), which caused its local increase and non-uniformity of temperature and gas distribution in a building.

Since the divergence of the technological parameters was determined at the beginning of a poultry raising cycle, it can be assumed that the causes of

these phenomena could be the imperfection of the existing system of heating-ventilation equipment control as well as the openings in the structures of a building and the baffle systems of ventilation devices.

a   b
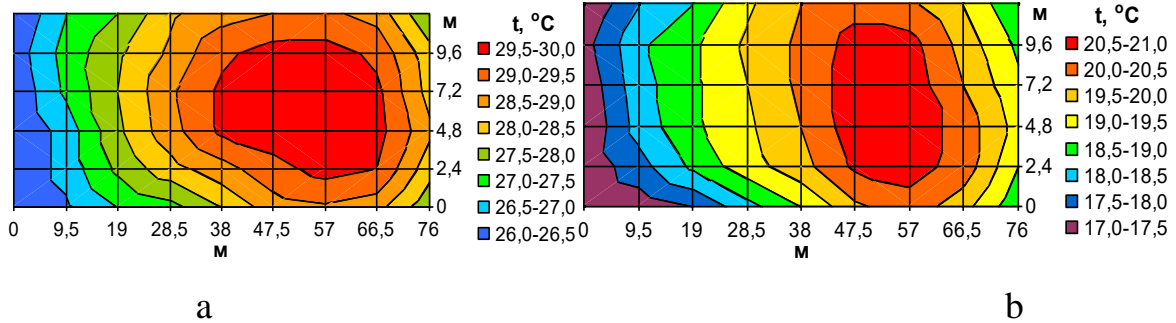
Fig. 6.3. Temperature distribution in a poultry building during a poultry raising cycle

a – day 14; b – day 42

According to the results of the measurements, statistical analysis has been conducted and the graphs of the distribution of root-mean square deviations and error dispersions of the controlled variables have been built in order to make a comparison with the specified parameters according to the coordinates X (length), Y (width) of displacement (Fig.6. 4).
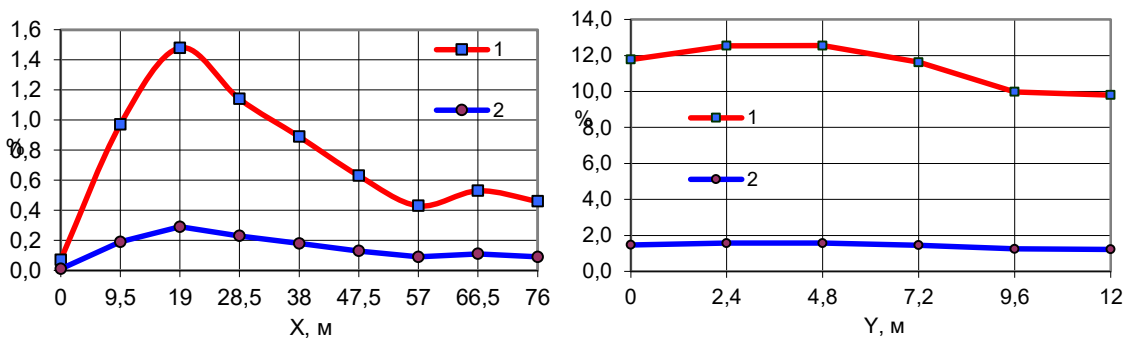
Fig. 6.4. Root-mean square deviations and error dispersions of temperature distributions

(1, 2) according to X, Y coordinates of displacement

Based on the results of the experimental investigations and the production inspection of the quality indicators of the air medium in a poultry house, numerical mathematical simulation has been conducted in order to evaluate the degree of the validity of the obtained results.

Finite element method (FEM) was used in the numerical calculation of hydrodynamics and heat transfer problems. Fig. 5 presents the FEM mesh built in ANSYS Meshing mesh generator based on Workbench framework by means of "CutCell" method. The minimum size of the boundary is equal to 0.05 m and the maximum one is 0.4 m. According to "Orthogonal Quality" criteria, the quality of the mesh is 0.75.

Fig.6.6-6.7 present the results of the numerical simulation for a half of the poultry building of the specified design. Fig. 6 shows that higher temperature is observed in the center of a poultry building. It is shown that temperature distribution in a poultry building is within the limits from +24 to +31 $^{\circ}$C (see Fig. 6). Fig. 7 presents the distribution of the temperature field in a poultry house at the distance of 15, 30, 45 and 60 m from extractor type fans. As expected, in the transient period of the year, the air being +4 $^{\circ}$C is concentrated near the flooring of a poultry house. At a height of 0.8 m near the birds the temperature is +17 $^{\circ}$C, which meets the norms.
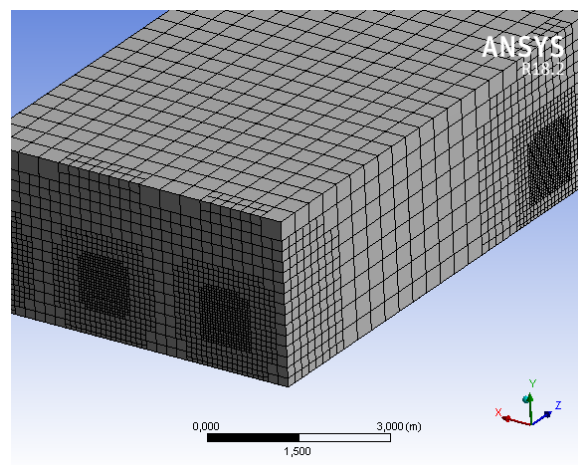
Fig. 6.5. Finite-element mesh generation
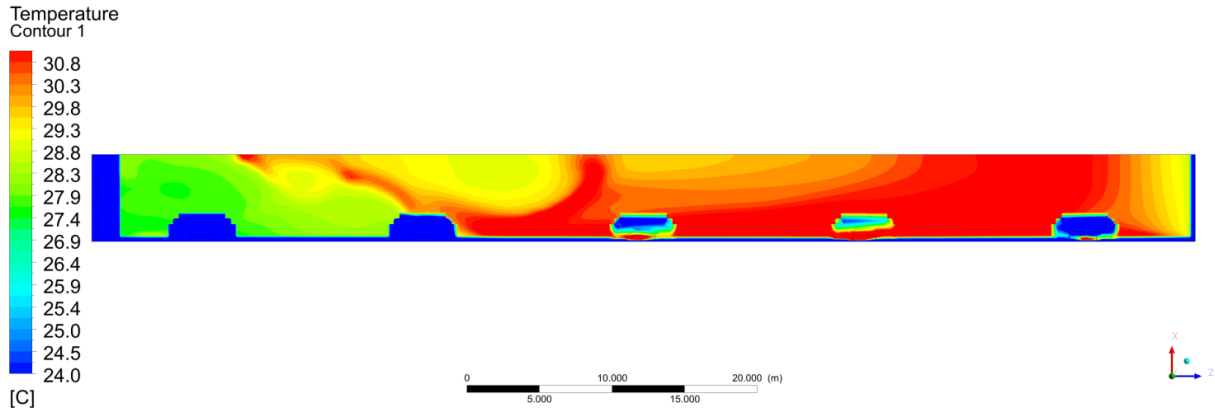
Fig. 6.6. Temperature field in a poultry house ranging from +24 to +31 ºC at a height of 0,3 m from the floor level along xz axis
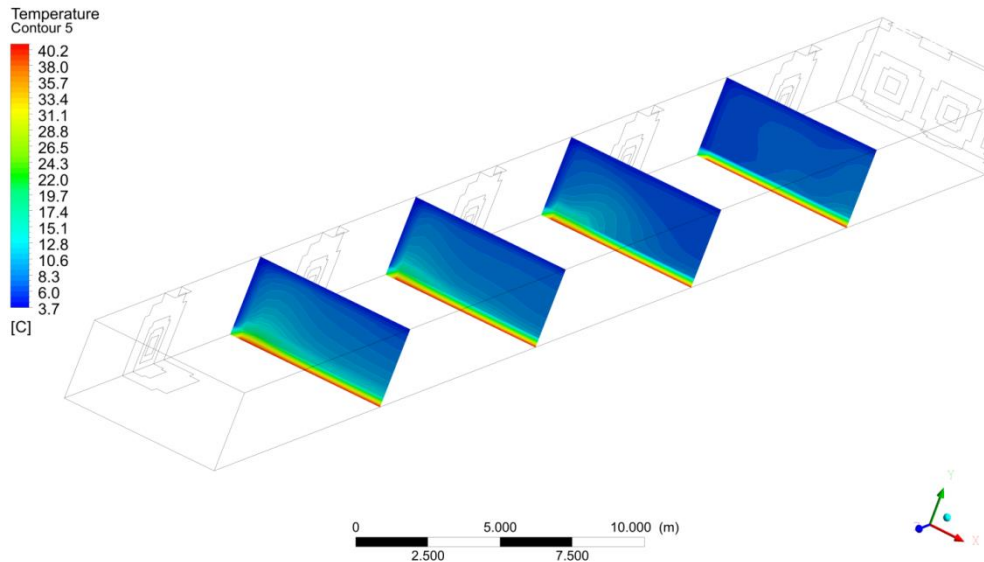
Fig. 6.7. Temperature field in a poultry house at a distance 15, 30, 45 and 60 m from extractor type fans along xy axis

The graphs in Fig. 6.8 characterize air temperature distributions along the length of the building and the ones obtained as a result of the numerical simulation and the experimental investigations (see Fig. 6.3 a) at a distance of 2.4 m (see Fig. 6.8 a) and 4.8 m (see Fig. 6.8 b). The deviation of the results does not exceed 6.5%.
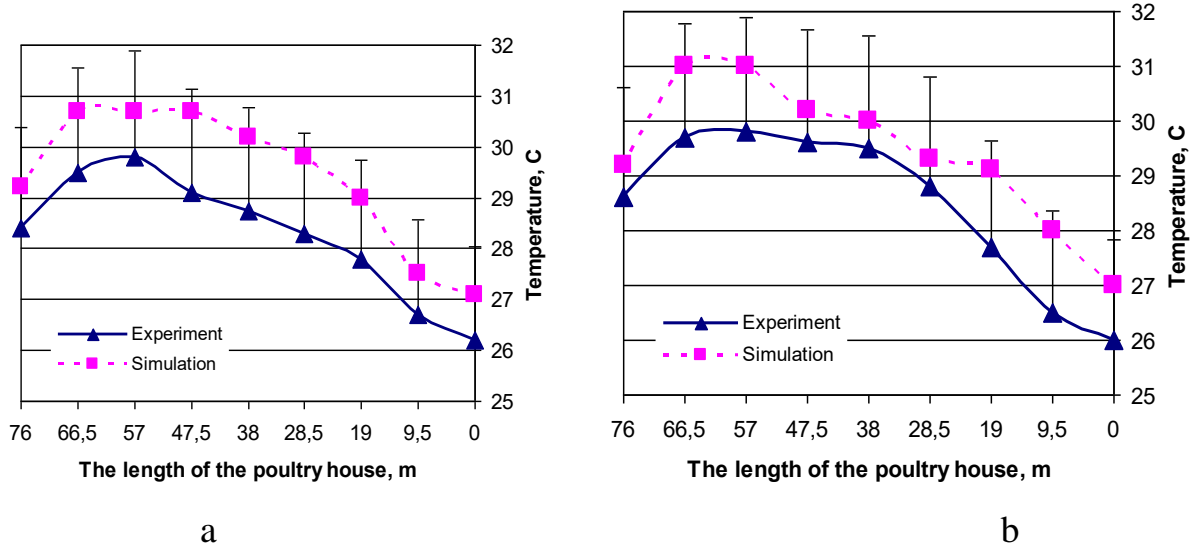
Fig. 6.8. Air temperature distribution along the length of a building

from the side wall of a poultry house for:

a – 2,4 m; b – 4,8 m

The ventilation system is controlled in terms of providing the predetermined temperature and gas concentration (NH_3). Under these conditions, depending on the balance of the inside and outside temperature, the efficiency of the ventilation system (VS) ranges from nominal (the maximum) L_n to the minimum L_{min}. The values of the outside temperatures T_{max} and T_{min} correspond to these values – the beginnings of cooling and heating seasons, when inside temperature control is determined by the nominal or the minimum values of air exchange, respectively:

$$n* = \frac{1}{L_n}\left[\frac{1}{\gamma c}\left(\frac{q_\Sigma(t)}{T_{in}-T} - \left(k_j F_j\right)_\Sigma\right)\right] \tag{6.1}$$

As already noted, the range of VS efficiency control should be from L_{min} to L_{max} at the change of outside temperatures from T_{min} to T_{max} that are determined from heat-balance equations reduced to the following form:

$$T_{min} = T_{in} - \frac{q_\Sigma(t)}{\gamma c L_{min} + \left(k_j F_j\right)_\Sigma} \; ; \; T_{max} = T_{in} - \frac{q_\Sigma(t)}{\gamma c L_{max} + \left(k_j F_j\right)_\Sigma}$$

Current ventilator efficiency values are determined by means of processing hourly data on the temperature of the outside air taken from data books. For a certain period of time, let us determine the number of hours of temperature duration within the range of $T_{max} - T_{min}$ at a pitch of 1 ^{o}C. The minimum VS efficiency is determined with the condition of NH_3 emission depending on the age of birds $L_{min} = f(t)$.

In the temperature range of $T_{max} - T_{min}$ with the pitch of 1 ^{o}C, according to the formula (6.1), VS running time with its correspondent efficiency is obtained. Running time with nominal efficiency is equal to the temperature duration of more than T_{max} and running time with the minimum efficiency – less than T_{min}. As a result of adding time intervals with the same efficiency based on the obtained data, it follows that VS running time in a nominal mode is about 15% of the total operating time and VS running time with the minimum velocity – 7%. The rest of the time – 78% – ventilators operate with the controlled efficiency.

In order to calculate energy consumption for heating a poultry house, firstly, it is necessary to determine the beginning of a bird raising period, since cycle distribution during a year greatly influences the overall energy consumption. According to the investigation data and the methodology presented in *(Ivanova V. M., 1987; Shutka O.V. and Sukach S.V., 2010)*, cycle arrangement in a row is determined. Thus, the beginning of a raising period, which falls on the first days of November, corresponds to rational cycle distribution, at which heat energy saving up to 15% is provided.

According to the data covered above and having assumed that, currently, the minimum period of broiler raising is equal to 43 days and 9 days of sanitary period, 7 raising cycles are obtained under the condition of their optimal arrangement. According to climatological reference books, graphs of distribution of the average monthly air temperature and the change of the inside

temperature in a poultry house within every raising cycle in the selected area (climatic zone) are built.

The energy consumed by heat-producing equipment of a broiler farm is calculated according to the heat balance equation:

$$Q = \int_{t_\Pi}^{t_K} \left[\left(k_j F_j + \gamma c L_{min}(t)\right)\left(T_{in} - T_{out}\right) - q_\Sigma(t) \right] dt \qquad (6.2)$$

While determining energy consumption during a cycle, when the preset temperature of the inside air is changed according to the birds' age, variable values in the expression (6.2) are T_{in} and T_{out} and after a 30-day age – only T_{out}. In order to simplify further calculations and transformations, let us set the constants:

$$\alpha = \left(k_j F_j + \gamma c L_{min}(t)\right); \ b = T_{max\_in} - T_{min\_out}; \ c = Q_{T_{in}} + Q_T - Q_{out} \qquad (6.3)$$

where T_{max_in} – inside air temperature during bird placing; T_{min_out} – minimum temperature of the outside air.

For the first and the last cycles of raising, in case of linear approximation of outside temperature distribution, $T_{min} = T_{max}$'.

Having substituted (6.3) into (2), for the first cycle we obtain:

$$Q = \int_{t_{ny}}^{t_{ny}+\tau} \left[\alpha\left(b - r\left(t - t_{ny}\right) + gt\right) - c\right] dt \qquad (6.4)$$

where τ – duration of the period of raising at changeable air temperature, twenty-four hours; t_{ny} – the beginning of broiler raising cycle, calendar day; r, g – constant coefficients of linear functions.

Having integrated and simplified the expression (6.4), we obtain:

$$Q = \tau\left[\alpha\left(b + gt_{ny} - \frac{(r-g)\tau}{2}\right) - c\right] \qquad (6.5)$$

Analogically, we obtain the dependence for calculating energy demand in the last raising cycle:

$$Q = \tau\left[\alpha\left(b - gt_{ny} - \frac{(r+g)\tau}{2}\right) - c\right] \qquad (6.6)$$

The number of twenty-four hours τ, during which it is necessary to heat the air, can be determined by differentiating the expressions (6.5) and (6.6). As a result, we obtain:

$$n_1 = \frac{\alpha(b + gt_{ny}) - c}{\alpha(r - g)} ; \quad n_1 = \frac{\alpha(b - gt_{ny}) - c}{\alpha(r + g)} \tag{6.7}$$

For the cycles of raising, in which the approximation of the outside temperatures causes significant errors, their distribution should be presented in the form of a quadratic dependence

$$T_{out} = T_{min.av} + kt^2 \tag{6.8}$$

where $T_{min.av}$ – the minimum average air temperature, which is typical of this area; k – constant coefficient of the parabolic function of temperature distribution.

From the expressions (6.2) and (6.8) we obtain the equation for calculation the necessary amount of heat from the 2nd to the 6th cycle of raising:

$$Q_{(2-6)} = \int_{t_{ny}}^{t_{ny}+\tau} \left[\alpha \left(b' - r(t - t_{ny}) + kt^2 \right) - c \right] dt \tag{6.9}$$

where $b' = T_{max\_in} - T_{min\_out}$ – the difference between the maximum inside temperature and the minimum (average monthly in the coldest period) outside temperature, ºC.

After integration and transformation, we obtain:

$$Q_{(2-6)} = \tau \left[\alpha \left(b - \frac{rt}{2} - kt_{ny}^2 - kt_{ny}\tau \frac{k\tau^2}{2} \right) - c \right] \tag{6.10}$$

In order to calculate heat demand according to the formula (6.10), it is necessary to substitute the correspondent to a certain cycle values of t_{ny}, which characterize the time of chicken placement, in it. This is the value that significantly influences heat energy consumption.

Based on the analysis and generalization of the results of the investigation on the distribution of the fields of air medium technological parameters in a poultry house, the function of the required air exchange is obtained and it

determined the minimum volume of fresh air (m³) and, correspondingly, the minimum artificial ventilation heat exchange in order to create the optimal microclimate conditions according to NH₃ content, which provides the minimum heat energy consumption for medium heating:

$$G = 24k \int_a^b q(i_{NH_3})di \qquad (6.11)$$

where k – the number of twenty-four hours in the cycles of broiler raising during the period under study; $q(i_{NH3})$ – functional dependence of the minimum necessary air exchange depending on the bird's age (from i = a to i = b), m³/h.

The amount of heat (J) required for heating the incoming air is determined as follows:

$$Q = c\rho G(T_{in.av} - T_{out.av}) \qquad (6.12)$$

where c – specific heat capacity of dry air, J/(kg·K); ρ – air density, kg/m³; $T_{in.av}$ – average inside air temperature, °K; $T_{out.av}$ – average outside air temperature, °K.

From the expressions (6.11), (6.12) we obtain the equation necessary to determine the required amount of heat to provide the preselected temperature in a poultry house during air exchange according to NH₃ content:

$$Q = 24kc\rho(T_{in.av} - T_{out.av}) \cdot \int_a^b q(i_{NH_3})di \qquad (6.13)$$

Heat consumption for heating the incoming air is determined by the range of ventilation system efficiency control, which was chosen with the condition of providing the maximum required demand of poultry for fresh air (m³/h):

$$L_{max} = L_n = nq_{max}m_{max} \qquad (6.14)$$

where n – the number of heads in a poultry house, unit; q_{max} – summer norm of air exchange per 1 kg of body weight, m³/h; m_{max} – weight of one bird at the end of a raising period, kg.

According to the technological conditions, the maximum control range of D in order to provide the necessary air exchange $L_{min}(i)$ in poultry houses for

young broilers should be 1:80, while the existing ventilation systems provide the maximum range of efficiency control about 1:10, its minimum limit corresponds to the value of $L_{max}(i)$ (Fig. 6.9).
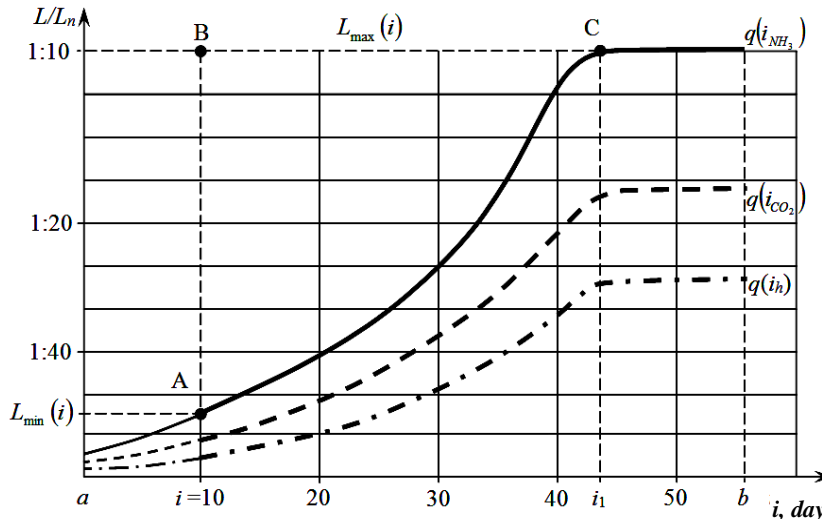
Fig. 6.9. Relative dependences of air exchange values on the birds' age in winter and transient periods of the year:

according to ammonia $q(i_{NH3})$ content, carbon dioxide $q(i_{CO2})$ content and excess water $q(i_h)$

According to the control range of the frequency of ventilator rotation, the calculation of the minimum value of air exchange (m^3/h) is conducted according to the formula:

$$L_{min} = L_n D \qquad (6.15)$$

The Figure below (see Fig. 6.9) presents the graphs of the relative dependences of the required efficiency L of a ventilation system, according to the current birds' need for fresh air q(i), on the age and the content of harmful substances.

The obtained results show that beginning from the moment of exhaust ventilation operation $i = 10$ and to the birds' age $i = i_1$ (43 day), there is overconsumption of the air (m^3), which is heated to the poultry house

temperature. In the adjusted scale, it is determined by the area of the ABC plot (see Fig. 6.9) as the difference of the integrals $L_{max}(i)$ and $q(i_{NH3})$ within the interval $i - i_1$:

$$G = L_{\max} \int_i^{i_1} di - \int_i^{i_1} q(i_{NH_3})di \qquad (6.16)$$

From the equations (6.12) and (6.16) we obtain the value of heat energy overconsumption (J), which is caused by insufficient range of ventilation system control:

$$\Delta Q = c\rho(T_{in.av} - T_{out.av}) \left(L_{\max} \int_i^{i_1} di - \int_i^{i_1} q(i_{NH_3})di \right) \qquad (6.17)$$

Thus, the investigation results presented above prove that specific heat and electric energy consumption can be decreased by means of extending the range of ventilation system control (not less than 1:50) with the help of variable-frequency asynchronous electric drive with adaptive control system, which is based on the analysis of microclimatic parameters of the air medium in poultry houses.

Conclusions to chapter 6

Based on the conducted research, it is possible to draw the following conclusions:

Numerical simulation of the processes of heat and mass transfer of the ventilated air in a poultry house in order to verify the results has been conducted together with the experimental investigations. According to the investigation results, with the help of ANSYS Fluent software, 3D temperature fields in a poultry house have been obtained;

Energy consumption and quality characteristics of the environment support technology depend heavily on the organization of the speed range of technological equipment;

The solution of the stated problems makes it possible to decrease energy consumption of the environment support technology during broilers raising, increase the quality of the air medium in poultry houses, reduce feed consumption and the loss of poultry stock and, as a result, increase economic efficiency of the production process and the quality of the finished product.

CHAPTER 7. PROBABILITY OF BOUNDARY EXHAUSTION OF RESOURCES AS FACTOR OF OPERATIONAL SAFETY FOR AGRICULTURAL AGGREGATES

The influence of the presence of fatigue cracks detected in the array of operational defects of typical parts of individual units on the condition of safety of tractors has been analyzed. In the work with the help of a specialized portable vibration current flow defectoscope the presence of cracks in the details of the units of tractors with different operating periods was estimated. The defectoscopic control of more than 500 parts of various applications was carried out in 50 tractors that were in service until 17 years since the date of issue in agricultural enterprises of Ukraine. Defectoscopic inspection was carried out during the defect of the details of these tractors received for repair. Based on statistically valid data, the kinetic dependences of the probability distribution of the accumulation of operational fractures of parts of tractor units in time were constructed. The cracks analyzed in the work were detected using a high-sensitivity pulsed vibration current flaw detector, which allowed us to quantify the size of the cracks that correspond to certain operating lifetime terms. It is established that the process of accumulation of a certain type of cracks has an exponential kinetics. The regularities considered in the work reflect the consequences of the statistical process of accumulation of an array of fatigue cracks in the details (knots) of tractors within the limits of the studied range of service life. Exceeding the maximum period of operation of aggregates dependence affects the change in the probability of accidents on mechanized and transport works. It is determined that the deadline for researching tractor types is 13-14 years.

The high level of injuries in the agroindustrial complex is due to the fact that most of the technological operations are carried out using morally obsolete

and used equipment [1]. However, researchers of occupational injuries in the agroindustrial complex primarily focus on organizational reasons [2] and working conditions [3], largely ignoring the unsatisfactory technical condition of the mobile means of agribusiness production.

At present, in the agroindustrial complex, in the face of high depreciation wear on wheel equipment, it is not fully possible to solve the issue of improving the safety of machine operators and drivers [4]. Studies on the setting of conditions for and the safety of work on tractors, harvesters or trucks generally belong to secondary [5].

The analysis of research on professional risk assessment in the agroindustrial complex showed that the used methods today largely do not determine the quantitative characteristics of the safety of the system of human-machine-environment (H-M-E) and can be used as an estimate of individual indicators [6]. On the other hand, in works dealing with the functioning of the mathematical model of the system H-M-E in agricultural production, the main emphasis is mainly on the reliability aspects of mobile technology [7]. But at the same time they do not consider the potential hazards for machine operators and other workers involved in the production process.

Thus, controlling the quality of maintenance and repair of mobile agricultural machinery, for the most part pay attention to the definition of technological and economic performance of the machine, without monitoring the existence of operational defects (cracks) in details. And this often leads to the implementation of mechanized work with an increased level of accident, which leads to the trauma of mechanics and auxiliary workers [8].

The comparison of such lines of analysis of the system H-M-E, as the reliability of equipment and labor protection during its operation, shows that they are based on the same probabilistic models of risk assessment failures and, respectively, the onset of accidents [9]. Therefore, in order to assess the probability of occurrence of emergencies it is expedient to involve approaches

of reliability theory, based on the statistics of failures of machinery or equipment.

The analysis of literary sources allows us to put forward the hypothesis that the statistical data of the defectoscopic control of the existence of operational cracks in the array of parts of the individual nodes determining the safety of the operation of the tractors can be used to establish the patterns of resource depletion, prediction of reliability and safety factors of long-life aggregates [10].

Obtaining of statistically substantiated data of the defectoscopic control during maintenance and repair of agricultural machinery constrains the non-adaptability of portable defectoscopes for the operational diagnosis of individual parts of tractors and self-propelled agricultural machines (SAM). In particular, there are currently no records of operational defects of parts of mobile machinery units after prolonged use. The purpose of the study is to substantiate the deadlines for the operation of mobile agricultural machinery with a high degree of damage to parts.

To achieve this goal you need to solve the following tasks:

1.   To analyze the possibilities of adaptation of portable defectoscopes for operative detection of operational damage in an array of parts units of tractor and SAM.

2.   Obtain and analyze the kinetic dependences of the accumulation of defects in the details of the knots of tractors of different durations of operation.

The basis of the research was the thesis that the probability of failure of individual tractor units is determined by a complex of existing cracks in details, which imposes special requirements for the periodicity and diligence of the conduct of defectoscopic control. At the same time, the reliability of the forecast depends on the quality of the received information on the presence of defects in the responsible details and elements of the structures of such objects. The proposed approach does not contradict the methods of statistical estimation of

the probability of failure-free operation of agricultural machinery, developed by other authors [4; 6; 7].

In the work with the help of a specialized portable vibration current flow defectoscope the presence of cracks in the details of the units of tractors UMZ-8040.2 with different operating periods was estimated. The defectoscopic control of more than 500 parts of various applications was carried out in 50 tractors that were in service until 17 years since the date of issue in agricultural enterprises of the Kiev and Chernihiv regions of Ukraine. Defectoscopic inspection was carried out during the defect of the details of these tractors received for repair.

The dependence of the kinetics of the accumulation of cracks on the surface of the details of the mechanical systems (knots) of the tractor proposed in the work is exponential within the studied range of operating life and is determined in terms of the fractal dimension of the surface. A dimensionless index of the fractal dimension of micro-plastic strain amplitudes, which is a kinetic characteristic of the cumulative inelasticity in the surface layer and is defined by the Hurst parameter H by the below formula, was chosen as a parameter characterizing the metal damage:

$$\frac{R(t)}{S(t)} = \frac{X(t)\max - X(t)\min}{S(t)}, \tag{7.1}$$

where: R/S is the normalized range, R is the deviation range X, $X(t)max$ is the maximum value for X, $X(t)min$ is the minimum value for X.

The range is cumulative deviation over N periods or the difference between the maximum and minimum calculated values of the parameter X:

$$X = \sum_{i=1}^{t}(n_i - M_N), \tag{7.2}$$

where: X is cumulative deviation over N periods, n_i is the deviation during a period of loading, M_N is the mean n_i over N periods.

The method of statistical measurement used in the work involves specifying objects of defectoscopic control in order to distinguish defective parts. The available details of the individual tractor units were divided into several categories:

1) high-stressed components with high probability of destruction;

2) the details, the technical condition of which is determined by the combined effect of force factors with aggressive environmental conditions;

3) the parts, which undergo a minor damaging operation;

4) the parts in which damage is detected only visually (small, non-metallic, etc.).

Within the framework of the proposed methodological approach, the potential fracture hazard and damage to the third and fourth categories of parts: fixing, rubber, non-metal, etc. were not taken into account. In the work for the detection of cracks, a portable vibration current defectoscope was used. This defectoscope meets the requirements related to the specifics of the control of parts of tractor units. The main ones are:

- versatility in relation to the metal of the investigated parts (automatic adjustment on the metal object of control);

- informative about the presence of damage in the investigated details (the smallest sizes of detected cracks: depth – more than 0.2 mm, length – more than 3 mm, width – more than 0.1 mm);

- the ability to change the sensitivity (the ability to set the minimum size of defects that can detect a defectoscope);

- no need for special preparation of controlled surface of parts (the defectoscope is practically not sensitive to surface roughness and is able to detect defects in surface roughness below 60 μm;

- absence of the edge effect and the effect of removal of the sensor, the wear of the sensor against friction on the monitored surface;

- detection of cracks at the maximum gap between the instrument sensor and the monitored surface to 3 mm.

The applied portable defectoscope has the ability to switch the range of sensitivity and selectivity of the device, that is, it is possible to detect cracks whose sizes are larger than certain values, which is especially important for the flaw detection of the entire range of tractor parts.

Before conducting defectoscopic investigations of details and structural elements it is mandatory to check the work of the defectoscope on control samples. Control samples of cracks of different lengths were obtained on metal samples of metal alloys as a result of the propagation of fatigue cracks from the stress concentrator applied to the edge of the sample.

The danger of the spread of cracks in the details and structural elements significantly depends on the size of the cross-section of the detail (structural element), where the crack originated and is developing. The methods of fracture mechanics use to calculate the degree of fracture hazard, and an approximate approach was implemented in order to isolate the details of detected cracks in certain ranges of relative length in this work. So, for example, according to this approach, the details of the steering control of tractor considered as parts of small, medium and large size.

According to the applied gradation, small size details include a billet, a swivel lever, an earring, a nut, a ball finger, bolts terminal, a lock pin, a hub liner, a hub, a bolt, a screw cover, a adjusting screw.

For parts of the average size of the steering control include: steering column (shaft), the body of hydro amplifier of the steering control, middle shaft, intermediate shaft, front shaft, steering tie rod tip, axis of adjusting screw, cardan hinges, rack, intermediate prop, splined bush, pin, right wall of the rack, worm, sector, rack, stem, piston. The details of the large size of the steering control include retractable pipe, brackets, semi axis, pipe of steering column, steering shaft and rotary shaft.

The kinetics of the accumulation of cracks in the details of systems and assemblies of tractors of different durability is presented in Fig. 1. The coordinates of the graphs are as follows: the ordinate axis – the probability of occurrence of the critical state $P = n_d / N$ (the ratio of the number of cracks n_d, detected in the total number of investigated, significant in terms of the limiting condition of operation safety, details N); axis of abscissa – relative durability $D = t_{ex} / t_{base}$ (ratio of the duration of operation of tractors t_{eks} relative to the base operation t_{base}, which in the calculation is 17 years). In Fig. 1 also describes the trend line equation and the accuracy of the approximation of R^2.

Scientific notation equations, as exponential function (Fig. 1), in contrast to the linear relationship explained by the analogy of the physical process of accumulation of scattered damage in the samples of metal during cyclic loading. The view of this analogy will continue to apply the methods of prediction of durability to failure details for evaluation of the limit technical condition tractors with an array of cracks in the details.
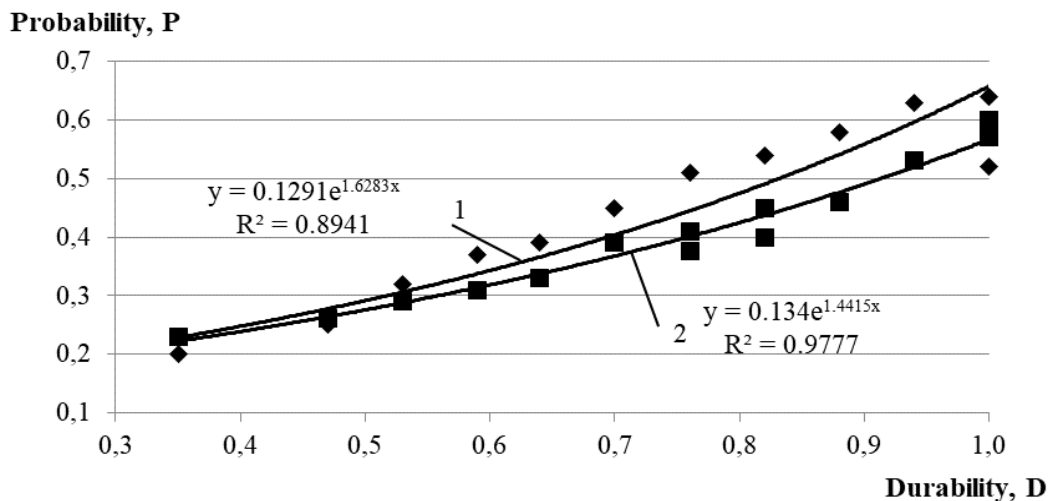
Fig. 7.1. Kinetics of the accumulation of cracks in the details of tractors of different durations of operation:

1 – steering system; 2 – hinged device of the tractor

Motorcycle hours of tractor use in agricultural enterprises during the calendar year are difficult to establish, since only one year of release of the unit

is known from the operating documentation. In the given work, the estimated duration of operation of tractors was obtained on the basis of the following assumptions:

- performed in the work the defectoscopic control allows with a certain degree of reliability and authenticity to detect fatigue cracks in the details of the knots of tractors involved in mechanized and transport work under the load, which led to the emergence of operational damage;

- believed that all the explored tractors of one year of issue worked practically the same hour resource;

- the basic choice was the 17-year lifetime of tractors, which is twice as higher of the resources specified by the manufacturer.

The regularities considered in the work reflect the consequences of the statistical process of accumulation of an array of fatigue cracks in the details (knots) of tractors within the limits of the studied range of service life. Analysis of the statistical process of accumulation of scattered damage of structural materials under fatigue should be submitted in terms of the fractal dimension of the surface - the Hurst parameter (H). The characteristic of the development of the statistical process in time can be approximated with a certain degree of reliability by the exponential function (Fig. 7.1). The general analysis of the kinetics of the accumulation of the array of cracks in the details of all systems (nodes) of tractors (Fig. 7.2) allows to predict the degree of kinetics outside the studied duration of operation.

Such an a priori forecast of the characteristics of the time series of the kinetics of the accumulation of fatigue cracks indicates a likely change in the dynamics of the appearance of damaged details, which, in case of exceeding the critical parameter of unit damage, corresponds to an increase in the probability of a sudden occurrence of emergency situations on mechanized or transport jobs. The regularities of the kinetics of the accumulation of operational defects in the array of details of separate systems (nodes) of tractors are similar to the kinetics

of the deformation hysteresis of the surface layer of metal structures represented by the parameter N. The difference lies in the different speeds of the dynamic processes of mechanical loading of laboratory samples and original parts. Consequently, comparing the boundary state of identical fracture processes to a single criterion, creates conditions for determining the predictive parameters of the state of critical damage. Proceeding from this self-similarity of the characteristics of the processes of destruction in the time, it is advisable to set the time of the onset of the critical state at a certain probability P. This criterion corresponds to the degree of accumulation of operational defects, the exceeding of which characterizes a significant increase in the probability of emergency situations on mechanized and transport works with the participation of tractors.
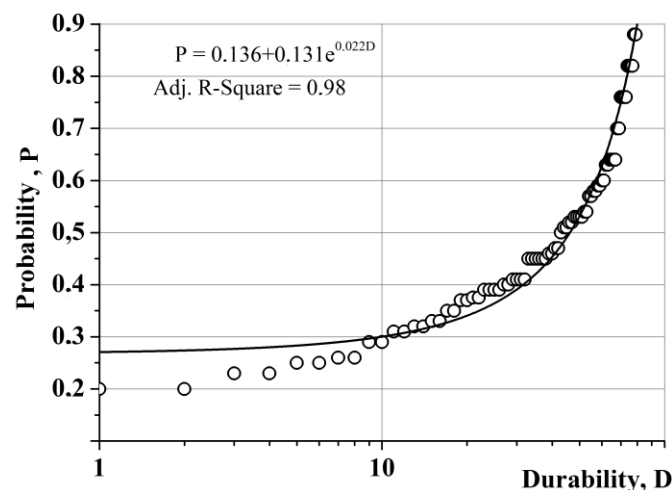
Fig. 7.2. Kinetic characteristic of accumulation of operational damage in an array of details of tractor units on the explore basis of long-term exploitation (17 years)

The relative number of details with operational cracks in each of the examined aggregates of the general ensemble of tractors is approximately the same for the whole sample of the details of each tractor. The critical durability of the tractor operation for a probability $R \approx 0.4$ is $D_{crit} = 0.7\text{-}0.8$, which corresponds to 13-14 years of operation. Consequently, this indicator can serve as a criterion for the discontinuation of tractor operation, the flaw detection of

parts in order to detect cracks and repair (replace) defective parts. In accordance with the Technical Rules for the safety of machines (approved by the Cabinet of Ministers of Ukraine dated January 30, 2013, No. 62) and the Technical Regulation of components and characteristics of wheeled agricultural and forestry tractors (approved by the Cabinet of Ministers of Ukraine from December 28, 2011, No. 1368) the requirements for trouble-free operation, that put forward to the technical condition of machine details is mostly qualitative (expected), instead of the introduction of quantitative indicators that could be obtained technically by means of control methods.

At present, the practice of detecting operational defects in details of tractors, self-propelled agricultural machines and cars is largely based on planiometric or organoleptic control methods, which is quite subjective. It is necessary to add to the Rules for the Technical Operation of Tractors and Mobile Agricultural Machinery the requirements of instrumental (using portable defectoscopes) detection of cracks of dangerous sizes in the details of the knots, and to consider the visual-planimetric control as not in compliance with the current requirements of this normative document. The significance of the impact of the defectoscopic control on the safety increases with the length of stay of tractors, combines and SAM in operation, in particular after 10-12 years. Introduction to the practice of activities of repair units of the methodology of operative defectoscopic control and the rules for assessing the risk of exploitation of mobile agricultural machinery with defects will significantly increase the level of detection of defective agricultural aggregates annually. The use of the proposed approaches in the Rules of Technical Operation of Tractors and Mobile Agricultural Machinery is aimed at reducing the number of accidents of agricultural aggregates and misadventures.

The obtained statistical data on the existence of operational cracks can also be used to calculate the probability of occurrence of emergencies involving mobile agricultural machinery. In this calculation technique, it is expedient to

use data not about the linear dimensions of the detected defects, but the available signs that revealed cracks of varying degrees of danger in terms of the destruction of the detail. This allows us to estimate the tractor's malfunction in the probabilistic aspect, depending on the implementations of a set of signs, that is, for possible variants of the presence or absence of cracks of the boundaried and admissible sizes.

Conclusions to chapter 7

1. The obtained experimental characteristics of the presence of dangerous mechanical defects in the details of the tractor units allowed to determine the durability of operation, after which the probability of accumulation of critical damage accident increases significantly.

2. The necessity of changes to the Rules of technical exploitation of tractors and other mobile agricultural machinery concerning the carrying out of instrumental (with the help of portable flaw detectors) detection of cracks in dangerous sizes in details is substantiated, in order to extend the term of the assigned resource as additional to the current requirements of visual-planimetric control.

3. For the investigated types of tractor units, a probabilistic criterion for the termination of the accident-free operation of the tractor was proposed, and the fractoscopy of the parts was performed in order to detect and eliminate cracks by replacing or repairing defective parts. The probability criterion of *P = 0.4* corresponds to 13-14 years, the operation depending on the force impact on agricultural units.

**CHAPTER 8. PROBABILITY OF TRAUMATIC SITUATIONS
IN MECHANIZED PROCESSES IN AGRICULTURE USING
THE MATHEMATICAL APPARATUS OF MARKOV CHAIN METHOD**

In this paper for exploring the mechanisms of the formation of traumatic situations, the conditions and circumstances that contribute to them, and the study of the course of events leading to dangers in mechanized processes in agriculture was used mathematical apparatus developed by the probability theory for Markov random processes with discrete states and continuous time, when the transition of a system from one state to another is possible at any unknown random time. It has been established that the processes of traumatic situations and their consequences can be represented by graph structures, using four states of the "man-machine-industrial environment" system: he working and defective conditions of the tractor (machinery), hit of the machine operator into a dangerous and emergency condition (situation). It has been made a system of Kolmogorov differential equations, in which unknown functions are the probabilities of states of the system as functions of time with the normative condition that the sum of these probabilities will be equal to 1. Introducing the matrix of the intensity of events, the Laplace transform was used to solve the system of differential equations, which allowed the system to be transformed into a linear algebraic system. Elements of the matrix of intensities of the flows of events that bind separate states of the graph were given taking into account the probabilities of accidents with mechanics, established on the basis of the statistics of occupational injuries and data of the accumulation of cracks in the array of tractor parts, determined as a result of defectoscopic control. The results of research allow in the medium and long term perspective to predict the probable states of the "human-machine-industrial environment" system in the risks of professional injury of agricultural machine operators.

The system of introduction of technical means of safety and preventive measures for the prevention of occupational injuries of agricultural workers should be based on an analysis of its causes through the improvement of available methods of probabilistic assessment of the risk of emergencies, taking into account the specific features of mechanized processes in the agro-industrial complex. Therefore, the study of the mechanism of the formation of traumatic situations, the conditions and circumstances that contribute to them, the study of the nature of the course of events that lead to the dangers of mechanized processes in the agro-industrial complex, is now an actual task. It is necessary to switch from qualitative methods for analyzing the causes of occupational injuries on the basis of expert assessments to quantitative methods for assessing the probability of occurrence of emergencies involving mobile agricultural machinery, which should take into account the degree of its serviceability.

Machine-tractor aggregates (MTA), machine operators - operators of mobile agricultural machinery and parameters of the production environment when performing mechanized works in agriculture should be considered as interconnected elements of a holistic system [1]. According to some researchers, the weak link of such a system can be workers with their false actions and violations of labor safety requirements, other researchers justify the high level of traumatism of machine operators by the influence of parameters of the production environment [2]. The common understanding is that the change in the state of any of the elements of the system machine - man - production environment (M-M-PE) necessarily leads to a change in the state of the system as a whole [3]. However, the important role of the technical condition of the machine and the functionality of the safety equipment set up on it in the formation of traumatic situations often left out of focus [4].

Changes in the system of M-M-PE by their nature are considered in a separate manner: as a gradual, for example, the accumulation of scattered operational damage in an array of details of the machine nodes or the

accumulation of employee weariness during the change, and suddenly occurring at certain moments of time (detachment of parts, loss concentration of operator or critical manifestation of environmental parameters) [5]. However, the gradual accumulation of operational defects in the part (element of the design) eventually leads to the emergence and spread of a major crack of critical size, which causes the sudden failure of the machine node (unit), and therefore the onset of a dangerous situation [6].

For the analysis of sudden changes in the M-M-PE system, a mathematical apparatus developed in the theory of probabilities for Markov random processes with discrete states and continuous time is used when the transition of a system from one state to another in any unknown, random, instantaneous time t [7]. However, in developed mathematical models, the transition from a system to a faulty state is viewed primarily as a consequence of the false actions of the machine operator (or other employee) without analyzing the degree of accumulation of operational defects in an array of parts of the unit, which may be determinative for the creation of an emergency (traumatic) situation.

In this paper, the method of calculation of professional risks of mechanizers is proposed on the basis of the analysis of the graph of the states of the processes of traumatic situations during the operation of the MTA [8].

According to the methodology [9] random processes with discrete states and continuous time are considered, and the transitions of system S from one state to another are described as occurring under the influence of certain events flows. Then the probability density of the transition λ gets the meaning of the intensities (densities) of the corresponding events flows. If all these flows are Poisson (ordinary and without an aftereffect, with constant or time-dependent intensity), then the process occurring in the system S will be Markovian.

The degree of deterioration of the technical condition of tractors after prolonged exploitation in the work [7] was estimated according to the data on

the intensity of accumulation of defects (cracks) in the array of tractor parts detected during the defectoscopic control of the responsible parts (construction elements) of tractors. In the used vibration current defectoscope it was possible to switch the sensitivity to the degree of defects of different sizes [4], which allowed the total number of identified operational defects to distinguish small-sized (on the threshold of the sensitivity of the defectoscope) that at the moment did not pose a threat to the safe operation of the tractor.

To analyze the traumatic situation that may occur on mechanized processes in the agroindustrial complex, a graph of states was presented, which is presented in Fig. 8.1
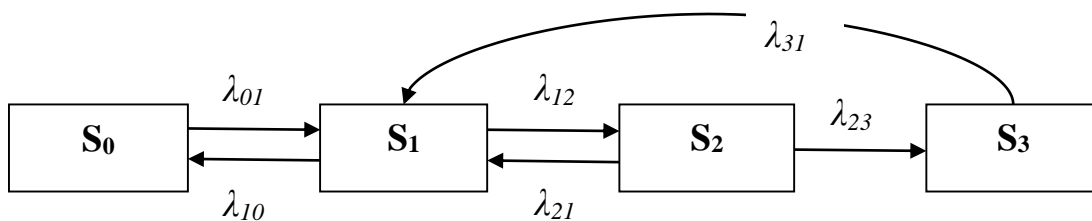
Fig. 8.1. A graph of the states of the process of the traumatic situation:

S_0 – the system is in the initial (proper) state; S_1 – the system is in a working conditionally conditional state; S_2 – the system is in a faulty state; S_3 – the state of the system is dangerous for workers servicing the agricultural unit

At the beginning of the MTA operation, the system is in good condition S_0, and after a certain period of time, from the effects of events of events with intensity λ_{01}, the state of the system deteriorates, however, it does not affect the system's robustness for some time and it can continue to function. Such a state can be characterized as a working (conditionally sound) state S_1. Being in the state of S_1, the system can return after a certain time to the state S_0 from the action of events of events with intensity λ_{10}. On the other hand, from the effects of events fluctuations with intensity λ_{12}, for example, due to non-compliance by the mechanician of the scheduled technical inspection or distribution of

truncated cracks in the details of the nodes (structural elements), the system can go into a faulty state S_2.

Consider the following options for the development of the event:

a) from the effects of events streams with intensity λ_{21} (for example, after repair of a certain node of a tractor or replacement of defective parts), the system returns to the state S_1, which may or may not continue, or subsequently, from the effects of events of events with an intensity of λ_{10}, may return to the state S_0;

b) from the events of events with intensity λ_{23} the system passes to the dangerous state S_3 with possible consequences in the form of injury to the machine operator or return to the state of S_1 from the effects of events with intensity λ_{31} (for example, due to capital repairs of the MTA).

Having analyzed the analyzed graph of states in Fig. 1, we determine the probabilities of the states of the analyzed system $P_0(t)$, $P_1(t)$, $P_2(t)$ and $P_3(t)$ as a function of time. These probabilities must satisfy the system of differential Kolmogorov equations, with probabilities of states of the system as unknown functions (8.1):

$$
\begin{cases}
\dfrac{dP_0}{dt} = -P_0\lambda_{01} + P_1\lambda_{10}, \\
\dfrac{dP_1}{dt} = -P_1\lambda_{10} - P_1\lambda_{12} + P_0\lambda_{01} + P_2\lambda_{21} + P_3\lambda_{31}, \\
\dfrac{dP_2}{dt} = -P_2\lambda_{21} - P_2\lambda_{23} + P_1\lambda_{12}, \\
\dfrac{dP_3}{dt} = -P_3\lambda_{31} + P_2\lambda_{23},
\end{cases}
\tag{8.1}
$$

where: $P_0 + P_1 + P_2 + P_3 = 1$ – is the normalization condition.

If we consider the vector-function $P(t) = (P_0(t); P_1(t); P_2(t); P_3(t))$ and the intensity matrix, then the system of Kolmogorov equations will have the form of a linear matrix system of differential equations (8.2):

$$
\Lambda = \begin{pmatrix}
-\lambda_{01} & \lambda_{10} & 0 & 0 \\
\lambda_{01} & -\lambda_{10} - \lambda_{12} & \lambda_{21} & \lambda_{31} \\
0 & \lambda_{12} & -\lambda_{21} - \lambda_{23} & 0 \\
0 & 0 & \lambda_{23} & -\lambda_{31}
\end{pmatrix}.
\tag{8.2}
$$

After solving this system of differential equations using the Laplace transform, one can find the probabilities of states of the analyzed system (8.3).

$$\begin{cases} \dfrac{d\vec{P}(t)}{dt} = \Lambda\vec{P}(t), \\ l\vec{P}(\cdot) = \sum_{i=0}^{3} P_i(0) = 1, P_i(0) \geq 0. \end{cases} \tag{3}$$

In the development of work [9] in Fig. 8.2 shows the kinetics of the accumulation of cracks in the steering system of tractors UMZ-8040.2 of different durations of operation with the allocation of the intensity of accumulation of small defects.
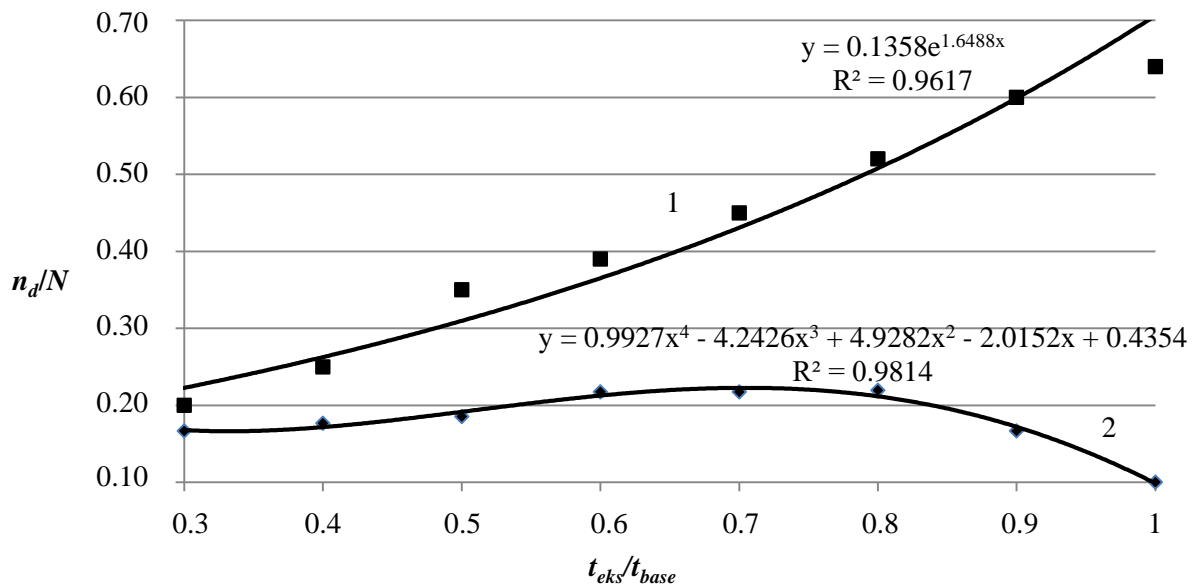
Fig. 8.2. Kinetics of the accumulation of cracks in the details of the steering system of tractors of different durations of operation:

1 – cracks without spacing in size; 2 – small cracks

The coordinates of the graphs are as follows: the ordinate axis – n_d/N – the relative number of detected cracks in the total number of investigated, significant from the point of view of safety of operation, details N; Axis abscissa – t_{eks}/t_{base} – ratio of the length of operation of tractors t_{eks} relative to the base duration $t_{base} = 17$ years. The kinetics of the accumulation of cracks is described

by the lines of the trend, the equations of which and the accuracy of the approximation are shown in Fig. 8.2.

In this paper, the probabilistic distribution of changes in the states of the M-M-PE system was obtained for a traumatic situation that may occur due to a malfunction of its steering system.

The following main reasons for the failure of the steering system of tractors were considered: the presence of operational defects (cracks) in details that are detected by defectoscopic control; presence of backlashes, curvature of details and other violations of the system, which are visual inspection and testing; violation of terms of technical inspection of tractors.

Elements of the matrix of the intensity of events (transition states of the system) were established on the basis of the following assumptions.

In the labor protection system for the diagnosis of malfunctions of tractor units and other mobile agricultural machinery, Safety Ratings have been developed, which specify the frequency and place of control of the normative parameters of the trouble-free operation of the machine nodes (unit), but the emphasis is made on the visual (optical) control without the use of defectoscopic equipment.

This allows you to detect a significant discrepancy in security parameters at the transitional stage. That is, non-compliance with the periodicity of such a control of the technical state will indicate the high probability of the system transition to a dangerous state.

In this paper, it was believed that the transition of the system from a normal state to a dangerous state (in relation to the safety of a machine operator), in addition to other circumstances related to the activities of the machine, may be due to the presence of a certain (critical) number of operational defects in a plurality of parts of the tractor's units that were defectoscopic control. That is, as a good condition of the system, the absence of operational defects or the presence of defects in the initial stages of their formation (that is,

only small size), which in the near future will not lead to sudden failures (accidents) of technology, were considered.

The failure of the system will be consistent with the absence of security equipment or cracking on the unit, which may subsequently overflow into the mains and cause the system failures (emergency situations). In the event that the company will not take measures to repair the unit, the situation becomes dangerous (corresponding to the dangerous state of the system). How dangerous it is possible to consider a situation (a dangerous state of the system), when the density of defects in an array of parts of the unit exceeds a certain critical value.

The number of tractors with a faulty steering system can be estimated from the data of 2018, when the mobile agricultural machinery held an annual state technical review. Thus, the number of tractors standing on the balance sheet of agricultural enterprises amounted to 190.375 units. Of these, 146.172 tractors were submitted for the state technical inspection. During the check, technical faults were detected in 33.383 tractors, which is 22.8%.

As a result of the analysis of diagrams in Fig. 2 it was proposed the following coefficients of intensity characterizing the intermediate states of the studied system:

1. We assume that at the initial stages of operation ($t_{eks} = 0.3$) the intensity ratio will be $\lambda_{00} = 1.00 - - 0.22 - 0.16 = 0.62$, which corresponds to the proper condition of the tractors.

2. At the intermediate stage of operation ($t_{eks} = 0.5$), the technical condition of tractors passes to the category conditionally serviceable due to the presence of details of operational defects ($\lambda_{01} = 0.38$). For tractors that are in the working condition (conditional condition), small cracks at present do not constitute a threat of sudden failure, the same $\lambda_{10} = 0.22$. Then the working conditional state of the tractors will characterize the intensity coefficient $\lambda_{11} = 1.00 - 0.38 - 0.22 = 0.40$.

3. For a faulty state, a significant accumulation of cracks of a critical (dangerous) size ($\lambda_{12} = 0.44 -- 0.22 = 0.22$) is characteristic for the maximum intensity of small cracks ($\lambda_{21} = 0.22$).

4. If the defectoscopic control of the responsible parts of the tractor is not carried out, the system at the exploitation phase ($t_{eks} = 0.9$) will be dangerous for workers ($\lambda_{23} = 0.6 - 0.17 = 0.43$).

5. In the case of a technical inspection of tractors in accordance with the Safety Data Acquisition Control Maps, the part of the parts of the tractor units will be found to be in conformity with the safety requirements, these parts will be replaced and the state of the tractor will pass from the dangerous to the working ($\lambda_{31} = 0.228$).

We will have a matrix of transition states of the system (8.4):

$$\Lambda = \begin{pmatrix} -0.38 & 0.22 & 0 & 0 \\ 0.38 & -0.44 & 0.22 & 0.228 \\ 0 & 0.22 & -0.65 & 0 \\ 0 & 0 & 0.43 & -0.228 \end{pmatrix}. \tag{8.4}$$

The set of probabilities of states of the system can be obtained after solving the Kolmogorov equation with the condition of normalization (8.5):

$$\begin{cases} P_0(t) = 0.907c_1 - 0.302c_2(0.477)^t - 0.052c_3(0.514)t - 0.608c_4(0.747)^t, \\ P_1(t) = 1.567c_1 + 0.495c_2(0.477)^t + 0.067c_3(0.514)t - 0.243c_4(0.747)^t, \\ P_2(t) = 0.53c_1 - 1.194c_2(0.477)^t - 1.015c_3(0.514)t - 0.149c_4(0.747)^t, \\ \quad P_3(t) = c_1 + c_2(0.477)^t + c_3(0.514)t + c_4(0.747)^t. \end{cases} \tag{8.5}$$

In order to fulfill the condition of valuation, it is necessary to put the constant $c_2 = c_3 = 0$; $c_1 = 0.25$; $c_4 = 0.01$.

The functions of states are represented in the following form (8.6):

$$\begin{cases} P_0(t) = -0.00608(0.747)^t + 0.23, \\ P_1(t) = -0.00243(0.747)^t + 0.39, \\ P_2(t) = -0.00149(0.747)^t + 0.13, \\ \quad P_3(t) = 0.01(0.747)^t + 0.25. \end{cases} \tag{8.6}$$

Graphs of calculated kinetic dependencies of probabilities P states of the system are presented in Fig. 8.3.
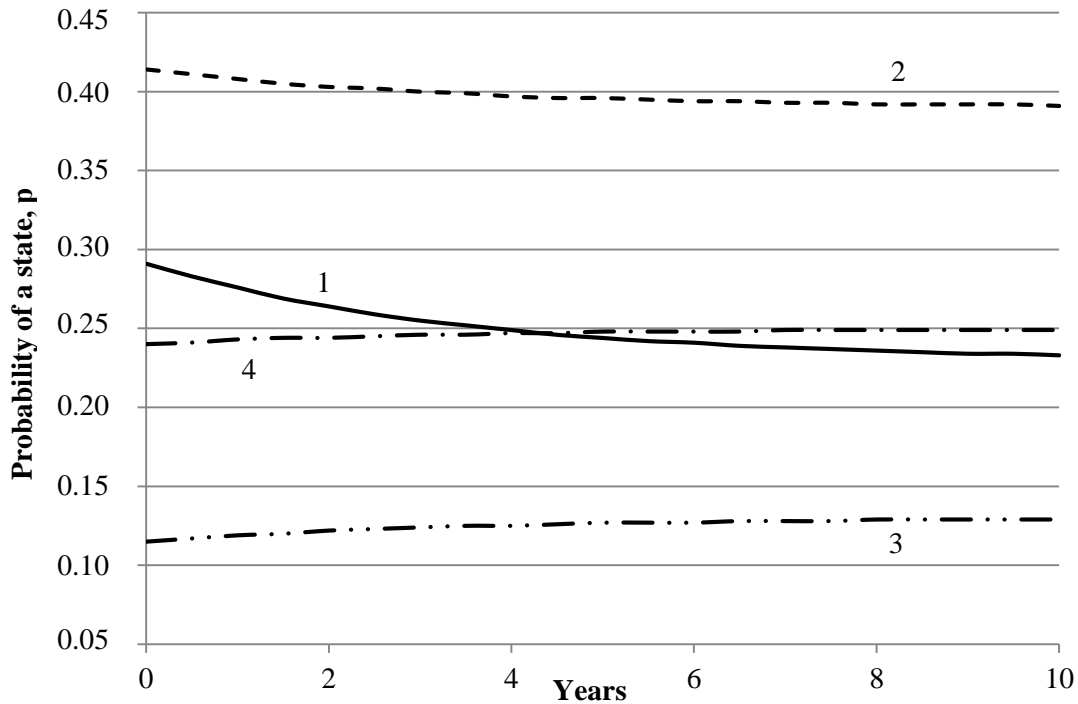
Fig. 8.3. Charts of kinetic dependences of probabilities P states of the system:

1 – the normal state S_0; 2 – conditional condition S_1; 3 – faulty state S_3; 4 – dangerous condition S_4

The final probabilities of the states of the system will be: $P_0 = 0.23$; $P_1 = 0.39$; $P_2 = 0.13$; $P_3 = 0.25$. This means that in the long run (10 years), 23% of the units will work in good condition S_0, 39% and 13% will switch respectively to defective S_1 and dangerous S_2 states, causing a dangerous situation to occur. The probability of a system transitioning to a critical state of S_3 (traumatizing the machine) in this case will be 25%. The probability of a system transitioning to a critical state of S_3 (traumatizing the machine) will be 25%.

Conclusions to chapter 8

1.	The method of investigation of changes in occupational risk at mechanized works in the agro industrial complex, taking into account the degree

of accumulation of operational defect in an array of parts of the MTA, is developed.

2.   It was established that the processes of the course of traumatic situations and their consequences can be represented by graph structures, confined to four states of the system "man-machine-industrial environment": a conditional, conditional and defective condition of the tractor (machine), the entry of the machine operator into a dangerous (emergency) state (situation).

3.   It is shown that the obtained results allow in the medium and long term to predict the probabilities of the states of the system "man-machine-industrial environment" in the categories of occupational risk of traumatizing agricultural mechanics.

CHAPTER 9. STUDYING TRUCK TRANSMISSION OILS USING THE METHOD OF THERMAL-OXIDATIVE STABILITY DURING VEHICLE OPERATION

Reliability of transport vehicles is determined by the processes occurring in tribological systems of "materials of mating parts – oil" type. These systems can be characterized by running-in modes, coefficient of friction, wear resistance and self-organization having a direct effect on operating capacity of oil. Comprehensive evaluation of oil properties during operation forms a prerequisite for priority solution of the issue of improving operational reliability of vehicle systems and units.

At present, reliability of mechanical systems is raised by selecting durable structural materials and oils for them. Choice and application of wear-resistant materials is studied more intensively and a significant progress has been achieved in machine designing. Choice of lubricants for mating various systems and units of machines operating in certain ranges of temperatures, loads and speeds refers to more complex problems. This is because one type of oil is often used in one unit and mating parts are made of structural materials having a wide range of mechanical properties. Besides, lubricant markets offer a wide variety of oils poorly substantiated for their use in various mechanisms of transport vehicles. Operating life of oils on mineral, synthetic and mixed bases is taken constant. It is regulated by producers based on machine-hours or run mileage for wheeled vehicles. These parameters do not take into consideration modes and conditions of operation, technical state of mating parts, state and availability of an oil filtering system and actual oil properties.

The process of friction and wear of the mating parts during operation depends to a large extent on the lubricant properties. Oil properties (viscosity,

oxidation, friction, dispersity, etc.) are formed with the help of additives in technological operations of oil production. Change of operational properties of oils is caused by oxidation processes, temperature and mechanical degradation, chemical reactions on the materials of mating parts as well as the products formed in oil ageing.

Oxidation of the working oil proceeds more intensively on working surfaces of the mating parts because of high temperatures and catalytic influence of the part materials. Besides, this process reflects connection and effect of elements of the "mating parts materials – oil" tribological system on operational reliability of systems and units of transport vehicles in general. In this regard, it is very important to determine state of working oils by controlling their thermal-oxidative stability. Diagnosis of this property of transmission oil enables improvement and finding possibility of forming a rational diagnostic database of technical state of the vehicle power units. This is a relevant scientific and technical problem.

As a rule, oxidation processes in oils are estimated by acid number and are standardized for some oil grades. Analysis of patents and scientific and technical literature has shown that there is a large variety of engineering methods and devices for assessing thermal-oxidative stability. The following indicators are proposed to be considered as main indicators: magnitude of viscosity change, electrical conductivity, number of deposits on parts, specific dielectric losses in presence and absence of a catalyst, coefficient of light absorption [1]. Auxiliary but not less important indicators of oil include sedimentation period, tendency to lacquer formation, optical density, concentration of insoluble contaminants, mass working and lacquer fractions, evaporability, corrosion properties, etc. [2]. However, most of these indicators are impractical because of lack of standardized industrial means of control. Part of the indicators of the oil state study requires expensive equipment and is only used in laboratory conditions.

Application of rapid methods for studying mating parts of assemblies and units on the basis of tribotechnical tests is described in [3]. Detection of abrasive particles in the medium is an important problem. It is realized with the use of friction machines but the authors did not offer solution to the problem of determining the quantity and size of abrasive particles during operation. The issue of application of non-destructive methods is solved on the basis of analysis of oils for vehicles. Particular attention is paid to controlling dielectric permeability, electromagnetic inspection of oils and other diagnostic parameters of the lubricant state [4]. Urgency of conducting non-destructive oil control is determined by increasing efficiency of forming diagnostic databases for vehicle units. Further improvement of technical service requires control of the load-carrying ability of oils during operation which was not realized by the authors by means of control of technical state of oils by rapid test methods.

Based on available theoretical and applied aspects of the oil state study, it is often impossible to draw a conclusion on operating state of the oil used in hydraulic systems even when diagnostic parameters are within their tolerance field [5]. In the process of operation of mating parts, abrasive particles fall into oil causing destruction of parts and increase in activation of their surface layers that makes impossible to establish exact mechanic effects in hard operating conditions. Therefore, the authors decided to replace certain executive mechanisms with pneumological elements and thus dispense with hydromechanic mechanisms.

It is important for technical maintenance to forecast service life of vehicle units [6]. In order to solve this problem, it is necessary to diagnose units in a timely and qualitative manner and perform necessary operations of technical service. It was proposed to solve this issue with the help of magnetic sensors and online control of stationary power units. Instead of further implementation in mobile machines, these methods have not found their application. It is also

impossible to develop recommendations regarding conformity of working oils to operating conditions on their basis.

The main cause of failure of power units is growing degree of wear and degradation of consumables [7]. These processes can be monitored in aggregate on the basis of oil diagnosis by spectral analysis. However, their actual development degree and behavior stages are difficult to assess. To cope with this problem, diagnostic data are analyzed and a model of the space of states of mating parts in the vehicle power units is constructed. Regarding the diagnostic data of oil efficiency in the zone of inter-boundary values of wear product concentration, they may have overshoots in the forecast period because of impossibility of comprehensive consideration of characteristics of working oils by spectroscopy and their reaction to temperature regimes.

Reliability and service life of wheeled vehicles generally depend on technical state of their power units. About 25 % of transport companies claim that they are facing failures of transmission switchboxes associated with oil state [7]. These failures are most of all related to extreme running regimes and elevated operating temperatures which cause growth of stress concentrators on the work surfaces of oil seals, bearings, and gear teeth. Growth of stress concentrators is stimulated by high oxidation of the oil and rapid worsening of its working state. Additives protect seals and improve thermal and oxidation balances and viscous stability [8]. Solution to these problems was achieved through the use of environmentally friendly oils with a certain complex of additives, which attack the mating parts weaker. However, in order to introduce them in vehicle operation, it is necessary to develop a control system that would determine an adequate model of change of technical state of working oils.

The use of oils that do not meet specifications, untimely diagnosis and replacement of oil contribute to its rapid oxidation and development of micro-pitting of parts potentially resulting in the unit failure [9]. These issues were solved on the basis of development of an additive complex for oils but the

authors did not provide control during operation. To prevent occurrence of such problem situations, it is necessary to develop a procedure for controlling technical state as for thermal-oxidative stability.

The use of environmentally friendly oils contributing to achievement of energy independence and security through their natural resource recovery is not always effective. Their use is limited by low thermal-oxidative stability and unsatisfactory properties during the cold period of operation of the vehicle systems and units [10]. Improvement of quality of working environmentally friendly oils facilitates search for a combination of additives based on a systematic approach. This reflects the need for creation and use of oils with high thermal-oxidative stability. At the same time, the issue of controlling oil by the indicator of thermal-oxidative stability during operation is not resolved yet which is a very persuasive necessity of introduction of such oils into production and development of instructions as regards their compliance.

Mineral oils operating in severe conditions are strongly subjected to oxidative reactions caused by access of oxygen, water and abrasive metal particles that affect oil performance [11]. The authors have carried out studies of oil oxidation using antioxidants and metal passivators to evaluate and compare thermal-oxidative stability. Thermal-oxidative stability was controlled by observing acid number and content of carbon clusters in oxidized samples of oil in a form of a sediment. All this did not accurately reflect change and action of additives and oil fractions. Implementation of such a scheme in operation requires significant time inputs for even a single study of technical state of the oil.

Environmentally friendly vegetable oils have satisfactory tribological and environmental properties but instead they lack full thermal and hydrolytic stability [12]. The effect of thermal oxidation on lubricating and physical-chemical properties of oil was determined in this study. A method of visible-light spectroscopy was introduced to estimate oil oxidation rate. However, this

method did not allow the authors to comprehensively describe the process of variation of temperature stability of the oil under study. It just established initial moments of structural change.

Therefore, it is necessary to develop methods for studying technical state of oils for the transmission units intended for liquid lubrication and for mobile machines on the basis of which one could judge on the oil compliance to operating conditions. These recommendations can be elaborated in more detail with introduction of complex procedures for determining thermal-oxidative stability of working oils.

The study objective was to identify patterns of change of thermal-oxidative stability of the working oil and develop a method for assessing its working state which would enable improvement of the system of technical maintenance and working out recommendations concerning oil conformity to operating conditions.

To achieve this objective, the following tasks were addressed:

– develop a procedure for studying oil state regarding thermal-oxidative stability and formulate necessary analytical expressions for its realization;

– obtain regularities of variation of characteristics of the transmission oil oxidation process during operation;

– substantiate expediency of use of a transmission oil based on the study of its state regarding thermal-oxidative stability.

The following oil grades were chosen for the study.

– YUKO TO-4 80W-85 (conformity to SAE 80W-85, API GL-4) with the following characteristics:

1) kinematic viscosity at 100 °C, mm^2/s: 12.0;

2) density at 20 °C, kg/m^3: 890;

3) viscosity index: 95;

4) flash temperature in open crucible, °C: 225;

5) congelation point, °C: –25.

– Tedex Gear GL-4 80W90 (conformity to SAE 80W-90, API GL-5) with the following characteristics:

1) kinematic viscosity at 100 °C, mm^2/s: 14.6;

2) density at 20 °C, kg/m^3: 920;

3) viscosity index: 105;

4) flash temperature in open crucible, °C: 228;

5) congelation point, °C: –33.

The above oil grades were sampled from KamAZ 6520 trucks (3 trucks) and MAN TGA 6×4 trucks (3 trucks) involved in transportation works at ATP 2004 enterprise, Kropyvnytsky, Ukraine. Samples were taken during each technical maintenance service No. 2 in a quantity of 250 ml of oil (by 40 ml for three repeat examinations) from each gearbox according to DSTU 4488:2005. The samples were taken in the oil level measuring and filling points of gearboxes of corresponding vehicle models.

To determine thermal-oxidative stability, TOS-10 (Electronprylad NTK) device was used (Fig. 1) which consisted of a mechanical and an electric unit. The mechanical unit containing a glass beaker with a heater insulated from external environment by thermal insulation and enclosed in a case with a handle. Output of the heater is connected to the electric unit through a plug. A glass container with a sample is put on a platform with hinges with a possibility of its removal. The platform is locked in the top position. A thermocouple and a glass stirrer connected to the electric motor ensuring the stirrer rotation are immersed in the vessel. The electric unit consists of TRM-200 thermoregulator and power sources for the heater and the micromotor.

a   b

c   d

Fig. 9.1. Instruments used in the study of thermal-oxidative stability of oils:

TOS-10 laboratory device for thermal oxidation of oils (Ukraine) (a); KFK-2 photoelectric colorimeter for measuring concentration (Russia) (b); TVE-0.21 laboratory balance (Ukraine) (c); VPZhT-2 viscosimeter (Ukraine) (d)

TVE-0.21 laboratory balance (Fig. 9.1, *c*) for a maximum weighing mass of 300 g and error value of 0.01 g is intended for measuring mass of the evaporated oil. Measurement was performed before the start and at the end of the oxidation process.

Photometric equipment is intended for estimation of pollution of industrial hydraulic, motor and transmission oils. Coefficient of light absorption is the indicator of oil evaluation in this case. Photoelectric device KFK-2 (Fig. 9.1, *b*) consists of optical and measuring units. The optical unit is intended for direct

photometry of oils with various transparencies. Photometric cuvette is intended to form a photometric layer of oil of a given thickness. Cuvettes of 3 mm in length were used in experimental determination of the coefficient of light absorption. Stabilized monochromatic light passes through a layer of the oil under study to the photodetector.

Depending on concentration of mechanical impurities and oil oxidation products, the photodetector receives light flows inversely proportional to concentration of impurities. Optical density of oil was measured on the KFK-2 device which enables measurement of optical density in a range from 0 to 2 units. Photometric examination of oil was carried out at an optical wavelength of 440 nm. The sensitivity coefficient in mode 2 was determined in 15 to 20 minutes after the device switch-on. The cuvette compartment was open during warming up. Working surfaces of the cuvette were cleaned with an alcohol-ether mixture before each measurement. A fresh portion (40 ml) of oil was poured into the measuring flask and diluted with 4 ml of solvent (benzene). The mixture was stirred and then three samples of 10 ml each were poured into cuvettes. The samples of pure oil needed setting of the photocolorimeter pointer to the zero mark. When the pointer moved from zero position, it was set back using the rotary knob "set 10 coarse" and "precise". Following the zero setting for a fresh oil sample, the photometer was ready to measure working oils. After replacement of the control oil solution in the KFK-2 cuvette holder with 40 ml of working oil diluted with 4 ml solvent (benzene), optical density of the oil under study was read from the device scale. Repeated measurements were performed three times in a row with calculation of the mean value of optical density of the oil.

It is known that resistance of working oils to oxidation determines their antioxidant properties. High intensity of oxidation occurs on surfaces of the parts subjected to high temperatures (above 90 °C). Tests for thermal-oxidative stability were carried out by means of a device simulating oxidation processes in

the working mating parts during operation of transmission oils in the truck gearbox. The process of study on thermal-oxidative stability was carried out as follows. A 250±0.1 ml oil sample was poured into device determining thermal-oxidative stability in which it was maintained at 180 °C with stirring at 350±3 rpm. To eliminate influence of metals on the oxidation processes, the glass and the stirrer were made of glass and the stirrer speed was optimized to achieve maximum oxidation rate while avoiding turbulence. The test time was 3 hours. The samples were weighed each hour to determine mass of the oil evaporated and samples were taken for photometry. The residual volume of the oil under test was re-oxidized.

Photometry of oxidized oils was carried out at a 2 mm thickness of oil layer. Limit values of the coefficient of light absorption and evaporability of the transmission oil were equal to 0.7 un. and 0.15 un., respectively. The determined limits were derived on the basis of tribological studies of oils according to ASTMD 2783. Based on the measurement results, graphic dependences of the coefficient of light absorption and evaporability on the oxidation time were plotted. The coefficient of thermal-oxidative stability, K_{TO}, was determined from the following formula:

$$K_{TOS} = K_{lf} + K_e, \tag{9.1}$$

where K_{lf} is the coefficient of light absorption; K_e is the coefficient of oil evaporability:

$$K_e = m_{bi} / m_i, \tag{9.2}$$

where m_{bi} is the mass at the beginning of the i-th oxidation, g; m_i is the mass after the i-th oxidation, g.

Kinematic viscosity of the oil under study was determined according to DSTU GOST 33-2003 by means of viscosimeter of VPZhT-2 type (ISO 3105-76). Graphic dependences of viscosity measurement during oil oxidation are presented by the coefficient of relative viscosity:

$$K_v = \nu_{0i} / \nu_i, \tag{9.3}$$

where ν_{0i} is the kinematic viscosity at the beginning of the *i*-th oxidation, m^2/s; ν_i is the kinematic viscosity after the *i*-th oxidation, m^2/s.

Reliability of the device readings and experimental data on determination of the coefficient of light absorption and evaporability was checked in three experiments with corresponding grades of oils in each diagnosis. In this case, absolute and relative deviations were determined. To process the study results, licensed Excel 2007 program was used which computed the mean square deviation, correlation coefficient, regression coefficient and mean approximation error.

The mean square deviation to estimate the magnitude of the random error in the diagnostic results was calculated from formula:

$$S_{D_j} = \sqrt{\frac{\sum(\overline{D_j} - D_{ji})}{n-1}}, \tag{9.4}$$

where *n* is the number of repetitions; $\overline{D_j} = \frac{1}{n}\sum_{i=1}^{n} D_{ji}$ is the diagnostic parameter; D_{ji} is the diagnostic parameter at the *i*-th diagnosis repetition. To characterize magnitude of the random error, a confidence interval and a confidence probability value were determined which allowed us to estimate degree of reliability of the diagnosis result. The confidence probability in measurements was limited by γ=0.95. Therefore, for each indicator measured at different test temperatures, the confidence interval was determined from formula:

$$\Delta\tau_{\overline{D_j}} = 2 \cdot \frac{t_\gamma \cdot S_{D_j}}{\sqrt{n}}, \tag{9.5}$$

where t_γ is Student's criterion for α=1−γ.

The mathematical model of development of the investigated processes was constructed and evaluated according to the method of least squares and the coefficient of determination:

$$R^2 = 1 - \frac{\sum_{i=1}^{n}(D_{ji} - D_{j.theor.})}{\sum_{i=1}^{n}(D_{ji} - \bar{D})^2},$$ (9.6)

where D_{ji}, $D_{j.theor.}$, $\bar{D}$ are actual, theoretical and mean values of the function of the process described by the *j*-th diagnostic parameter.

Diagnosis of the transmission oil according to the above techniques is important for technical service at the enterprises operating transport equipment. Therefore, they were selected to ensure minimum time for implementation.

Samples of working oil were taken from gearboxes of operated vehicles for studying and determining thermal oxidation stability of oils. The studied oils contained thickening additives resistant to degradation. All data of the technical state of transmission oils are shown in Tables 9.1, 9.2.

Table 9.1

Averaged data of the state of the YUKO TO-4 80W-85 transmission oil (KamAZ 6520, 3 trucks.) regarding thermal-oxidative stability during operation of the vehicles in 2018

Run, 1000 km	Coefficient of light transmission	Coefficient of evaporability	Coefficient of thermal-oxidative stability	Coefficient of relative viscosity
0	0.45	0.141	0.591	1.6
12	0.68	0.145	0.825	1.9
24	0.72	0.147	0.867	2.1
36	0.79	0.151	0.941	2.4
48	0.81	0.158	0.968	2.52

The experimental data in Table 1 are graphically represented in Fig. 9.2, 9.3 and their mathematical models were obtained for a coefficient of determination not less than 0.95.
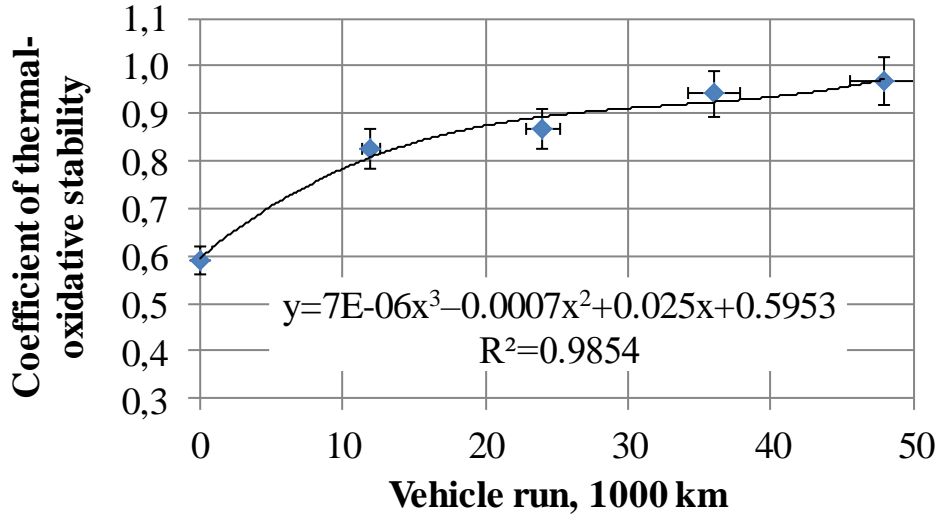
Fig. 9.2. Variation of the coefficient of thermal-oxidative stability of the YUKO TO-4 80W85 transmission oil depending on the vehicle run
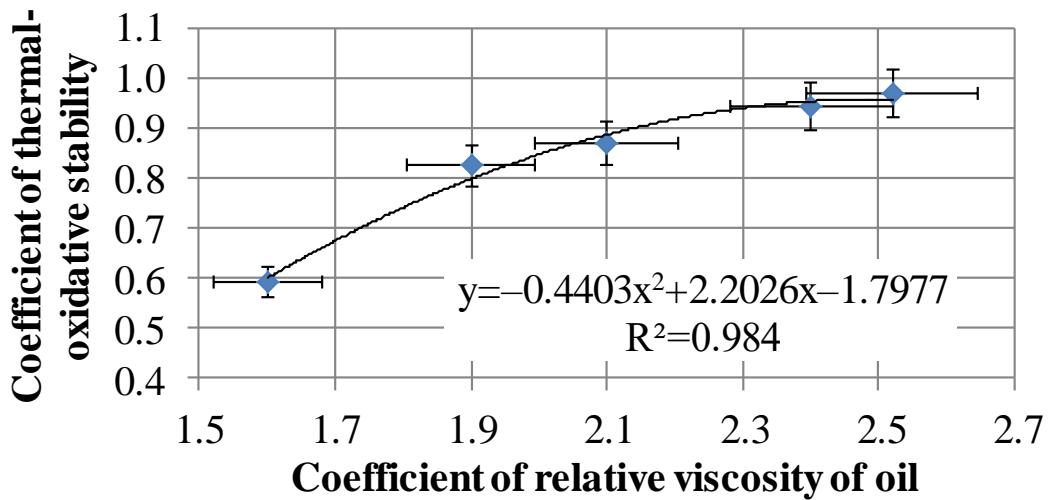
Fig. 9.3. Variation of the coefficient of thermal-oxidative stability of the YUKO TO-4 80W85 transmission oil depending on the coefficient of relative viscosity of the oil

Table 9.2

Averaged data of the study of the Tedex Gear GL-4 80W90 (MAN TGA 6×4-3) transmission oil by thermal-oxidative stability during operation of vehicles in 2018

Run, 1000 km	Coefficient of light transmission	Coefficient of evaporability	Coefficient of thermal-oxidative stability	Coefficient of relative viscosity
0	0.55	0.121	0.671	1.7
12	0.57	0.127	0.697	1.85
24	0.66	0.129	0.789	2.04
36	0.69	0.131	0.821	2.1
48	0.71	0.135	0.845	2.15

The experimental data in Table 2 are graphically represented in Fig. 9.4, 9.5 and mathematical models with indicated boundaries and estimates were obtained. The coefficient of determination was greater than or equal to 0.95.

The equation shown on the figure:

$$y = -4\text{E-}06x^3 + 0.0002x^2 + 0.001x + 0.6685$$
$$R^2 = 0.9808$$
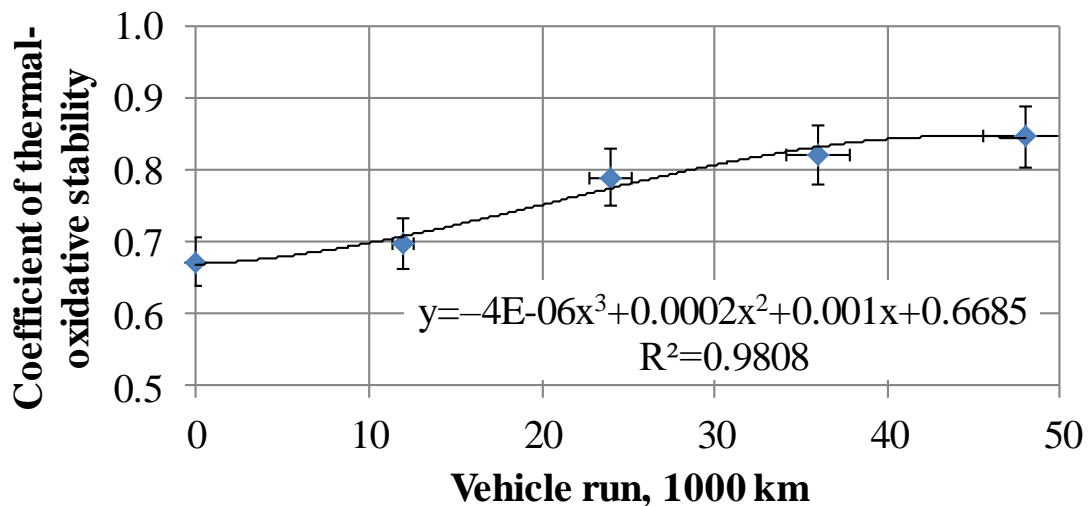
Fig. 9.4. Variation of the coefficient of thermal-oxidative stability of the Tedex Gear GL-4 80W90 transmission oil depending on the vehicle run.
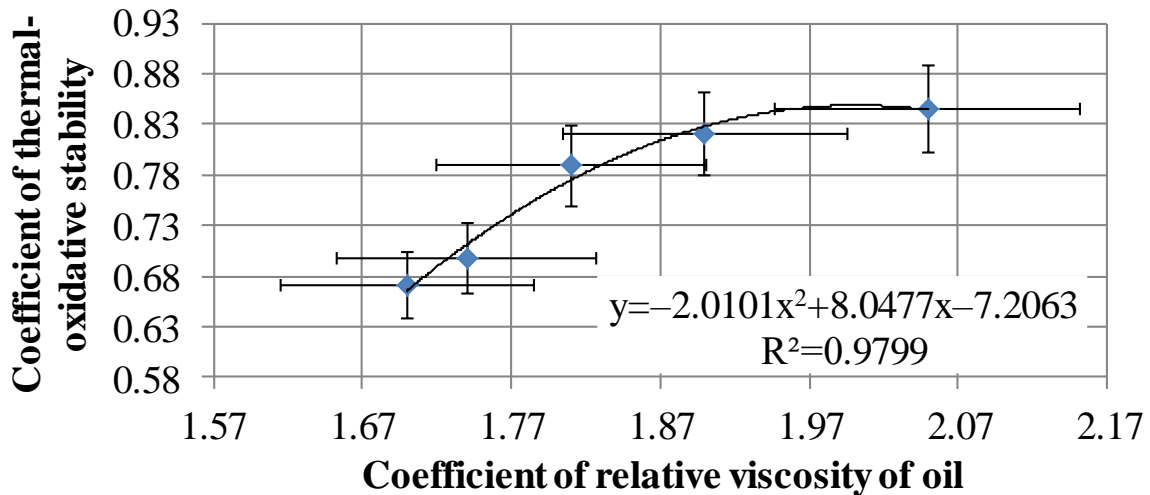
Fig. 9.5. Variation of the coefficient of thermal-oxidative stability of the Tedex Gear GL-4 80W90 transmission oil depending on the coefficient of relative viscosity of oil

Variation of thermal-oxidative stability of the transmission oil also reflects variation of relative viscosity of oil which additionally takes into consideration conditions of action of additives, their additional elements and formation of clusters of waste inclusions in the oil. Control of these inclusions and subsequent oil efficiency were determined by the oil stability relative to the temperature factor.

The process of the transmission oil oxidation stimulates changes in optical properties, volatility and viscosity. Under these conditions, it should be assumed that viscosity changes as a result of action of the set of additives and formation of clusters of oxidation products, therefore, oil efficiency should be evaluated by the coefficient of thermal-oxidative stability which is determined from expression (9.1). This coefficient characterizes amount of excess thermal energy absorbed by the products of oxidation and evaporation of acid inclusions in the oils under study.

Analyzing the results of the study of thermal oxidation stability of the YUKO TO-4 80W-85 transmission oil in KamAZ 6520 (3 pcs.), replacement of

oil every 48 thousand km does not provide conformity to operating conditions. This is evidenced by Fig. 1 according to which mathematical model of variation of thermal-oxidative stability at a run of 14 thousand km is beyond the permissible limits. In addition, in the range of 14–48 thousand km, the level of this diagnostic parameter of the oil exceeds the value of 0.85 units. This character of the process development reflects nonconformity of the oil of the studied grade to operation modes of KamAZ 6520 trucks.

Increase in viscosity of transmission oil provides initial conditions for lubrication of gearbox teeth but cannot provide proper friction mode in operation. In such conditions, incoming of the required portion of oil is impeded which contributes to overheating of the gearbox parts and thus intensifies the process of oil oxidation. Fig. 3 shows variation of relative viscosity of the YUKO TO-4 80W-85 transmission oil. Change of this parameter by more than 1.96 characterizes degradation of additives and formation of wear product clusters. Transformations in such short runs occurred because of non-conformity of the used oil grade to the modes of operation of the KamAZ 6520 trucks. Therefore, its use should be reconsidered for the trucks operated by ATP 2004 enterprise, Kropyvnytsky, Ukraine, taking into consideration the results of study of respective vehicle models.

When analyzing the results of study of thermal-oxidative stability of the Tedex Gear GL-4 80W90 transmission oil for MAN TGA 6×4 trucks (3 trucks), its conformity to operation conditions was found ensured. This conclusion was made on the basis of absence of a significant increase in the mathematical model in Fig. 9.4 and also the level of thermal-oxidative stability of oil lower than 0.85 un. during trial period of operation. When analyzing behavior of dependence of variation of the coefficient of thermal-oxidative stability of the oil depending on growth of its viscosity, it was found consistent with the loading regimes. Also, this behavior of development of the mathematical model in Fig. 9.5 shows gradual degradation of the oil components during operation. These regimes are

rational and show the oil conformity to the technical maintenance of transport vehicles.

The results of experimental studies of the coefficient of thermal-oxidative stability indicate that the results of studies of coefficients of light transmission, evaporability and relative viscosity must be taken into consideration when determining operating capacity of the transmission oil. The above-mentioned has formed the basis for development of a procedure for determining expiry term of oil operating capacity based on the study results.

Limitations of the study of the coefficient of light transmission were established only for percentage of benzene in the test sample of the working oil which should not exceed 10 %. It was because a significant scatter of recurrent output experimental results took place. It is desirable to conduct study of thermal-oxidative stability in a temperature range no more than 180–182 °C with laminar stirring of the working oil. In turn, this ensures gradual oxidation of oil throughout its volume in a measuring flask without local overheating which additionally prevents formation of significant carbon clusters in it.

Study of thermal-oxidative stability of transmission oils makes it possible to determine whether the oil grade was correctly selected. Further studies of this diagnostic parameter will make it possible to solve the problem of selecting the complex of additives for oils and establish possibility of their addition during operation. Further study of the technical state of transmission oils by their thermal-oxidative stability will enable establishment of the vehicle runs at which working oil additives should be used for a guaranteed period of oil operation.

Conclusions to chapter 9

1. Experimental studies have established variation of thermal-oxidative stability depending of the vehicle run using results of studies of the coefficients of light transmission, evaporability, and relative viscosity. The corresponding

regression equations of variation of the coefficient of thermal-oxidative stability depending on the vehicle run and the ratio of relative viscosity of YUKO TO-4 80W-85 and Tedex Gear GL-4 80W90 transmission oils during operation of KamAZ 6520 and MAN TGA 6×4 trucks were obtained.

2. It was found that YUKO TO-4 80W-85 transmission oil does not provide its functional capacity for a 14-48 thousand km run for KamAZ 6520 trucks. This was evidenced by acquiring of values of the function of the mathematical model which describes change of thermal-oxidative stability of the oil depending on relative viscosity. It was 0.968 un. for the studied vehicle runs which is greater than the permissible level of 0.85 un. Behavior of variation of the coefficient of thermal-oxidative stability depending on relative viscosity in certain zones outside the permissible limits characterizes destruction of additives and formation of clusters of wear products which also characterizes noncompliance of the given oil to operating conditions.

3. Tedex Gear GL-4 80W90 transmission oil used in MAN TGA 6×4 trucks, met the operating conditions by its thermal-oxidative stability. This is evidenced by acquisition of a maximum value by function of the mathematical model describing variation of thermal-oxidative stability of oil depending on relative viscosity for the studied vehicle runs. Relative viscosity was 0.8450 un. which is less than the permissible level. Behavior of variation of thermal-oxidative stability depending on relative viscosity reflects gradual degradation of additives in the working oil.

CHAPTER 10. COMPUTATIONAL FLUID DYNAMICS INVESTIGATION OF HEAT-EXCHANGERS FOR VARIOUS AIR-COOLING SYSTEMS IN POULTRY HOUSES

The paper presents the improved environment control system in a poultry house. The processes of heat- and mass-exchange in the developed heat-exchangers for various ventilation systems have been investigated. Computational Fluid Dynamics analysis of the heat-exchangers of two various designs for tunnel and side ventilation systems has been carried out. The fields of velocities, temperatures and pressures in the channels under study have been obtained. The conditions of a hydrodynamic flow in the channels have been analyzed. The intensity of heat-transfer between a hot heat carrier and a cold one through their separating wall has been estimated. The most efficient heat-exchanging apparatus has been determined and the application potential of such a design has been substantiated.

The increase in the productivity of poultry plants is connected with the necessity to create the optimal controlled environment in poultry houses. Here, an important task is the development of new approaches and principles of solving the problem of incoming-air cooling and heating in poultry houses during summer and winter periods. This problem is of prime importance due to the decrease of poultry plant productivity caused by the imperfection of the existing controlled environment systems in summer seasons under high temperatures and moisture of the outside air. It is worth mentioning that the existing power supply systems in poultry houses require heavy energy expenditures and costs for providing a controlled environment in poultry buildings. Thus, the necessary prerequisite to resource conservation in this branch is conducting new investigations on the improvement of controlled environment systems at poultry plants.

Papers [1, 2] present Computational Fluid Dynamics (CFD) modelling of the flows of air and heat-mass exchange in the poultry buildings equipped with a side ventilation system. The authors of [1, 2] suggest that the method of side mechanical ventilation is more effective compared to other methods and is able to decrease heat stress and increase poultry operation productivity in summer seasons. As a result of the mathematical modelling conducted in [1, 2], the distributions of air flow velocities, pressures and temperatures in poultry houses with side ventilation systems have been obtained. The results of the conducted mathematical modelling have been compared to the experimental research data and the difference does not exceed 12%. According to the calculations presented by the authors of the research [1, 2], it has been concluded that insufficient air velocity as well as the absence of a cooling system increases poultry heat stress resulting in the decrease of beeding productivity. This is promoted by non-uniform air flow in the area of bird location and dead-air zones, that make the conditions for poultry thermoregulation worse.

The paper [4, 5] considers the system of outside air cooling by means of a heat-exchanger of a specific design [6, 7], which uses subterranean well water as a cooling medium. Mathematical modelling of heat- and mass-exchange processes in the course of air ventilation in the poultry buildings, where the arrangement of ventilation equipment is high adjusted, has been conducted. As a result of the numerical modelling, the fields of velocities, temperatures and pressures in a poultry house have been determined.

In the course of developing new types of heat-exchanger designs, such factors as their small-size characteristics, the efficiency of heat transfer through the surface that separates heat carriers, pressure loss in the circuits of every heat carrier and other parameters that characterize heat exchange units are of great importance [8]. Another important analysis tool for determining the efficiency of the developed heat exchanger design is a detailed mathematical modelling of mass and energy transfer processes in a heat exchanger [9-17]. Such modelling

allows for analyzing local hydraulic and thermal characteristics on heat exchange surfaces, determining their thermal efficiency and estimating hydraulic losses that determine the capacity of the pumps used for bleeding heat carriers.

The most wide-spread designs of heat-exchangers, which are mainly used in heat-exchange equipment, are recuperative heat-exchangers.

As a rule, shell-and-tube heat-exchangers have staggered or in-line arrangement of tube banks and their conditions of hydrodynamic flow and heat transfer have been investigated in details in a number of scientific papers [18-21].

However, hydrodynamics and hear transfer in the case of small-diameter tube banks have been under-investigated. It is worth mentioning that the use of such heat exchange surfaces in shell-and-tube heat-exchangers allows for improving their physical and cost performance compared to the known designs.

The aim of the research is the development and numerical modelling of a shell-and-tube heat-exchanger of a new design as an element of environment control system used in various types of ventilations systems in summer seasons.

Two types of ventilation systems were considered, namely, a tunnel one and a side one. Heat-exchangers aimed at cooling the incoming air in a summer season were designed for those ventilation systems.

A poultry house was of a traditional type for 50000 birds used for breeding floor meat birds. There were automatic blinds arranged in the side walls with the total of 80 pieces 0.3×0.85 m in size (Fig. 1). In addition, on the front end walls, there were wetted pads 5.3×1.1 m is size arranged.

When considering those two separate systems, heat-exchangers were mounted instead of wetted pads and automatic blinds.
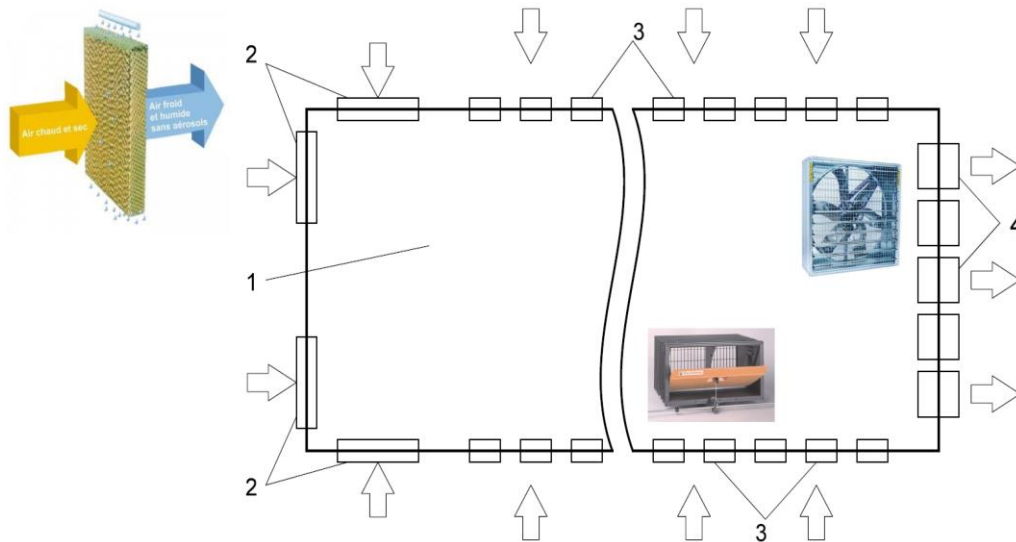
Fig. 10.1. Layout of an evaporating cooling system and side ventilating blinds in a poultry house:

1 – poultry building; 2 – wetted pads; 3 – ventilating blinds; 4 – exhaust blowers.

Let us consider a heat-exchanger with a rectangular-section shell under transverse tube bank flow. There is a distinctive arrangement geometry of tubes d=10 mm in diameter (Fig. 2). It is different from traditional staggered and in-line tube banks. The heat-exchangers, which contain transverse tube bank flow, are made of tube rows, where the adjacent tubes of every row are tangent to each other and the tubes of every row are arranged with a sequential displacement about the row axis, here, the adjacent tubes are displaced by 1 mm apart from each other [22]. In both types of heat-exchangers (HE), the width between the tubes is equal to 15 mm., the number of tubes in depth in one header is equal to 51 pcs.

All the calculations were performed under the air-flow rate of 1036 thousand m³/h. The air being +40 ºC at the entry, which flows through the outside hot-air cooling channels in a poultry house in summer seasons, was chosen to be a heat carrier. On the exit from a heat-exchanger, the air temperature decreased to nearly +20ºC. Subterranean well water [4-5] was used

as a coolant. In its turn, the temperature of the cold water, which moved inside the tubes, was equal to +10 ºC at the entry.

The system of heat carrier movement is of cross pattern. In order to obtain sufficient cooling of the incoming air from +40 to +20 ºC, heat-exchangers were designed by the entry size of blinds and wetted pads. Due to the requirement of such a substantial air exchange (1036 thousand m³/h) and heat transfer between heat carriers, the number of headers in heat-exchanging units is different.
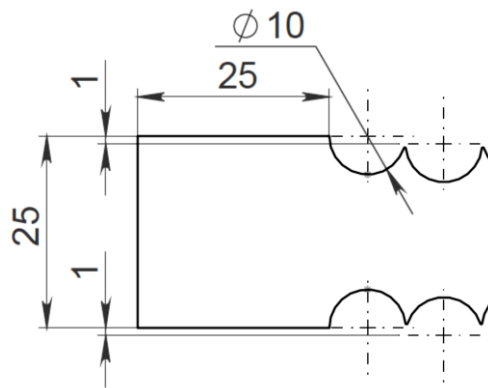
Fig. 10.2. Arrangement of tubes in a matrix, (view from above).

Table 1 presents the design data of both heat exchangers for various ventilation systems.

Table 10.1.

Design data of heat-exchangers for various ventilation systems

Ventilation system	Air consumption for all HEs, m³/h	Water consumption for all HEs, m³/h	Air consumption for one HE, m³/h	Height of HE, m	Width of HE, m	Number of headers, pcs	Number of tubes in one HE, pcs	Number of HE, pcs	Total length of tubes, m
Side	1036880	382.4	12961	0.3	0.85	3	5202	80	124848
Tunnel	1036704	372.0	86392	1.0	2.65	2	5406	12	64872

CFD modelling of hydrodynamic processes and heat transfer processes in the channels with close-together arrangement of tube banks was conducted. For

this purpose, ANSYS Fluent software package was used. The mathematical model is based on Navier-Stokes equation [23], energy-conservation equation applied for convective currents and the equation of continuity. The standard k-ε turbulence model was used in the calculations [24].

Navier-Stokes equation:

$$\left. \begin{array}{l} \rho\left(\dfrac{\partial u}{\partial t}+u\dfrac{\partial u}{\partial x}+v\dfrac{\partial u}{\partial y}\right)=-\dfrac{\partial p}{\partial x}+\mu\left(\dfrac{\partial^2 u}{\partial x^2}+\dfrac{\partial^2 u}{\partial y^2}\right), \\[3mm] \rho\left(\dfrac{\partial u}{\partial t}+u\dfrac{\partial u}{\partial x}+v\dfrac{\partial u}{\partial y}\right)=-\dfrac{\partial p}{\partial y}+\mu\left(\dfrac{\partial^2 u}{\partial x^2}+\dfrac{\partial^2 u}{\partial y^2}\right), \end{array} \right\}; \tag{10.1}$$

where ρ – medium density, kg/m^3; μ – medium dynamic viscosity, Pa•s; p - pressure, Pa; u, v – velocity field of vectors; t – time, s.

A continuity equation:

$$\frac{\partial u}{\partial x}+\frac{\partial v}{\partial y}=0; \tag{10.2}$$

An energy-conservation equation:

$$\rho C_p\left(V_x\frac{\partial T}{\partial x}+V_z\frac{\partial T}{\partial y}\right)=\frac{\partial}{\partial x}\left(\lambda\frac{\partial T}{\partial x}\right)+\frac{\partial}{\partial y}\left(\lambda\frac{\partial T}{\partial y}\right). \tag{10.3}$$

where T – point temperature, ºK; λ – coefficient of medium heat transfer capacity, W / m • ºK; C_p – specific heat capacity of a medium, J/kg • ºK.

Boundary Conditions

The boundary conditions are given in the following form (see figure 1).

At the inlet to the channel:

$$x=0; W=W_0; T=T_0. \tag{10.3}$$

At the outlet from the channel:

$$x=H; \partial W/\partial x=0. \tag{10.4}$$

On the walls of the tubes:

$$T(x=x_{tubeinside})(y=y_{tubeinside})=T_{wall0}. \tag{10.5}$$

On the walls of the casing:

$$\left|\frac{\partial T_{tube\ shall.}}{\partial y}\right|_{y=0}=0. \tag{10.6}$$

Conditions for sticking the liquid on the tubes walls:

$$x = x_{tube\ ext.};\ y = y_{tube\ ext.}.$$ (10.7)

Conditions for sticking on the walls of the casing:

$$y = H;\ W = 0;\ y = 0.$$ (10.8)

For a standard k-ε model, the equation of turbulence has the following form:

$$\frac{\partial}{\partial t}(\rho k) + \frac{\partial}{\partial x_i}(\rho k u_i) = \frac{\partial}{\partial x_j}\left[\left(\mu + \frac{\mu_t}{\sigma_k}\right)\frac{\partial k}{\partial x_j}\right] + G_k + G_b - \rho\varepsilon - Y_M + S_k$$, (10.9)

$$\frac{\partial}{\partial t}(\rho\varepsilon) + \frac{\partial}{\partial x_i}(\rho\varepsilon u_i) = \frac{\partial}{\partial x_j}\left[\left(\mu + \frac{\mu_t}{\sigma_\varepsilon}\right)\frac{\partial \varepsilon}{\partial x_j}\right] + G_{1\varepsilon}\frac{\varepsilon}{k}(G_k + G_{3\varepsilon}G_b) - C_{2\varepsilon}\rho\frac{\varepsilon^2}{k} + S_\varepsilon$$, (10.10)

where G_k – the generation of turbulence kinetic energy due to the mean velocity gradients; G_b – the generation of turbulence kinetic energy due to buoyancy; Y_M – the contribution of the fluctuating dilatation in compressible turbulence to the overall dissipation rate; $C_{1\varepsilon}$, $C_{2\varepsilon}$, and $C_{3\varepsilon}$ – constants; σ_k and σ_ε – the turbulent Prandtl numbers for k and ε, respectively; S_k and S_ε – user-defined source terms.

Grid generation was performed in ANSYS Meshing generator based on Workbench framework. In the course of grid generation for a heat-exchanger of all the designs, local grid control was applied. The minimum bound size was $2.5 \cdot 10^{-4}$ m. The generation of a quadrilateral grid was conducted with the use of boundary layer construction with total thickness approach (Total Thickness). The thickness of the first layer was $5 \cdot 10^{-5}$ m, the number of layers was 6 (Fig. 10.3). Grid quality index, that is Orthogonal Quality, for both types of heat-exchangers is within the limits from 0.561 to 0.564.
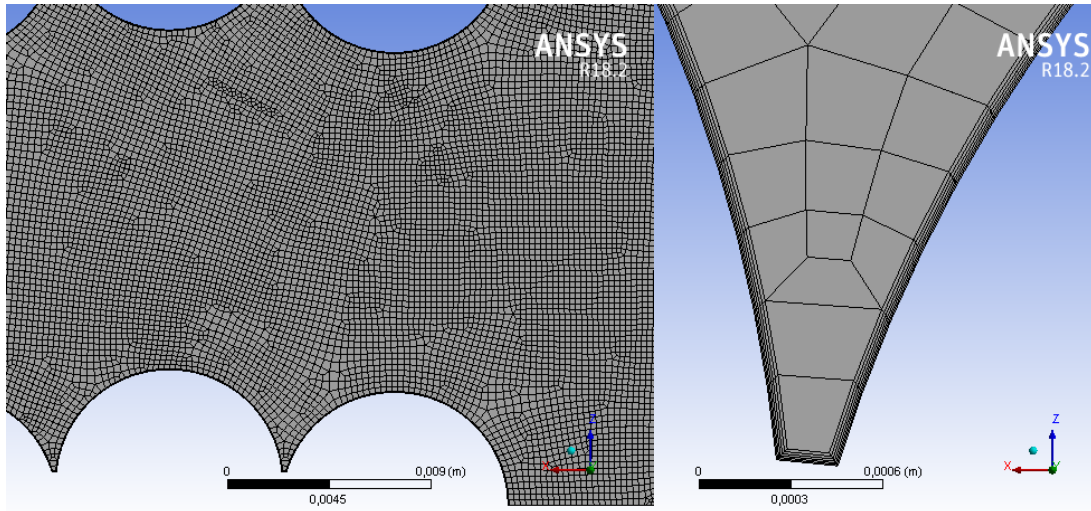
Fig. 10.3. Grid generated in ANSYS Meshing:

a – complete channel; b – boundary layer.

The results of the conducted numerical calculations are presented in Fig. 10.2-10.6. The incoming hot air enters a heat-exchanger on the right side. Fig. 10.2-10.3 show the change in temperatures for various ventilation systems. In the case of a tunnel ventilation, the temperature in a heat-exchanger decreases from +40 to +22.5 ºC (Fig. 10.4), and in the case of a side one, it decreases from +40 to +19.7 ºC (Fig. 10.5).

When comparing heat-exchangers by pressure drop across a channel (see Fig. 10.6-10.7), which were designed for various system types, it is obvious that they differ in about 3.3 times. More detailed results can be seen in Table 10.2.
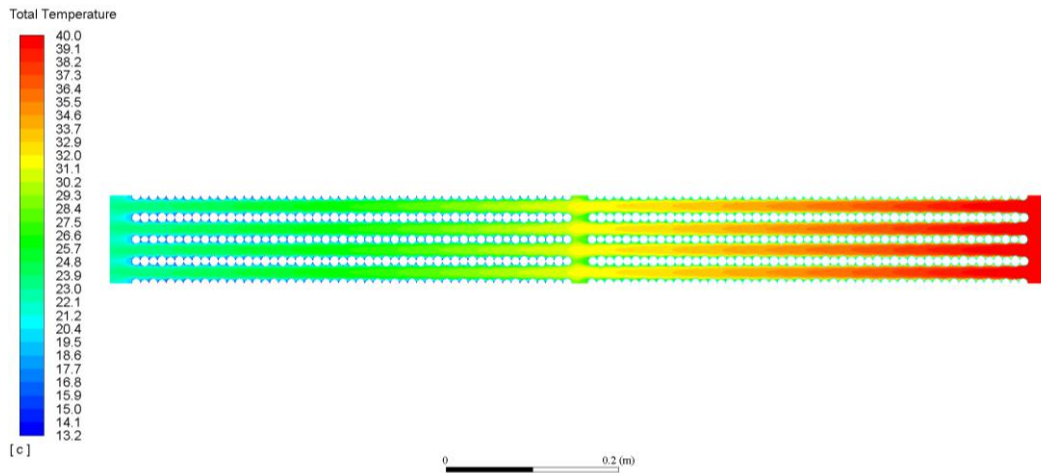
Fig. 10.4. Air temperature field in a heat exchanger for a tunnel ventilation system, ⁰C
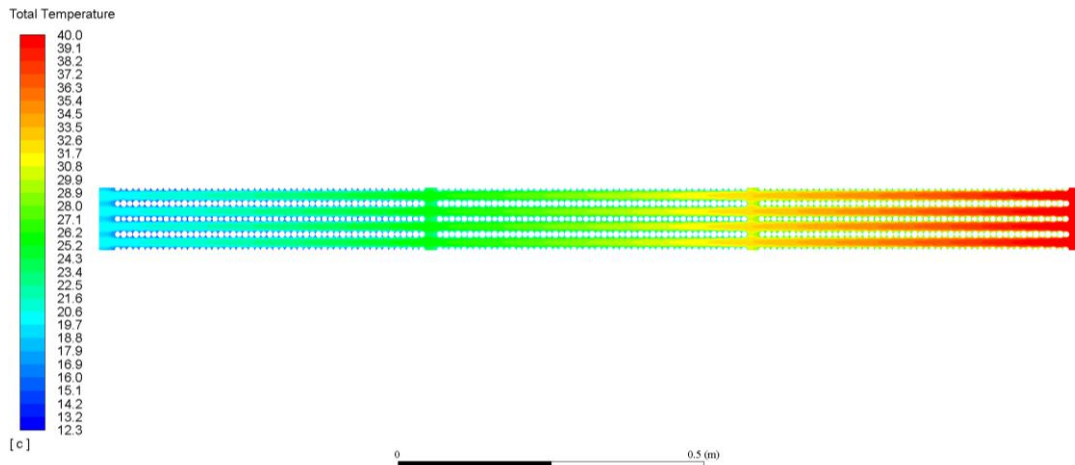
Fig. 10.5. Air temperature field in a heat exchanger for a side ventilation system, ⁰C
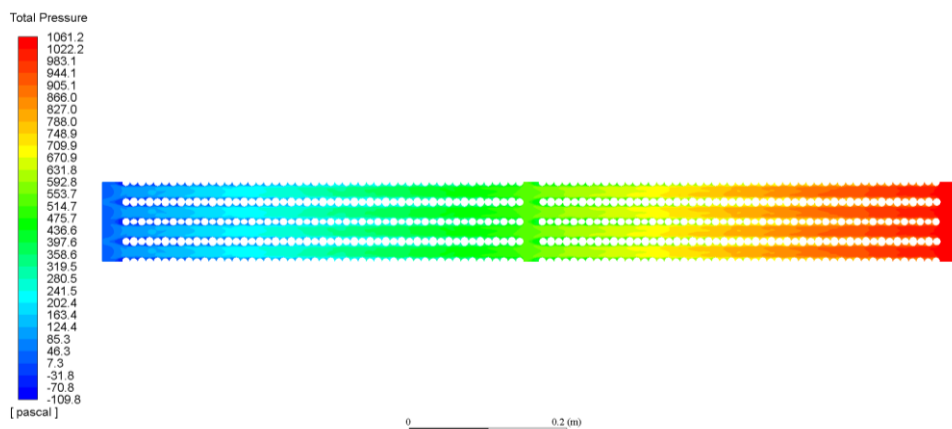
Fig. 10.6. Pressure drop across a HE channel for a tunnel ventilation system, Pa
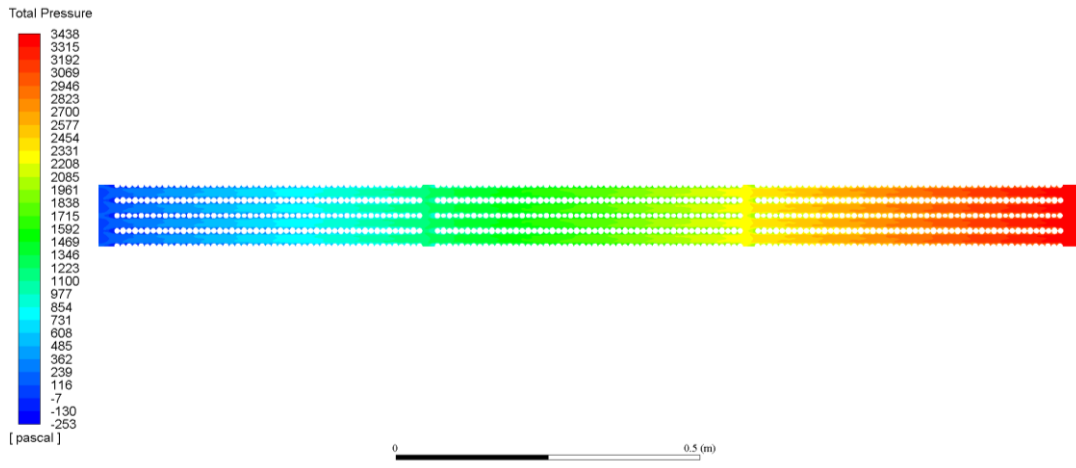
Fig. 10.7. Pressure drop across a HE channel for a side ventilation system, Pa

Fig. 8 presents a velocity vector at the entry to a HE channel for various ventilation systems. The process of air flowing about the tubes and boundary layer separation from its surface are shown. There are dead-air spaces in the form of a vortex observed between the tubes, thus the heat transfer coefficient in these spaces is decreased. In the case of a tunnel ventilation system (Fig. 8a, Fig. 9) the maximum air velocity at certain points is equal to 17.6 m/s and the average velocity in the narrowest channel passage is 15.1 m/s. In the case of a side ventilation system (Fig. 8b, Fig. 10) the maximum velocity is 27.2 m/s and the average one is equal to 23.5 m/s. Table 2 presents a more detailed review of the results of numerical modelling for various ventilation systems.

a   b
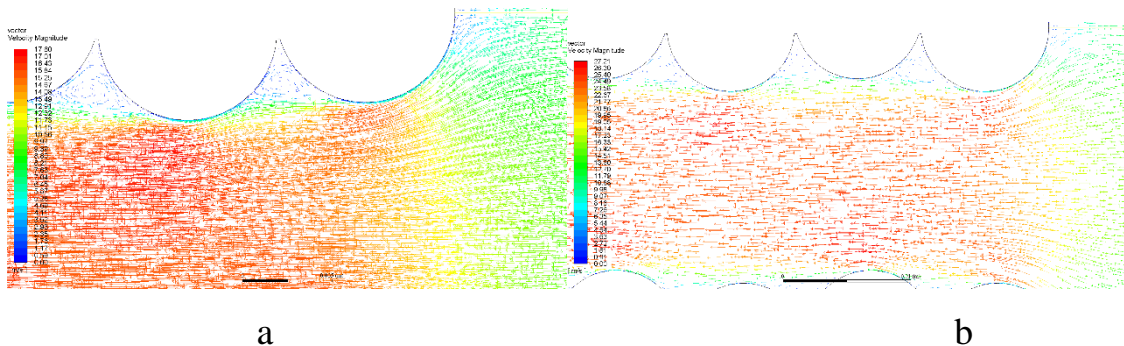
Fig. 10.8. Air flow velocity vector on entering HE, m/s:

a – for a tunnel ventilation system, b – for a side ventilation system.
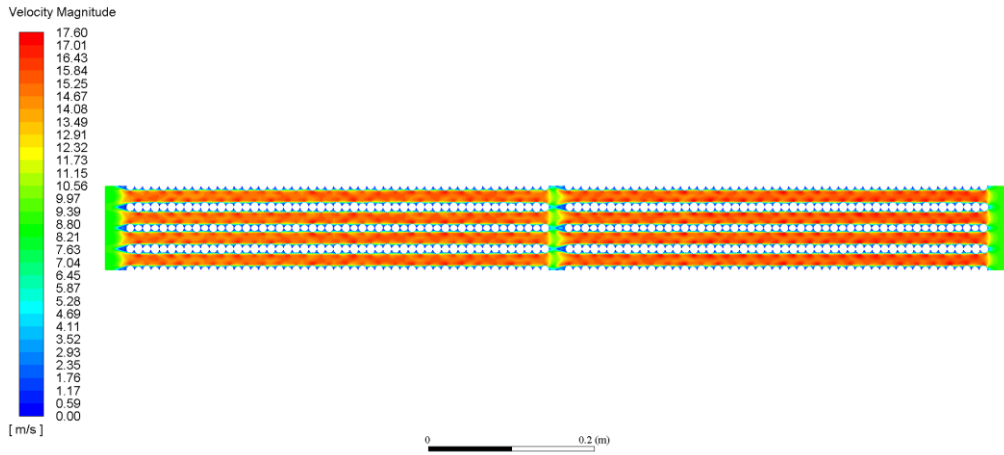
Fig. 10.9. Air velocity in a channel for a tunnel ventilation system, m/s
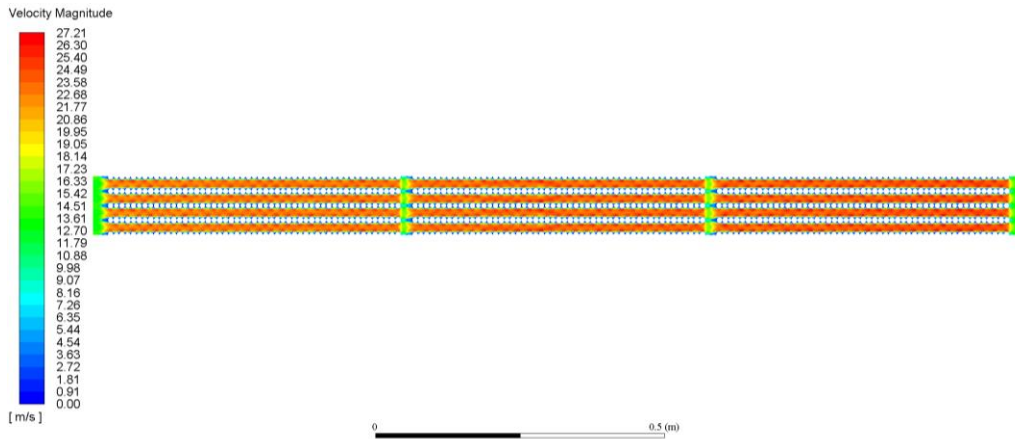
Fig. 10.10. Air velocity in a channel for a side ventilation system, m/s

Table 10.2

Results of numerical modelling of various ventilation systems

Ventilation system	Air temperature on exit from HE, °C	Water temperature on exit from HE, °C	Pressure drop in a HE channel, Pa	Maximum air velocity in a HE channel, m/s	in the narrowest section of a HE	Heat power of one HE, kW	Heat power of all HEs, kW
Side	19.66	23.95	3286	27.21	23.53	77.550	6204.00
Tunnel	22.55	23.16	991	17.60	15.10	474.72	5696.64

In the course of designing and manufacturing a heat-exchanger for an environment control system in poultry houses, it is necessary to take into account numerous parameters. They include pressure drop in heat-exchanger channels that influences the capacity and the productivity of ventilation systems; the temperature on the exit from a HE, which enters a poultry house and cools down the inside air in the building and other. The project has been based on the development of a HE for two ventilation systems. In the case of a tunnel ventilation system, pressure drop is equal to 991 Pa, which is 3.3 times less compared to a side ventilation system. The exit temperature is equal to +23 ºC, which meets the requirements for project engineering. However, the disadvantage is financial costs for purchasing, tube cutting and HE welding. According to Table 1, in order to make a HE for a tunnel ventilation system, it is necessary to use 64872 m of tubes, which is in 1.92 less compared to the second option. Both a tunnel and a side ventilation system are effective enough. In order to provide normalized environment conditions in a poultry house, taking into account all the aspects of technical and economic analysis, it is offered to choose a HE for a tunnel ventilation system. Such expenditures are justified due to the increase of bird mass in summer periods. However, not all the poultry plants can afford to install such a system.

Conclusions to chapter 10

1. A new design of a shell-and-tube heat exchanger with close-together tube arrangement in tube banks has been suggested and developed.

2. CFD modelling of the processes of heat- and mass-exchange in tube banks of various geometry under close-together tube arrangement has been conducted with the help of ANSYS Fluent software package. The fields of velocities, temperatures and pressures in the channels under study have been obtained. The conditions of the hydrodynamic flow in the channels have been

analyzed and the intensity of heat transfer between a hot and a cold heat carrier through a separating wall has been estimated.

3. The most efficient and the most cost-effective HE has been determined to be for a tunnel ventilation system due to the decrease of the number of tubes in 1.92 times and the decrease in pressure drop in 3.3 times.

CHAPTER 11. RATIONALE OF ACCEPTABLE RISK OF USING TRACTORS WITH OPERATIONAL DAMAGES OF RESPONSIBLE DETAILS

For calculating risk and safety indicators of the tractor it is proposed to use the data of defectoscopic control of the array of responsible tractor details and to analyze the kinetics of accumulation of the total damage in the array of these details by analogy with the estimation of the boundary elasticity of the surface layer of metal by multi-cycle fatigue. It is established that the dependence of the kinetics of the cracks accumulation in the details of systems (units) of the tractor with a high degree of reliability can be described by exponential diagrams within the studied range of service life, which is typical for the pattern of monotonic accumulation in model samples of structural materials of scattered fatigue damage. The description of the kinetics of dispersion of the relative number of defective parts using a 4 degree polynomial allowed to establish a certain maximum corresponding to the interval of 12-13.5 years of the tractor operating life. This maximum corresponds to the maximum intensity of the formation of operational cracks for the studied interval of the duration of operation of the tractor and the probability of accumulation in the array of details of the critical (limit) number of defects. This can serve as a criterion for discontinuing the tractor, performing parts flaws to detect cracks and repairing (replacing) defective parts. On the basis of the kinetic diagram of accumulation of operational defects in the array of tractor details, the method of estimating the residual life of tractors after a certain duration of operation is proposed. This method uses approaches to analyze the kinetics of damage to metallic materials that have undergone mechanical loading, using the Hearst parameter as a criterion, the limiting value of which does not depend on the mechanical loading parameters.

The problem of ensuring the reliable operation of mobile agricultural machinery is becoming more urgent, since the speed of its aging far exceeds the pace of technical re-equipment of the agricultural sector of Ukraine [1]. Therefore, to predict the failure of tractors, combines and machine-tractor units and, therefore, to prevent possible emergencies in the field and roads, there is a problem of reliable determination of their residual resource, in particular how safe their further operation will be after the assigned resource is exhausted [2].

Determining the degree of performance of the machine is important, not less than determining the magnitude of the risk of its operation for the operator or other employees, because the magnitude of the risk should not exceed an acceptable level [3]. At present, acceptable risk levels are generally set for industries and sub-sectors of the economy based on industrial injury statistics, as well as for large-scale nuclear facilities, the chemical and metallurgical industries [4]. The operation of mobile agricultural machinery is also considered to be of high risk, but the concept of acceptable (acceptable) risk for mechanical work has no regulatory definition [5]. This does not allow to establish the degree of danger of finding agricultural machinery on the fields, farms and roads of machines without technical means of safety, with exhaustion of the established resource of machinery [6].

Therefore, the introduction of a production risk management system, in which it is necessary to implement the principles of risk prevention, acceptability and minimization, taking into account all potential workplace threats, is relevant for agriculture [7]. This should be guaranteed by the manager of the enterprise (employer) a certain level of safety for the employees [8].

Establishing time limits for machine operation, should not only rely on strength and economic performance [9], but also take into account the basic provisions of the concept of risk, which will justify the resource of safe operation [10]. Along with the terms "strength", "resource", "reliability", technicians and operators must evaluate the "safety", "risk" and "security" of

employees [11]. And this should apply not only to important and critical production sites, but also to long-lasting machines [12].

In this paper, to evaluate the risk and safety performance of machines, it is proposed to use the results of studies of defects in materials and structural elements [13], since with increasing the life of the machine, the risk of accidents due to the accumulation of operational defects is continuously increasing [14].

Nowadays traditional and new methods and means – optical, physical, mechanical, etc. – are used to diagnose the technical condition of machines during routine work [15]. There are virtually no universal methods for detecting several defect parameters, and the most common methods (external examination and magnetic powder flaw detection) allow only large operational cracks to be detected when the risk of damage is already high [16].

The results of this analysis show that, given the high level of complexity of the control of surface preparation, due to the high complexity of the control of preparation of the controlled surface [17], it is advisable to use most of the methods of defectoscopy developed for the examination of local zones with possible damage, rather than general metalwork [18]. For general inspection of metal structures, methods of defectoscopic control, which do not require careful preparation of the surface [19], should be applied, as it was implemented in the framework of this work to study defects in the array of tractor parts [20].

In this work, a portable eddy-current defectoscope (Fig. 1) was used to detect cracks. It is allowing the detection of cracks longer than 3 mm and practically insensitive to surface roughness (capable of detecting defects at surface roughness Rz 60 and less). The developed device is characterized by the absence of the edge effect, the effect of the sensor removal, allows to detect cracks with a maximum gap between the sensor and the controlled surface up to 3 mm [21]. This made it possible to carry out defectoscopic inspection of a large array of responsible details of tractors (more than 1,200 parts were studied in 50

tractors of different years of manufacture) without preparing a controlled surfaces [22].

Fig. 11.1. Portable eddy-current defectoscope

Flaw control was performed during major repairs of tractors with disassembly of separate units.

In order to specify the objects of flaw detection and to narrow the field of detection of cracks, the available details of individual tractor units were divided into several categories:

1) high voltage parts with high probability of failure;

2) details, the technical condition of which is conditioned by the aggregate action of force factors with aggressive environmental conditions;

3) parts subject to minor damage;

4) details in which damage is detected only visually (small, non-metallic, etc.).

The proposed methodological approach did not take into account the potential cracking and damage of the third and fourth categories of parts: fasteners, rubber, nonmetallic, etc.

A stepwise sensitivity switch was installed on the defectoscope used to change the minimum size of cracks found in the ranges of 3, 5, and 7 mm in length, respectively (conventionally named small, medium, and large, depending on the cross-section of the workpiece). As a result of this methodological approach, both kinetic dependences of accumulation of operational defects accumulation in components of units with increasing duration of operation of tractors were constructed, as well as kinetic dependences of intensity of origin of small cracks in the array of controlled parts.

Flawed inspection of components was carried out for tractors that had been involved in mechanical and transport work for some time, and were subjected to a force load, which led to the emergence of operational cracks. Some of these defects were discovered during the repair of tractors with the disassembly of knots. The same was considered with a certain degree of certainty that all the tractors under study at one year of production were in operation for the same period. The 17-year service life of the tractors of the brand under study, which is twice their estimated life, was chosen as the base one.

It is imperative that the defectoscope is inspected for test pieces before defectoscopic examination of parts and structural members. Control samples of cracks of various lengths were obtained on sheet metal alloy samples as a result of the propagation of fatigue cracks from the stress concentrator applied at the edge of the sample.

In order to assess the acceptable permissible risk of using mobile agricultural machinery, generalized data were analyzed on the performance of defectoscopic inspection of tractor units [23], which are presented in Table 11.1.

The kinetics of the accumulation of cracks in the details of systems and assemblies of wheeled tractors of different duration of operation are presented in Fig. 11.2 and Fig. 11.3.

Table 11.1

Generalized results of defectoscopic inspection of tractor parts of different years of production

№	The name of the tractors unit	Years of operation of tractors (in brackets indicate the number of tractors whose parts have undergone defective inspection)								Total
		15 (3)	14 (8)	13 (4)	12 (7)	11 (7)	10 (7)	9 (8)	7 (7)	
	Steering system									
1	A total of cracks were detected	10	20	10	23	10	13	12	8	114
2	All details were investigated	22	47	18	43	27	41	48	40	303
3	The relative number of defective parts	0.45	0.42	0.56	0.53	0.7	0.32	0.25	0.2	
	Hinged device									
4	A total of cracks were detected	3	18	7	22	9	10	10	9	95
5	All details were investigated	8	48	15	55	29	34	38	39	278
6	The relative number of defective parts	0.4	0.37	0.46	0.4	0.31	0.29	0.26	0.23	
	Engine parts									
7	A total of cracks were detected	4	22	11	17	10	16	9	7	108
8	All details were investigated	7	45	23	38	26	50	29	28	263
9	The relative number of defective parts	0.56	0.48	0.47	0.44	0.39	0.32	0.31	0.25	
	Rear axle									
10	A total of cracks were detected	6	16	7	14	9	8	7	8	80

11	All details were investigated	13	43	20	41	27	25	23	30	232
12	The relative number of defective parts	0.46	0.37	0.35	0.34	0.33	0.32	0.3	0.27	
	Gearbox									
13	A total of cracks were detected	12	11	5	8	9	9	9	7	81
14	All details were investigated	29	35	16	25	31	32	42	39	273
15	The relative number of defective parts	0.41	0.31	0.31	0.32	0.29	0.28	0.21	0.18	
	A total of cracks were detected in all tractors	35	87	40	84	47	56	47	39	435
	All the details of all tractors were investigated	79	218	92	202	140	182	180	176	1269
	The relative number of parts of all tractors with defects	0.44	0.39	0.43	0.41	0.33	0.3	0.26	0.22	
	Dispersion of the relative number of defective parts	0.0040	0.0040	0.0101	0.0071	0.0017	0.0004	0.0016	0.0013	0.0040

The coordinates of the graphs are as follows: the ordinate axis is the probability of occurrence of a critical state $P = n_d/N$ (the ratio of the number of detected cracks n_d in the total set of investigated, meaningful from the point of view of the limit state of operational safety, details N); the abscissa axis is the relative durability of $D = t_{eks}/t_{baz}$ (the ratio of the duration of operation of the tractors t_{eks} to the base duration t_{baz}, which is 17 years in the calculations). The experimental data for the individual tractor operating ranges are described by the trend lines of exponential type. In Fig. 11.2 and Fig. 11.3, their equations and the reliability of the approximation of R^2 are written. The obtained results correspond to the normal distribution.
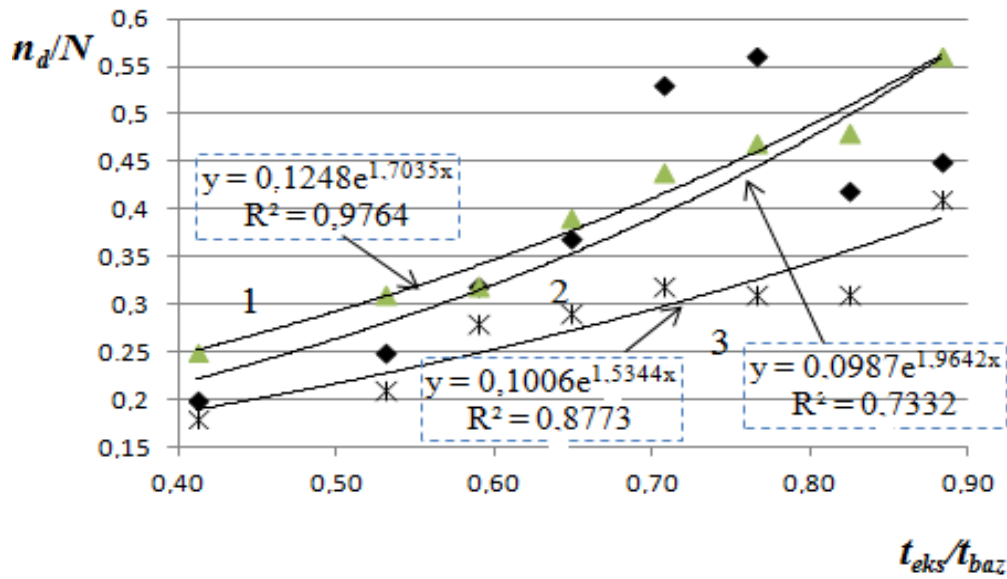
Fig. 11.2. Kinetics of cracks accumulation in engine parts (curve 1), steering system (curve 2) and gearboxes (curve 3) of wheeled tractors of different duration of operation
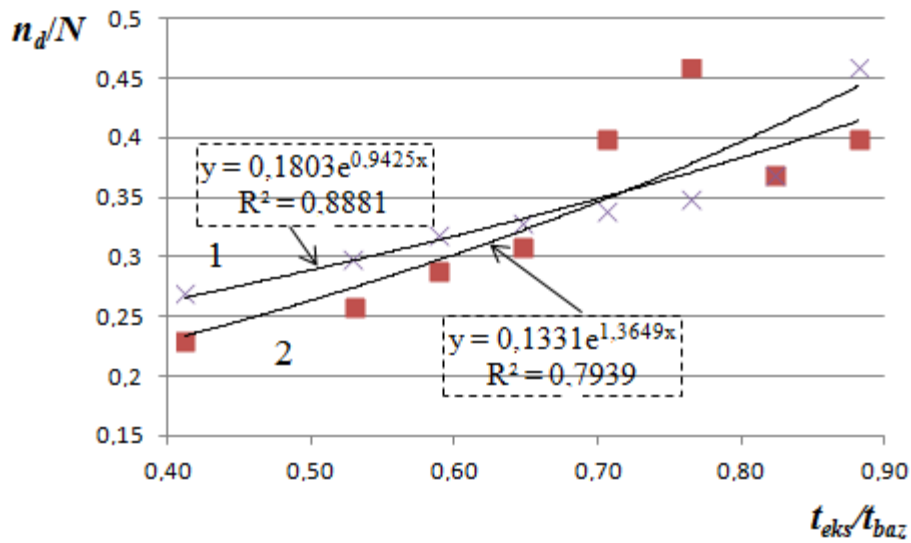
Fig. 11.3. Kinetics of the accumulation of cracks in the details of the rear axle (curve 1) and the hinged device (curve 2) of wheel tractors of different duration of operation

The exponential form for graph representation in Fig. 11.2 and Fig. 11.3 are selected for the maximum confidence of the approximation of R^2 by the

trend line. The reliability of linear dependence approximation is lower, as evidenced by the data in the Table 11.2.

Table 11.2

Comparison of the reliability of the approximation R^2 for different tractor units

The name of the tractors unit	The reliability of the approximation R^2	
	Exponential dependence	**Linear dependence**
Steering system	0.7332	0.6537
Hinged device	0.7939	0.7399
Engine parts	0.9764	0.9707
Rear axle	0.8881	0.8311
Gearbox	0.8773	0.8656

The exponentiality of the trend line in Fig. 11.2 and Fig. 11.3 reflect a certain increase in the intensity of defect accumulation in the array of tractor parts with an increase in service life, which was found in the presence of a maximum in Fig.11.3. This made it possible to propose a criterion for the risk of continuation of the tractor without defectoscopic control.

The dispersion kinetics σ of the obtained values of the relative number of defective parts for the considered knots and tractor systems was analyzed (Fig. 11.4). The graphs in Fig. 11.4 is based on the statistical processing of a data set of 40 elements, and each point on the graph corresponds to a variance of 5 values obtained as a result of averaging the results of defectoscopic control of at least 232 tractor parts. The results of the calculation of the dispersion were described by a polynomial of 4 degrees with a clear maximum corresponding to the duration of operation in the range of 0.7-0.8 relative duration of operation, which is 12-13.5 years. The presence of this maximum can be explained by the

maximum intensity of the formation of operational cracks in the given duration of operation of the tractor, which indicates the danger of its further use without proper control of the technical condition with the involvement of means of flaw detection to detect large (critical size) cracks.

The same critical duration of the tractor operation (12-13.5 years) can serve as a criterion for termination of the tractor operation, flaw detection of parts to detect cracks and repair (replacement) of defective parts. The highest correlation coefficients characterize the kinetics of the accumulation of cracks in: the steering system and attachment; engine and rear axle with tractor gearbox (Table 11.3).

From the diagram of Fig. 5 shows that the dispersion of accumulation of operational defects is significantly different for different systems (units) of the tractor. The description of the results of studies of the kinetics of the accumulation of damage by exponential dependences is preferred over linear dependencies not only in view of the approximation reliability.

The equation shown on the chart:

$$y = -1.3322x^4 + 2.794x^3 - 2.0255x^2 + 0.5947x - 0.0567$$
$$R^2 = 0.6701$$
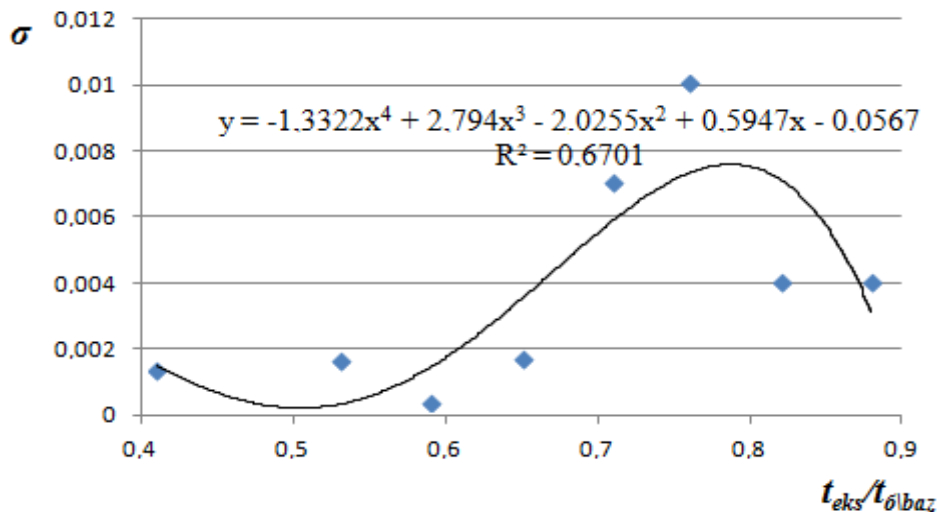
Fig. 11.4. Kinetic of dispersion σ of obtained values of the relative number of defective parts for the considered components and tractor systems

The lowest is for the rear axle and gearbox consisting of the same parts, and the highest for the steering system. This imposes high demands on the flaw detection of parts of this system, the destruction of which can lead to accidents with a high risk of injury to employees.

Table 11.3

Correlation coefficients of kinetics of accumulation of operational defects for different tractor systems (units)

Name of tractors system (units)	Hinged device	Engine	Rear axle	Gearbox
	Correlation coefficients			
Steering system	0.977094	0.823954	0.601399	0.766263
Hinged device	-	0.877112	0.682509	0.789921
Engine	-	-	0.925974	0.936178
Rear axle	-	-	-	0.94546
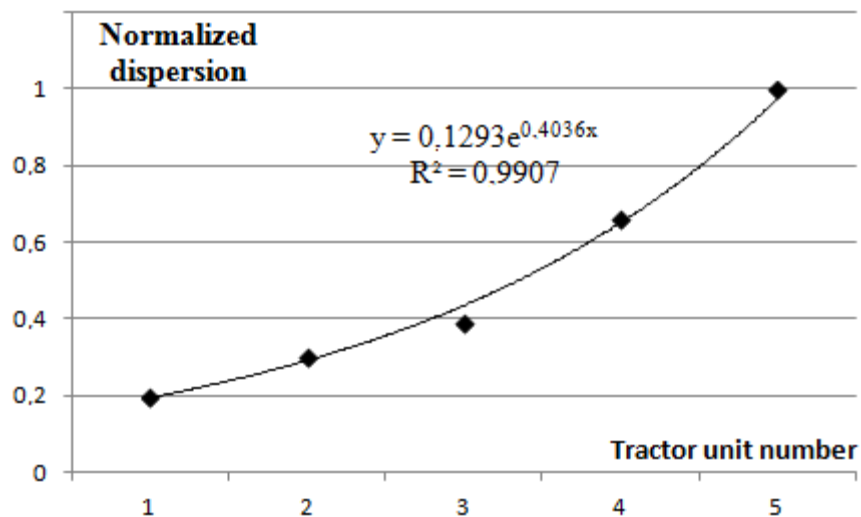
Fig. 11.5. Diagram of dispersion of accumulation of operational defects for different tractor systems (units):

1 – rear axle; 2 – transmission; 3 – hinged device; 4 – the engine;

5 – steering system

Presented in Fig. 11.2 and Fig. 11.3, the dependences of the kinetics of the accumulation of cracks in the details of tractor systems (units) are exponential within the investigated operating life span. It should be noted that the exponential dependence is characteristic of the laws of monotonic accumulation in samples of structural materials of scattered fatigue damage represented by the Hearst parameter (*H*).

To predict the remaining life of a machine with an exhausted service life, you need to solve two problems:

−   to evaluate the current technical status on the basis of data collected during examination (diagnosis, defect) of materials;

−   to determine the residual resource on the basis of forecasting the development of this state to the limit.

As a rule, the current technical condition of the machine is evaluated according to various parameters, and the residual resource is predicted according to the determining parameter of the technical condition of the machine.

The proposed in this work methodology for predicting the residual life of a metal structure is based on the principles implemented in the method of analysis of the damage kinetics of metallic materials that have undergone mechanical loading, in accordance with changes of the Hearst parameter *H*. Diagrams of accumulation of operational defects in the arrays of parts of individual systems (units) of tractors were analyzed analogously to the graphs of kinetics of statistical parameters of deformation hysteresis of the surface layer of metal structures.

The same as the criterion of the degree of accumulation of operational defects, which can cause accidents in mechanized and transport works with the participation of tractors, by analogy in this work, the probability of accumulation in the array of details of the critical (limit) number of defects was taken.

In Fig. 6 presents a diagram to illustrate the proposed in this paper method for the estimation of residual resource (D_{lim} - D_{fact}) of tractors after a certain duration D_{fact} of operation based on a kinetic diagram of the accumulation of operational defects in the array of wheeled tractor parts, obtained by averaging the defect control data. The coordinates of the diagram correspond to the coordinates of the diagrams in Fig. 11.2 and Fig. 11.3.

The plot shows $y = 0{,}1196e^{1,5541x}$ and $R^2 = 0{,}9073$, with axes $P = n_d/N$ (vertical) and $D = t_{eks}/t_{baz}$ (horizontal), marking P_{lim}, P_{fact}, D_{fact}, and D_{zim}.
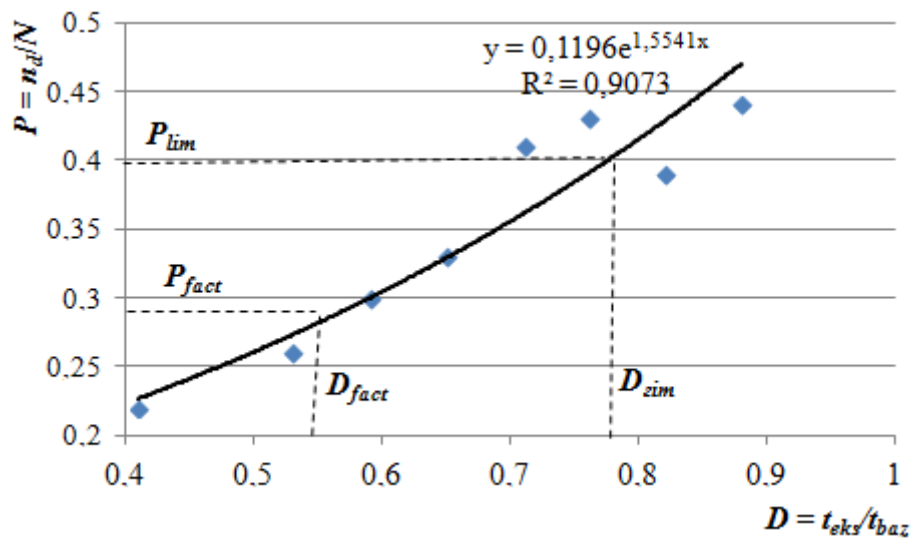
Fig. 11.6. Scheme of the method of estimating the residual life of tractors after their long operation

In Fig. 11.4 shows the relative duration of operation, when the intensity of cracks is maximum, and therefore, if this value is exceeded, the probability of sudden destruction of tractor units and the creation of accidents in mechanized or transport operations is increased. For the studied wheeled tractor units, this value (D_{lim}) is approximately the same and is in the range of 0.7-0.8 relative operating life, that is about 12-13.5 years. The actual duration (D_{fact}) of tractor operation can be estimated by detecting a certain number of defects (cracks) in an array of parts, calculating their relative number in the total set of investigated parts, and drawing the horizontal line to the curve of intensity of the accumulation of operational cracks, as shown in Fig. 11.6.

The procedure for estimating the residual life of the tractors or their individual units (systems) after prolonged operation is as follows.

1.   With the help of a portable flaw detector, carry out flaw detection of the array of responsible tractor parts.

2.   Determine which part ($P_{fact} = n_0/N$) of the array of parts has operational defects relative to the total number of parts N that are subject to flaw control.

3.   According to the year of tractor production, set its relative duration of operation ($D_{fact} = =t_{exp}/t_{baz}$) relative to the base term ($t_{baz} = 17$ years).

4.   Through the point with coordinates (P_{fact}, D_{fact}) in Fig. 11.6 conduct an exponential curve with parameters corresponding to the trend line parameters of the exponential accumulation defect accumulation curve obtained by averaging the data. With some approximation, we can take the parameters of the exponent $a = 0.119$; $b = 1.5541$.

5.   For the limit accumulation of operational defects $P_{lim} = 0.4$, we draw a horizontal line to intersect with the exponential curve. The abscissa of the intersection point will correspond to the maximum duration of operation of the tractor D_{lim}, and the difference ($D_{lim} - D_{fact}$) to its residual resource.

To estimate the residual life of individual units (systems) of tractor, it is necessary to use the parameters of the corresponding exponential curves shown in Fig. 11.2 and Fig. 11.3. However, it should be noted that the general analysis of the kinetics of the obtained data (Fig. 11.2 and Fig. 11.3) does not allow to reliably predict the parameters of the kinetics of cracks accumulation in the details (units) of the tractors beyond the studied service life (17 years).

In other areas we may also find some analogues to the proposed methodology for estimating the residual life of tractors after prolonged use. Thus, in a sufficient statistical base of experimental data on the occurrence of defects was collected and analyzed to determine the technical condition of induction motors. The performed researches made it possible to construct the

criterion of maximum accumulation of defects in induction motors, which made it possible to predict the technical condition of the induction motor in the aggregate of accumulated defects and to stop it in a timely manner, avoiding significant damage to the machine components and accidents.

Conclusions to chapter 11

1.   The analysis of the generalized data of defectoscopic inspection of tractors made it possible to justify the terms of use of mobile agricultural machinery without exceeding the acceptable permissible risk.

2.   It is shown that the results of the calculation of the dispersion of the obtained values of the relative number of defective parts for the considered systems (units) tractor can be described by a polynomial with a clear maximum corresponding to the duration of operation in the range of 0.7-0.8 relative duration of operation, which is 12-13.5 years. The presence of this maximum corresponds to the maximum intensity of the formation of operational cracks, which indicates the danger of further use of the machine without proper inspection of the technical condition with the use of flaw detection to detect large (critical) cracks.

3.   The methodology of estimation of residual life of tractors or their separate units (systems) after long operation on the basis of data of defectoscopic control is developed. This methodology is based on the approaches of the method of analysis of the kinetics of damage of metallic materials that have undergone mechanical loading, according to changes in the Hearst parameter, whose limit value, expressed by a fixed value, does not depend on the parameters of mechanical loading

REFERENCES

1.   Aksenov A.G., (2018), Onion set bulb position during planting with vibration-pneumatic planting device, *Agri Res & Tech:Open Access J.*, issue 16 (3), pp. 1-6, California / United States;

2.   Aliev E.B., Bandura V.M., Pryshliak V.M., Yaropud V.M., Trukhanska O.O., (2018), Modeling of mechanical and technological processes of the agricultural industry, *INMATEH - Agricultural Engineering*, vol. 56, issue 3, pp. 95-104, Ed. INMA, Bucharest / Romania;

3.   Allmaras S.R., Johnson F.T., Spalart P.R., (2012), Modifications and Clarifications for the Implementation of the Spalart-Allmaras Turbulence Model, 7th International Conference on Computational Fluid Dynamics, pp. 9-13, Big Island/Hawaii;

4.   Ambekar A.S., Sivakumar R., Anantharaman N. & Vivekenandan M. (2016). CFD simulation study of shell and tube heat exchangers with different baffle segment configurations. Applied Thermal Engineering, Vol. 108, 999-1007. https://doi.org/10.1016/j.applthermaleng.2016.08.013.

5.   Amudhan, A., Karthicka, N., Manonmanis, K., Parimalamurugaveni, S. (2015). Interpretation of the properties of refined rice bran oil as bio lubricant. International Journal of Applied Engineering Research, 10 (55), 3952–3955. Available at: https://www.scopus.com/inward/record.uri?eid=2-s2.0-84942418557&partnerID=40&md5=c3484681ecdc1ca4f2f1652bcf6dd976

6.   ANSYS, (2017), ANSYS Fluent Theory Guide. Release 18.2, Published in the USA, 832 p.;

7.   ANSYS. (2017). ANSYS FLUENT Theory Guide. Release 18., Inc. Southpointe 275 Technology Drive Canonsburg.

8.   Asejeva A., Kopiks N., Viesturs D., (2013), Optimal distribution of the amount of work among the tractor aggregates considering set agrotechnical

terms. *Proceedings of the International scientific conference "Economic science for rural development"*: *Production and cooperation in agriculture. Finance and taxes*, No 30, pp. 38-42, Jelgava / Latvia;

9.   Astashev V., Krupenin V. Efficiency of vibration machines. Proceedings of 16th International Scientific Conference "Engineering for rural development". Jelgava, Latvia, May 24-26, 2017, Latvia University of Agriculture. Faculty of Engineering. Vol. 16, pp. 108-113.

10. Aulin, V., Chernovol, M., Pankov, A., Zamota, T., Panayotov, K. (2017). Sowing machines and systems based on the elements of fluidics. INMATEH – Agricultural Engineering, 53 (3), 21–28. Available at: http://dspace.kntu.kr.ua/jspui/bitstream/123456789/7278/1/53-03%20Aulin%20.pdf

11. Aulin, V., Hrinkiv, A., Dykha, A., Chernovol, M., Lyashuk, O., Lysenko, S. (2018). Substantiation of diagnostic parameters for determining the technical condition of transmission assemblies in trucks. Eastern-European Journal of Enterprise Technologies, 2 (1 (92)), 4–13. doi: https://doi.org/10.15587/1729-4061.2018.125349

12. Aven T. Risk assessment and risk management: Review of recent advances on their foundation. European Journal of Operational Research, 2016, vol. 253, issue 1, pp. 1-13. Scopus.

13.   Badegaonkar U.R., Dixit G., Pathak K.K., (2010), An experimental investigation of cultivator shank shape on draft requirement. *Archives of Applied Science Research*, no. 2, issue 6, pp. 246-255, Chhattisgarh / India;

14.   Bailly C., Comte-Bello G., (2015), Turbulence. Series: Experimental Fluid Mechanics, Springer International Publishing, 360 p., Heidelberg/Germany;

15.   Barwicki J., Gach St., Ivanovs S., (2012), Proper utilization of soil structure for crops today and conservation for future generations. *Proceedings of*

11th International Scientific Conference "Engineering for Rural Development", vol. 11, pp. 10-15, Jelgava / Latvia;

16. Bayram H., Sevilgen G. (2017). Numerical Investigation of the Effect of Variable Baffle Spacing on the Thermal Performance of a Shell and Tube Heat Exchanger. Energies, Vol. 10, 8, 19. https://doi.org/10.3390/en10081156.

17. Blanes-Vidal V., Guijarro E., Balasch S. & Torres A.G. (2008). Application of computational fluid dynamics to the prediction of airflow in a mechanically ventilated commercial poultry building. Biosystems Engineering, vol.100, 1, 105-116.

18. Blanes-Vidal V., Guijarro E., Balasch S., Torres A.G., (2008), Application of computational fluid dynamics to the prediction of airflow in a mechanically ventilated commercial poultry building, Biosystems Engineering, vol.100, no.1, pp. 105-116, San Diego/USA;

19. Bulgakov V., Adamchuk V., Arak M., Petrychenko I., Olt J., (2017), Theoretical research into the motion of combined fertilising and sowing tractor-implement unit. *Agronomy Research*, vol. 15(4), pp. 1498-1516, Tartu / Estonia;

20. Bulgakov V., Adamchuk V., Ivanovs S., Kaletnik H. Experimental investigation of technical and operational indices of asymmetric swath reaper machine-and-tractor aggregate. Proceedings of 18th International Scientific Conference "Engineering for rural development". Jelgava, Latvia, May 22-25, 2019, Latvia University of Agriculture. Faculty of Engineering, vol. 18, pp. 256-263. Scopus. WoS.

21. Bulgakov V., Ivanovs S., Adamchuk V., Nowak J. Theoretical investigation of steering ability of movement of asymmetric swath headerand-tractor aggregate. Proceedings of 17th International Scientific Conference "Engineering for rural development". Jelgava, Latvia, May 23-25, 2018, Latvia University of Agriculture. Faculty of Engineering. Vol. 17, pp. 301-308.

22.	Bulgakov V., Ivanovs S., Nadykto V., Kuvachov V., Masalabov V., (2018), Research on the turning ability of a two-machine aggregate, *INMATEH - Agricultural Engineering*, vol. 56, issue 3, pp. 139-147, Ed. INMA, Bucharest / Romania;

23. Bulgakov V., Nadykto V., Ivanovs S., Nowak J. Research of variants to improve steerability of movement of trailed asymmetric harvesting aggregate. Proceedings of 18th International Scientific Conference "Engineering for rural development". Jelgava, Latvia, May 22-25, 2019, Latvia University of Agriculture. Faculty of Engineering, vol. 18, pp. 136-143. Scopus. WoS.

24.	Bulgakov V., Nikolaenko S., Holovach I., Ivanovs S., Vartukapteinis K. Theoretical investigations of oscillations of root crop head cleaner hanged on integral row-crop tractor. Proceedings of 16th International Scientific Conference "Engineering for rural development". Jelgava, Latvia, May 24-26, 2017, Latvia University of Agriculture. Faculty of Engineering. Vol. 16, pp. 1395-1408.

25.	Bulgakov V., Pascuzzi S., Nadykto V., Ivanovs S. A mathematical model of the plane-parallel movement of an asymmetric machine and tractor aggregate. Journal of Agricultural Engineering. Vol. 49, No 1, 2018, pp. 258-271.

26. Bulgakov V., Pascuzzi S., Nadykto V., Ivanovs S. A mathematical model of the plane-parallel movement of an asymmetric machine and tractor aggregate. Journal of Agricultural Engineering, 2018, vol. 49, no 1, pp. 258-271. Scopus.

27. Bustamante E., Calvet S., Estelles F., Torres A.G. & Hospitaler A. (2017). Measurement and numerical simulation of single-sided mechanical ventilation in broiler houses. Biosystems Engineering, vol.160, 55-68.

28.	Bustamante E., Calvet S., Estelles F., Torres A.G., Hospitaler A., (2017), Measurement and numerical simulation of single-sided mechanical

ventilation in broiler houses, Biosystems Engineering, vol.160, pp. 55-68, San Diego/USA;

29. Cabezas-Gomez L., Navarro H. A., Saiz-Jabardo J.M., Hanriot S.D. & Maia C.B. (2012). Analysis of a new cross flow heat exchanger flow arrangement - Extension to several rows. International Journal of Thermal Sciences, Vol. 55, 122-132. https://doi.org/10.1016/j.ijthermalsci.2012.01.001.

30. Cabezas-Gomez L., Saiz-Jabardo J.M., Navarro H.A. & Barbieri P.E.L. (2014). New thermal effectiveness data and formulae for some cross-flow arrangements of practical interest. International Journal of Heat and Mass Transfer, Vol. 69, 2014, 237-246. https://doi.org/10.1016/j.ijheatmasstransfer.2013.10.022.

31. Cheng, Q. Y., Li, H., Rong, L., Feng, X. L., Zhang, G. Q., & Li, B. M. (2018). Using CFD to assess the influence of ceiling deflector design on airflow distribution in hen house with tunnel ventilation. Computers and Electronics in Agriculture, 151, 165-174. doi:10.1016/j.compag.2018.05.029, Netherlands;

32. Constantin N., Cojocaru I., (2008), Large working capacity technical equipment for overturning the stubble field and preparing the germinating bed in all types of soil designed to tractors of 120-220 HP, *Scientific Papers INMATEH*, no. 26, pp. 102-108, Bucharest / Romania;

33. Constantin N., Irimia D., Persu C., (2012), Testing the multifunctional aggregate for soil tillage works – MATINA, *INMATEH Agricultural Engineering*, vol. 36, issue 1, pp. 5-12, Bucharest / Romania;

34. Corinne Berzin, José R. León. Estimating the Hurst parameter. Statistical Inference for Stochastic Processes. Springer Verlag, 2007, vol. 10 (1), pp. 49-73. Scopus.

35. Croitoru Şt., Vladut V., Voicea I., Gheorghe Gh., Marin E., Vlăduţoiu L., Moise V., Boruz S., Pruteanu A., Andrei S., Păunescu D., (2017), Structural and kinematic analysis of the mechanism for arable deep soil loosening, *Proceedings of the 45th International Symposium on Agricultural*

Engineering "Actual Tasks on Agricultural Engineering", pp. 207-216, Opatija / Croatia;

36. David A., Voicu Gh., Persu C., Gheorghe G., (2014), The Determination of the Resistant Forces for Deep Loosening of Soil Machines with Active Organs. *INMATEH Agricultural Engineering*, vol. 42, issue 1, pp. 5-12, Bucharest / Romania;

37. Dell'aquila A., 2007. Towards new computer imaging techniques applied to seed quality testing and sorting. In: Seed Science and Technology, 35. Jg., Nr. 3, pp. 519-538.

38. Development of a method and an apparatus for tribotechnical tests of materials under loose abrasive friction / Lutsak D., Prysyazhnyuk P., Burda M., Aulin V. // Eastern-European Journal of Enterprise Technologies. 2016. Vol. 5, Issue 7 (83). P. 19–26. doi: https://doi.org/10.15587/1729-4061.2016.79913

39. Dewangan A., Singh Rajput N., (2017), Stress Analysis of Cultivator: A Survey Approach. Crop cultivation. *International Research Journal of Engineering and Technology*. vol. 04, issue 01, pp. 692-696, Delhi / India;

40. Dinesh J., (2009), Modelling and Simulation of a Single Particle in Laminar Flow Regime of a Newtonian Liquid, *Excerpt from the Proceedings of the COMSOL Conference*, pp. 1-9, Bangalore / India;

41. Draganov B.Kh. & Khalatov A.A. (2010). Exergoeconomic optimization of surface heat exchangers. Thermal Engineering, Vol. 57, 10, 888-891. https://doi.org/10.1134/S0040601510100113.

42. Drga R., Janacova D., Charvatova H. Simulation of the PIR detector active function. Proceedings of 20th International conference on Circuits, Systems, Communications and Computers (CSCC 2016), July 14-17, 2016, E D P Sciences, 17 Ave Du Hoggar Parc D Activites Coutaboeuf Bp 112, F-91944 Cedex A, France, vol. 76, UNSP 04036.

43. Duan F., Živanovi´c R., Al-Sarawi S., Mba, D. Induction motor

parameter estimation using sparse grid optimization algorithm. IEEE Trans. Ind. Inf, 2016, vol. 12, pp. 1453-1461. Scopus.

44. Dubbini M., Pezzuolo A., De Giglio M., Gattelli M., Curzio L., Covi D., Yezekyan T., Marinello F. Last generation instrument for agriculture multispectral data collection. CIGR Journal, vol. 19, 2017, pp. 158-163.

45. El Maakoul A., Laknizi A., Saadeddine S., El Metoui M., Zaite A., Meziane M. & Ben Abdellah A. (2016). Numerical comparison of shell-side performance for shell and tube heat exchangers with trefoil-hole, helical and segmental baffles. Applied Thermal Engineering, Vol. 109, 175-185. https://doi.org/10.1016/j.applthermaleng.2016.08.067.

46. Erokhin M., Pastukhov A., Kazantsev S. Operability assessment of drive shafts of John Deere tractors in operational parameters. Proceedings of 18th International Scientific Conference "Engineering for rural development". Jelgava, Latvia, May 22-25, 2019, Latvia University of Agriculture. Faculty of Engineering, vol. 18, pp. 28-33. Scopus. WoS.

47. Fidaros D., Baxevanou C., Bartzanas T., Kittas C., (2018), Numerical study of mechanically ventilated broiler house equipped with evaporative pads, Computers and Electronics in Agriculture, vol. 149, pp. 101-109, doi:10.1016/j.compag.2017.10.016, Netherlands;

48. Filho A. A. P., Luna F. M. T., Cavalcante C. L. Oxidative stability of mineral naphthenic insulating oils: Optimization of commercial antioxidants and metal passivators // IEEE Transactions on Dielectrics and Electrical Insulation. 2019. Vol. 26, Issue 1. P. 240–246. doi: http://doi.org/10.1109/TDEI.2018.007513

49. Galat U.N., Ingale A.N., (2016), Failure Investigation & Analysis of Agricultural 9 Tyne Cultivator Used In Various Soil Condition. *International Journal on Recent and Innovation Trends in Computing and Communication*. vol. 4, issue 1, pp. 173–179, Delhi / India;

50.   Gheorghiță N.E., Biriș S.Șt., Ungureanu N., Ionescu M., (2018), Contributions to the analysis of the vibratory working tools by FEM. *International Symposium ISB INMA TEH Agricultural and Mechanical Engineering*, 01-03 November, pp. 579-582, Bucharest / Romania;

51.   Gheres M.I., (2014), Mathematical model for studying the influence of tillage tool geometry on energy consumption. *INMATEH Agricultural Engineering*, vol. 42, issue 1, pp. 5-12, Bucharest / Romania;

52. Gorobets V., Bohdan Y., Trokhaniak V. & Antypov I. (2019). Investigations of heat transfer and hydrodynamics in heat exchangers with compact arrangements of tubes. Applied Thermal Engineering, vol. 151, 46-54, doi:10.1016/j.applthermaleng.2019.01.059.

53.   Gorobets V., Bohdan Y., Trokhaniak V., Antypov I., (2019), Investigations of heat transfer and hydrodynamics in heat exchangers with compact arrangements of tubes, Applied Thermal Engineering, vol. 151, pp. 46-54. doi:10.1016/j.applthermaleng.2019.01.059, London/United Kingdom;

54. Gorobets V.G., Bohdan Yu.O., Trokhaniak V.I. & Antypov I.O. (2018). Experimental studies and numerical modelling of heat and mass transfer process in shell-and-tube heat exchangers with compact arrangements of tube bundles. Paper presented at the MATEC Web of Conferences, vol. 240, 02006. https://doi.org/10.1051/matecconf/201824002006.

55. Gorobets V.G., Trokhaniak V.I. & Bohdan Yu.O. (2016). Heat exchanger. UA Patent No. 111751.

56. Gorobets V.G., Trokhaniak V.I., Antypov I.O. & Bohdan Yu.O. (2018). The numerical simulation of heat and mass transfer processes in tunneling air ventilation system in poultry houses. INMATEH: Agricultural Engineering, vol.55, 2, 87-96.

57.   Gorobets V.G., Trokhaniak V.I., Antypov I.O., Bohdan Yu.O., (2018), The numerical simulation of heat and mass transfer processes in

tunneling air ventilation system in poultry houses, INMATEH: Agricultural Engineering, vol.55, no.2, pp.87-96, Bucharest/Romania;

58.   Gorobets V.G., Trokhaniak V.I., Rogoskii I.L., Titova L.L., Lendiel T.I., Dudnyk A.O., Masiuk M.Yu. The numerical simulation of hydrodynamics and mass transfer processes for ventilating system effective location. INMATEH. Agricultural Engineering. Bucharest. Romania, vol. 56, No 3, 2018, pp. 185-192. Scopus. WoS.

59.   Günther D., Reininghaus J., Prohaska S., Weinkauf T. et al., 2011. Efficient computation of a hierarchy of discrete 3d gradient vector fields. In: Topological Methods in Data Analysis and Visualization, vol. II, pp. 15-29.

60. Gurcanli E., Bilir S., Sevim M. Activity Based Risk Assessment and Safety Cost Estimation for Residential Building Construction Projects. Safety Science, 2015, vol. 80, pp. 1-12. Scopus.

61. Gyansah L., Ansah A.K. Fatigue Crack Initiation Analysis in 1060 Steel. Res. J. of Appl. Sc. Eng. and Tech, 2010, vol. 4, issue 2, pp. 319-325. Scopus.

62.   Hevko B.M., Hevko R.B., Klendii O.M., Buriak M.V., Dzyadykevych Y.V., Rozum R.I., (2018), Improvement of machine safety devices. *Acta Polytechnica,* vol. 58, no. 1, pp. 17-25, Prague / Czech Republic.

63.   Hevko R.B., Yazlyuk B.O., Liubin M.V., Tokarchuk O.A., Klendii O.M., Pankiv V.R., (2017), Feasibility study of the process of transportation and stirring of mixture in continuous-flow conveyers. *INMATEH: Agricultural engineering*, vol. 51, issue 1, pp. 49-58. Bucharest / Romania;

64.   Hutorov, A.O., Lupenko, Y.O., Yermolenko, O.A., Dorokhov V.O., 2018. Strategic management of the agrarian sector of economy based on the analysis of value chains. In: Bulletin of the Transilvania University of Brasov, Series II: Forestry, Wood Industry, Agricultural Food Engineering, vol. 11 (60), no. 2, pp. 101-114.

65.   International Rules for Seed Testing, 2011. In: ISTA Documents, International Seed Testing Association, Bassersdorf, Switzerland, p. 97.

66. Interpretation of the properties of refined rice bran oil as bio lubricant / Amudhan A., Karthicka N., Manonmanis K., Parimalamurugaveni S. // International Journal of Applied Engineering Research. 2015. Vol. 10, Issue 55. P. 3952–3955. URL: https://www.scopus.com/inward/record.uri?eid=2-s2.0-84942418557&partnerID=40&md5=c3484681ecdc1ca4f2f1652bcf6dd976

67.   Ivanova V. M., (1987), Prediction of heat consumption by livestock buildings (Прогнозирование теплопотребления животноводческими помещениями), Mechanization and electrification of agriculture (Механизация и электрификация сельск. хоз-ва.), vol. 10, pp. 43-46, Moscow/Russia;

68.   Ivanovs S., Bulgakov V., Nadykto V., Kuvachov V. Theoretical investigation of turning ability of two-machine sowing aggregate. Proceedings of 17th International Scientific Conference "Engineering for rural development". Jelgava, Latvia, May 23-25, 2018, Latvia University of Agriculture. Faculty of Engineering. Vol. 17, pp. 314-322.

69.   Kanehl P., (2010), *Particle model of the Magnus effect*, Bachelor Thesis. Mathematisch Naturwissenschaftliche Fakultät Ernst-Moritz-Arndt-Universität, 35 p., Greifswald / Germany;

70. Khamidullina E.A., Timofeeva S.S., Smirnov G.I. Accidents in Coal Mining from Perspective of Risk Theory. IOP Conference Series: Materials Science and Engineering, 2017, vol. 262, 012210. Scopus.

71. Khmelnik S.I. (2018). Navier-Stokes equations. On the existence and the search method for global solutions. Mathematics in Computers – MiC, Bene-Ayish, Israel;

72. Kim G.W., Lim H.M. & Rhee G.H. (2016). Numerical studies of heat transfer enhancement by cross-cut flow control in wavy fin heat exchangers. International Journal of Heat and Mass Transfer, Vol. 96, 110-117. https://doi.org/10.1016/j.ijheatmasstransfer.2016.01.023.

73. Klendii M.B., Klendii O.M., (2016), Interrelation between incidence angle and roll angle of concave disks of soil tillage implements. *INMATEH: Agricultural engineering,* vol. 49, issue 2, pp. 13-20, Bucharest / Romania;

74. Knapczyk A., Francik S., Pedryc N., Hebda T. Bibliometric analysis of research trends in engineering for rural development. Proceedings of 17th International Scientific Conference "Engineering for rural development". Jelgava, Latvia, May 23-25, 2018, Latvia University of Agriculture. Faculty of Engineering. Vol. 17, pp. 700-707.

75. Komiwes V., Mege P., Meimon Y., Herrmann H., (2006), Simulation of granular flow in a fluid applied to sedimentation, *Granular Matter*, Vol. 8 (1), pp. 41-54, Bern / Switzerland;

76. Kotov B.I., Spirin A.B., Tverdokhlib I.V., Polyevoda Y.A., Hryshchenko V.O., Kalinichenko R.A., (2018), Theoretical researches of cooling process regularity of the grain material in the layer, *INMATEH - Agricultural Engineering*, vol. 54, issue 1, pp. 87-94, Ed. INMA, Bucharest / Romania;

77. Kreivaitis, R., Padgurskas, J., Gumbytė, M., Makarevičienė, V. (2014). The thermal stability of rapeseed oil as a base stock for environmentally friendly lubricants. Mechanics, 20 (3). doi: https://doi.org/10.5755/j01.mech.20.3.5278

78. Kroulík, M., Húla, J., Rybka, A., Honzík, I., 2016. Pneumatic conveying characteristics of seeds in a vertical ascending airstream. In: Research in Agricultural Engineering, Czech Republic, vol. 62, pp. 56-63.

79. Kypris O., Nlebedim I.C., Jiles D. Measuring stress variation with depth using Barkhausen signal. J. Magn. Magn. Mater, 2016, vol. 407, pp. 377-395. Scopus.

80. Leoni G.B., Klein T.S. & Medronho R.D. (2017). Assessment with computational fluid dynamics of the effects of baffle clearances on the shell side flow in a shell and tube heat exchanger. Applied Thermal Engineering, Vol. 112,

497-506. https://doi.org/10.1016/j.applthermaleng.2016.10.097.

81. Li, J., Liu, J., Sun, X., Liu, Y. (2018). The mathematical prediction model for the oxidative stability of vegetable oils by the main fatty acids composition and thermogravimetric analysis. LWT, 96, 51–57. doi: https://doi.org/10.1016/j.lwt.2018.05.003

82. Lin J.-M., Wang W., Dai Y.-H. On-Line Monitoring of Particle in Oil Based on Electromagnetic NDT Technique // Studies in Applied Electromagnetics and Mechanics. 2015. Vol. 40. P. 329–336. doi: http://doi.org/10.3233/978-1-61499-509-8-329

83. Ling Z.Y., He Z.B., Xu T., Fang X.M., Gao X.N. & Zhang Z.G. (2017). Experimental and Numerical Investigation on Non-Newtonian Nanofluids Flowing in Shell Side of Helical Baffled Heat Exchanger Combined with Elliptic Tubes. Applied Sciences-Basel, Vol. 7, 1, 17. https://doi.org/10.3390/app7010048.

84. Luo A.C.J., Guo Y. Vibro-impact Dynamics. Berlin: Springer-Verlag, 2013. 213 p.

85. Lupu, M., Canja, C., Padureanu, V., 2017. The Influence of Moisture Content of Wheat Single Kernel on the Energy Consumption by Shearing Process. In: Bulletin of the Transilvania University of Brasov, Series II: Forestry, Wood Industry, Agricultural Food Engineering, vol. 10 (59), no. 1, pp. 119-124.

86. Lupu, M., Padureanu, V., Canja, C.M., 2014. Wheat Resistance Analysis on the Subject of Energy Consumption in the Grinding Process. In: Bulletin of the Transilvania University of Brasov, Series II: Forestry, Wood Industry, Agricultural Food Engineering, vol. 7 (56), no. 2, pp. 59-62.

87. Lutsak, D., Prysyazhnyuk, P., Burda, M., Aulin, V. (2016). Development of a method and an apparatus for tribotechnical tests of materials under loose abrasive friction. Eastern-European Journal of Enterprise Technologies, 5 (7 (83)), 19–26. doi: https://doi.org/10.15587/1729-

4061.2016.79913

88.   Masek J., Novak P., Jasinskas A. Evaluation of combine harvester operation costs in different working conditions. Proceedings of 16th International Scientific Conference "Engineering for rural development". Jelgava, Latvia, May 24-26, 2017, Latvia University of Agriculture. Faculty of Engineering. Vol. 16, pp. 1180-1185.

89. Mellal M., Benzeguir R., Sahel D. & Ameur H. (2017). Hydro-thermal shell-side performance evaluation of a shell and tube heat exchanger under different baffle arrangement and orientation. International Journal of Thermal Sciences, Vol. 121, 138-149. https://doi.org/10.1016/j.ijthermalsci.2017.07.011.

90. Mishin V.I., Chuenko R.N., Makarevich S.S., (2013), Conditions for stable joint operation of asynchronous machines of different types in an autonomous electromechanical system. Russian Electrical Engineering, vol. 84, no. 9, pp. 518-527, Moscow/Russia;

91. Mishin V.I., Lut N.T., Makarevich S.S., Chuenko R.N., (2016), Analogs and characteristics of compensated asynchronous machines with different numbers of phases. Russian Electrical Engineering, vol. 87, no. 12, pp. 653-660, Moscow/Russia;

92.   Mohamed Hemisa, Ruplal Choudhary, 2012. A coupled mathematical model for simultaneous microwave and convective drying of wheat seeds. In: Biosystems Engineering, no. 112, pp. 202-209.

93. Najafi P., Asoodar M. A., Marzban A., Hormozi M. A. Reliability analysis of agricultural machinery: A case study of sugarcane chopper harvester. AgricEngInt: CIGR Journal. March, 2015, vol. 17, no. 1, pp. 158-165. Scopus.

94. Nilesh N.J., Harshal R.A., Amol P.G., (2015), Design and fabrication of onion seed sowing machine, *International Journal on Recent Technologies in Mechanical and Automobile Engineering*, issue 2, pp. 1-10, Pahang / Malaysia;

95.   Novotny J. Technical and natural sciences teaching at engineering faculty of FPTM UJEP. Proceedings of 15th International Scientific Conference

"Engineering for rural development". Jelgava, Latvia, May 23-25, 2016, Latvia University of Agriculture. Faculty of Engineering. Vol. 15, pp. 16-20.

96. Nykyforchyn H., Lunarska E., Tsyrulnyk O., et al. Environmentally assisted "in-bulk" steel degradation of long term service gas trunkline. Engineering Failure Analysis, 2010, vol. 17, pp. 624-632. Scopus.

97. On-line detection of incipient trend changes in lubricant parameters / Salgueiro J. M., Peršin G., Hrovatin J., Juricic Đ., Vižintin J. // Industrial Lubrication and Tribology. 2015. Vol. 67, Issue 6. P. 509–519. doi: https://doi.org/10.1108/ilt-09-2013-0097

98. Pădureanu V., Lupu M., Steriu V., 2013. Theoretical researches concerning the process of crushing wheat grains using the finite elements method. In: Bulletin of the Transilvania University of Braşov, Series II, vol. 6(55), no. 1, pp. 143-150.

99. Pal E., Kumar I., Joshi J.B. & Maheshwari N.K. (2016). CFD simulations of shell-side flow in a shell-and-tube type heat exchanger with and without baffles. Chemical Engineering Science, Vol. 143, 314-340. https://doi.org/10.1016/j.ces.2016.01.011.

100. Pavel Kic, Aivars Aboltins, 2014. Drying process of two special plants. In: Engineering for Rural Development, vol. 13, pp. 137-142.

101. Pinzi S., Cubero-Atienza A.J., Dorado M.P. Vibro-acoustic analysis procedures for the evaluation of the sound insulation characteristics of agricultural machinery. Journal of Sound and Vibration, vol. 266 (3), 2016, pp. 407-441.

102. Pisarenko G., Voinalovych O., Rogovskii I., Motrich M. Probability of boundary exhaustion of resources as factor of operational safety for agricultural aggregates. Proceedings of 18th International Scientific Conference "Engineering for rural development". Jelgava, Latvia, May 22-25, 2019, Latvia University of Agriculture. Faculty of Engineering, vol. 18, pp. 291-298. Scopus. WoS.

103.   Pourvosoghi N., Nikbakht A. M., Sharifian F., Najafi R., (2018), Numerical analyses of air velocity and temperature distribution in poultry house using computational fluid dynamics, INMATEH: Agricultural Engineering, vol. 56, no. 3, pp. 109-118, Bucharest/Romania;

104.   Razzaghi E., Sohrabi Y., (2016), Vibratory soil cutting a new approach for the mathematical analysis. *Soil and Tillage Research*. vol. 159, pp. 33-40, Kiel / Germany;

105.   Rejovitzky E., Altus E. On single damage variable models for fatigue. International Journal of Damage Mechanics, 2013, vol. 22, no. 2, pp. 268-284. Scopus.

106.   Rogovskii I., Grubrin O. Accuracy of converting videoendoscopy combine harvester using generalized mathematical model. Scientific Herald of National University of Life and Environmental Science of Ukraine. Series: technique and energy of APK. Kyiv, Ukraine. vol. 298, 2018, pp. 149-156. doi: 10.31548/me.2018.04.149-156.

107.   Rogovskii I., Titova L., Novitskii A., Rebenko V. Research of vibroacoustic diagnostics of fuel system of engines of combine harvesters. Proceedings of 18th International Scientific Conference "Engineering for rural development". Jelgava, Latvia, May 22-25, 2019, Latvia University of Agriculture. Faculty of Engineering, vol. 18, pp. 291-298. Scopus. WoS.

108.   Rogovskii I., Titova L., Trokhaniak V., Trokhaniak O., Stepanenko S., (2019), Experimental study on the process of grain cleaning in a pneumatic microbiocature separator with apparatus camera. *Bulletin of the Transilvania University of Brasov, Series II: Forestry, Wood Industry, Agricultural Food Engineering*, vol. 12 (61), issue 1, pp. 117-128, Brasov / Romania;

109.   Rogovskii I.L., Titova L.L., Trokhaniak V.I., Rosamaha Yu.O., Blesnyuk O.V., Ohiienko A.V., (2019), Engineering management of two-phase coulter systems of seeding machines for implementing precision farming

technologies. *INMATEH Agricultural Engineering*, vol. 58, issue 2, pp. 137-146, Bucharest / Romania;

110. Rogovskii I.L., Titova L.L., Trokhaniak V.I., Solomka O.V., Popyk P.S., Shvidia V.O., Stepanenko S.P., (2019), Experimental studies of drying conditions of grain crops with high moisture content in low-pressure environment, *INMATEH - Agricultural Engineering*, vol. 57, issue 1, pp. 141-146, Ed. INMA, Bucharest / Romania;

111. Rohokale A.B., Shewale P.D., Pokharkar S.B., Sanap K.K., (2014), A review on multi-seed sowing machine, *International Journal of Mechanical Engineering and Technology (IJMET)*, vol. 5, pp. 180-186, Tamil Nadu / India;

112. Rojano F., Bournet P. E., Hassouna M., Robin P., Kacira M., Choi C. Y., (2019), Modelling the impact of air discharges caused by natural ventilation in a poultry house. Biosystems Engineering, vol. 180, pp. 168-181. doi:10.1016/j.biosystemseng.2019.02.001, San Diego/USA;

113. Ruzhylo M.J., Skorokhod T.A. On empirical distributions in spaces of growing dimensions. Discrete distributions. Random operators and stochastic equations, The Netherlands, 2005, vol. 3, pp. 210-219. Scopus.

114. Ruzhylo, M.J., Skorokhod T.A. On empirical distributions in spaces of growing dimensions. Continuous distributions. Random operators and stochastic equations, The Netherlands, 2005, vol. 4, pp. 184-193. Scopus.

115. Salgueiro, J. M., Peršin, G., Hrovatin, J., Juricic, Đ., Vižintin, J. (2015). On-line detection of incipient trend changes in lubricant parameters. Industrial Lubrication and Tribology, 67 (6), 509–519. doi: https://doi.org/10.1108/ilt-09-2013-0097

116. Sergejeva N., Aboltins A., Strupule L., Aboltina B. Mathematical knowledge in elementary school and for future engineers. Proceedings of 17th International Scientific Conference "Engineering for rural development". Jelgava, Latvia, May 23-25, 2018, Latvia University of Agriculture. Faculty of Engineering. Vol. 17, pp. 1166-1172.

117. Shahril S.M., Quadir G.A., Amin N.A.M. & Badruddin I.A. (2017). Thermo hydraulic performance analysis of a shell-and-double concentric tube heat exchanger using CFD. International Journal of Heat and Mass Transfer, Vol. 105, 781-798. https://doi.org/10.1016/j.ijheatmasstransfer.2016.10.021.

118. Sharma B. K., Perez J. M., Erhan S. Z. Soybean Oil-Based Lubricants: A Search for Synergistic Antioxidants // Energy & Fuels. 2007. Vol. 21, Issue 4. P. 2408–2414. doi: https://doi.org/10.1021/ef0605854

119. Shen Qiang, Xu Li-li, Wang Jun-qiang, Yang Wei-min, (2015), The performance of Agricultural science and technology transformation Fund of different Technical Fields, *International Conference on Engineering Management, Engineering Education and Information Technology*, issue 1, pp. 94-98, Madrid / Spain;

120. Shih-Heng T., Ming-Hsiang S., Wen-Pei S. Development of digital image correlation method to analyse crack variations of masonry wall. Sadhana, 2008, vol. 6, pp. 767-779. Scopus.

121. Shutka O.V., Sukach S.V., (2010), Model of the ventilation complex in the tasks of stabilizing the temperature regime in the room (Модель вентиляційного комплексу в задачах стабілізації температурного режиму в приміщенні), Transaction of Kremenchuk Mykhailo Ostrohradskyi National University (Вісник КДУ ім. М. Остроградського), vol. 3, no. 62, pp. 57–62, Kremenchuk/Ukraine;

122. Sowing machines and systems based on the elements of fluidics / Aulin V., Chernovol M., Pankov A., Zamota T., Panayotov K. // INMATEH – Agricultural Engineering. 2017. Vol. 53, Issue 3. P. 21–28. URL: http://dspace.kntu.kr.ua/jspui/bitstream/123456789/7278/1/53-03%20Aulin%20.pdf

123. Spalart P.R., Rumsey C.L. (2007), Effective inflow conditions for turbulence models in aerodynamic calculations, Aiaa Journal, vol. 45, no. 10, pp. 2544-2553 doi:10.2514/1.29373, Reston/USA;

124.   Srivastava A.K., Goering C.E., Rohrbach R.P., Buckmaster D.R., (2016), Soil tillage. Chapter 8, Engineering Principles of Agricultural Machines, *Monography*, 2nd ed., St. Joseph, Michigan: ASABE. Copyright American Society of Agricultural and Biological Engineers, pp. 169-230, Michigan / USA;

125.   Stroescu, Gh., Păun, A., 2018. Technology for obtaining environmentally-friendly seeds and sowing material for vegetable species, In: Proceedings of international Symposium ISB-INMATEH – Agricultural and Mechanical Engineering, 1-3 Nov., pp. 467-472.

126.   Stuart Nelson, 2015. Properties of agricultural materials and their applications. In: Monograph. Athens, GA, USA, Academic Press, 229 p.

127.   Substantiation of diagnostic parameters for determining the technical condition of transmission assemblies in trucks / Aulin V., Hrinkiv A., Dykha A., Chernovol M., Lyashuk O., Lysenko S. // Eastern-European Journal of Enterprise Technologies. 2018. Vol. 2, Issue 1 (92). P. 4–13. doi: https://doi.org/10.15587/1729-4061.2018.125349

128.   Thakre P.B. & Pachghare P.R. (2017). Performance Analysis on Compact Heat Exchanger. Materials Today-Proceedings, Vol. 4, 8, 8447-8453.

129.   The mathematical prediction model for the oxidative stability of vegetable oils by the main fatty acids composition and thermogravimetric analysis / Li J., Liu J., Sun X., Liu Y. // LWT. 2018. Vol. 96. P. 51–57. doi: https://doi.org/10.1016/j.lwt.2018.05.003

130.   The thermal stability of rapeseed oil as a base stock for environmentally friendly lubricants / Kreivaitis R., Padgurskas J., Gumbytė M., Makarevičienė V. // Mechanics. 2014. Vol. 20, Issue 3. doi: https://doi.org/10.5755/j01.mech.20.3.5278

131.   Trokhaniak V., Klendii O., (2018), Numerical simulation of hydrodynamic and heat-mass exchange processes of a microclimate control system in an industrial greenhouse, Bulletin of the Transilvania University of Brasov, Series II: Forestry, Wood Industry, Agricultural Food Engineering, vol.

11 (60), no. 2., pp. 171-184, Brasov/ Romania;

132. Trokhaniak V.I., Rutylo M.I., Rogovskii I.L., Titova L.L., Luzan O.R., Bannyi O.O. Experimental studies and numerical simulation of speed modes of air environment in a poultry house. INMATEH. Agricultural Engineering. Bucharest, 2019, vol. 59, no 3, pp. 9-18. Scopus. WoS.

133. Tutunaru L.F., Nagy E.M., Coța C., (2014), Influence of tillage tools cutting edge wear over technical and economic indicators. *INMATEH Agricultural Engineering*, vol. 44, issue 3, pp. 5-12, Bucharest / Romania;

134. Tyutrin S. Improving reliability of parts of mounted mower according to monitoring results by fatigue gauges from tin foil. Proceedings of 18th International Scientific Conference "Engineering for rural development". Jelgava, Latvia, May 22-25, 2019, Latvia University of Agriculture. Faculty of Engineering, vol. 18, pp. 22-27. Scopus. WoS.

135. Van Rensselar J. Trends in industrial gear oils // Tribology and Lubrication Technology. 2013. Vol. 69, Issue 2. P. 26–33. URL: https://www.scopus.com/inward/record.uri?eid=2-s2.0-84873974634&partnerID=40&md5=9e4c6b38cc445f867bc21d4c67302f50

136. Viba J., Lavendelis E. Algorithm of synthesis of strongly non-linear mechanical systems. In Industrial Engineering – Innovation as Competitive Edge for SME, 22 April 2006. Tallinn, Estonia, pp. 95-98.

137. Vlăduţ D.I., Biriş S., Vlăduţ V., Cujbescu D., Ungureanu N., Găgeanu I., (2018), Experimental researches on the working process of a seedbed preparation equipment for heavy soils, *INMATEH - Agricultural Engineering*, vol. 55, issue 2, pp. 27-34, Ed. INMA, Bucharest / Romania.

138. Vlăduţ V., Gheorghe G., Marin E., Biriş S. Șt., Paraschiv G., Cujbescu D., Ungureanu N., Găgeanu I., Moise V., Boruz S., (2017), Kinetostatic analysis of the mechanism of deep loosening system of arable soil. *45th International Symposium "Actual tasks on agricultural engineering"*, 21-24 February, ISSN 1848-4425. pp. 217-227, Opatija / Croatia;

139. Voinalovych A.V., Motrich M.N. Control of the technical state of agricultural aggregates by facilities of fault detection. Mechanization in agriculture. Sofia. Bulgaria, Year LXI, ISSN 0861-9638, issue 12, 2015, pp. 29-31.

140. Voinalovych O., Hnatiuk O., Rogovskii I., Pokutnii O. Probability of traumatic situations in mechanized processes in agriculture using mathematical apparatus of Markov chain method. Proceedings of 18th International Scientific Conference "Engineering for rural development". Jelgava, Latvia, May 22-25, 2019, Latvia University of Agriculture. Faculty of Engineering, vol. 18, pp. 563-269. Scopus. WoS.

141. Xi L., Songlin Z. Changes in mechanical properties of vehicle components after strengthening under low-amplitude loads below the fatigue limit. Fatigue and Fracture of Engineering Materials and Structures, 2019, vol. 32, no. 10, pp. 847-855. Scopus.

142. Xiong P., Yang Z., Sun Z., Zhang Q., Huang Y., Zhang Z., (2018), Simulation analysis and experiment for three-axis working resistances of rotary blade based on discrete element method. *Nongye Gongcheng Xuebao, Transactions of the Chinese Society of Agricultural Engineering*, vol. 34, issue 18, pp. 113-121, Beijing / Chine.

143. Yan S.-F., Ma B., Zheng C.-S. Remaining useful life prediction for power-shift steering transmission based on fusion of multiple oil spectra // Advances in Mechanical Engineering. 2018. Vol. 10, Issue 6. P. 168781401878420. doi: https://doi.org/10.1177/1687814018784201

144. Yata V.K., Tiwari B.C., Ahmad, I. Nanoscience in food and agriculture: research, industries and patents. Environmental Chemistry Letters, vol. 16, 2018, pp. 79-84.

145. Zagurskiy O., Ohiienko M., Rogach S., Pokusa T., Titova L., Rogovskii I. Global supply chain in context of new model of economic growth.

Conceptual bases and trends for development of social-economic processes. Monograph. Opole. Poland, 2018, pp. 64-74.

146. Zaica A., Visan A.L., Paun A., Gageanu P., Bunduchi G., Zaica A., Stefan V., Manea D., 2016. The coating process of corn grains using a treatment machine with brush screw conveyor. In: Proceedings of the 44th International Symposium on Agricultural Engineering: Actual Tasks on Agricultural Engineering, Croatia, 23-26 Febr., pp. 333-345.

147. Zajicek M. & Kic P. (2012). Improvement of the broiler house ventilation using the CFD simulation. Agronomy Research, vol. 10, Special Issue 1, 235-242.